

Multiple mantle metasomatism beneath the Leizhou Peninsula, South China: Evidence from elemental and Sr-Nd-Pb-Hf isotope geochemistry of the late Cenozoic volcanic rocks

Journal:	<i>International Geology Review</i>
Manuscript ID	TIGR-2018-0204.R4
Manuscript Type:	Data Article
Date Submitted by the Author:	11-Nov-2018
Complete List of Authors:	Sun, Pu; Institute of Oceanology Chinese Academy of Sciences, Marine geology NIU, Yaoling; Institute of Oceanology, Chinese Academy of Sciences; Durham University Guo, Pengyuan; Institute of Oceanology Chinese Academy of Sciences Chen, Shuo; Institute of Oceanology Chinese Academy of Sciences Duan, Meng ; Institute of Oceanology Chinese Academy of Sciences Gong, Hongmei; Institute of Oceanology, Chinese Academy of Sciences Wang, Xiaohong; Institute of Oceanology Chinese Academy of Sciences Xiao, Yuanyuan; Institute of Oceanology Chinese Academy of Sciences
Keywords:	South China, Cenozoic volcanism, mantle metasomatism, low-F melt, recycled UCC material

SCHOLARONE™
Manuscripts

- 1
2
3
4 1. These rocks show incompatible element enrichment but variable isotopic depletion;
5
6 2. High bulk-rock Sr does not indicate recycled oceanic gabbro in the mantle source;
7
8 3. A low-F melt with high Sr enriched the incompatible elements of the mantle source;
9
10 4. A recently recycled UCC material is present in the mantle source region.

13
14
15
16
17
18
19
20
21
22
23
24
25
26
27
28
29
30
31
32
33
34
35
36
37
38
39
40
41
42
43
44
45
46
47
48
49
50
51
52
53
54
55
56
57
58
59
60

For Peer Review Only

1
2
3 1 **Multiple mantle metasomatism beneath the Leizhou Peninsula, South**
4
5 2 **China: Evidence from elemental and Sr-Nd-Pb-Hf isotope**
6
7 3 **geochemistry of the late Cenozoic volcanic rocks**

8
9
10 4
11
12
13
14 5 Pu Sun ^{1, 2, 3 *}, Yaoling Niu ^{1, 2, 3, 4, 5 **}, Pengyuan Guo ^{1, 2, 3}, Shuo Chen^{1, 2, 3}, Meng Duan
15
16
17 6 ^{1, 2, 3}, Hongmei Gong ^{1, 2, 3}, Xiaohong Wang ^{1, 2, 3}, Yuanyuan Xiao ^{1, 2, 3}

18
19 7 ¹ Institute of Oceanology, Chinese Academy of Sciences, Qingdao 266071, China

20
21 8 ² Laboratory for Marine Geology, Qingdao National Laboratory for Marine Science and Technology,
22
23 9 Qingdao 266061, China

24
25 10 ³ Center for Ocean Mega-Science, Chinese Academy of Sciences, 7 Nanhai Road, Qingdao, 266071,
26
27 11 China

28
29 12 ⁴ Department of Earth Sciences, Durham University, Durham DH1 3LE, UK

30
31 13 ⁵ School of Earth Science and Resources, China University of Geosciences, Beijing 100083, China

32
33 14 Correspondence:

34
35 15 * Mr. Pu Sun (pu.sun@foxmail.com)

36
37 16 ** Professor Yaoling Niu (yaoling.niu@durham.ac.uk)

38
39
40 20 **Abstract.** We analyzed whole-rock major and trace elements and Sr-Nd-Pb-Hf isotopes
41
42 21 of the late Cenozoic volcanic rocks in the Leizhou Peninsula, South China to investigate
43
44 22 their mantle source characteristics. These volcanic rocks, collected from Jiujiang,
45
46 23 Tianyang and Huoju areas of the Leizhou Peninsula, are characterized by incompatible
47
48 24 element enrichment but variable isotopic depletion. The volcanic rocks from Jiujiang
49
50 25 and Tianyang show prominent primitive-mantle-normalized positive Nb, Ta and Sr
51
52 26 anomalies and depleted Sr-Nd-Pb-Hf isotope compositions, whereas those from Huoju

1
2
3 27 show slight positive to negative Nb and Ta anomalies, a prominent positive Pb anomaly,
4
5 28 and more enriched Sr-Nd-Pb-Hf isotope compositions. Two types of mantle
6
7 29 metasomatism are required to explain the geochemical characteristics of these rocks.
8
9
10 30 The Jiujiang and Tianyang samples were largely derived from a mantle source
11
12 31 metasomatized recently by a low-F melt. Such low-F melt is generated within the
13
14 32 asthenospheric mantle, which is enriched in volatiles and incompatible elements with
15
16 33 positive Sr anomaly and depleted Sr-Nd-Pb-Hf isotope compositions. The Huoju
17
18 34 samples were largely derived from a mantle source metasomatized by recycled upper
19
20 35 continental crust (UCC) material. These two types of mantle metasomatism beneath the
21
22 36 Leizhou Peninsula are consistent with trace element characteristics of mantle
23
24 37 mineralogy (e.g., clinopyroxene vs. amphibole), which reflects source evolution in
25
26 38 space and time (e.g., tectonic setting change).

30
31
32
33 40 **Key words:** South China; Cenozoic volcanism; mantle metasomatism; low-F melt;
34
35 41 recycled UCC material

36
37
38
39
40 43 **1. Introduction**

41
42
43
44
45 45 Studies of oceanic basalts have revealed mantle chemical heterogeneity on all
46
47 scales. Although the origin of mantle heterogeneity is controversial, seafloor
48
49 subduction has long been inferred to be significant in causing the heterogeneity (e.g.,
50
51 48 [Hofmann and White, 1982](#); [Zinder and Hart, 1986](#); [Hart, 1988](#); [Farley, 1995](#); [Stracke](#)
52
53 49 [et al., 2003](#); [Willbold and Stracke, 2006](#)). Seafloor subduction can carry terrigenous
54
55 and pelagic sedimentary materials into the upper mantle, which has been inferred to be
56
57 significant in forming geochemically enriched mantle sources (e.g., [Weaver, 1991](#);
58
59
60

1
2
3 52 Chauvel et al., 1992; Farley, 1995; Jackson et al., 2007). On the other hand, a low
4 degree (low-F) melt derived within the seismic low velocity zone (LVZ) beneath
5 oceanic lithosphere, which is highly enriched in volatiles, alkalis and incompatible
6 elements, has been suggested to metasomatize the mantle source of intraplate volcanic
7 rocks (Hanson, 1977; Wood, 1979; Halliday et al., 1995; Niu et al., 1999, 2002, 2012;
8 Niu and O'Hara, 2003; Niu, 2005, 2008, 2014; Pilet et al., 2008). The presence of LVZ
9 has also been observed beneath continental lithosphere of eastern Asia, eastern
10 Australia and western America through seismic tomography (Ekström and Dziewonski,
11 1998), which has been thought to be significant in forming geochemically enriched
12 continental intraplate basalts (e.g., Niu, 2005, 2014; Guo et al., 2016; Sun et al., 2017).
13
14

15 62 Late Cenozoic intraplate volcanic rocks are widespread in Southeast Asia (Fig. 1a),
16 including those in the South China Sea Basin (Yan et al., 2006; Yan et al., 2015), in the
17 Indochina Peninsula (Hoang and Flower, 1998), and in the Hainan Island and Leizhou
18 Peninsula (Tu et al., 1991, 1992; Flower et al., 1992; Zhang et al., 1996; Ho et al., 2000;
19 Xu et al., 2002; Zou and Fan, 2010; Wang et al., 2011, 2013; Liu et al., 2015). They are
20 characterized by OIB (oceanic island basalts)-like incompatible element enrichment but
21 varying extent of Sr-Nd isotope depletion with a Dupal-type Pb isotope signature (Tu
22 et al., 1991, 1992; Flower et al., 1992; Hoang and Flower, 1998; Chen et al., 2009; Zeng
23 et al., 2013). Over the last decade, a mantle plume has been popularly invoked to
24 explain the petrogenesis of these volcanic rocks, largely inferred from a mantle seismic
25 tomography beneath the region (Lebedev and Nolet, 2003; Zhao, 2004; Yan and Shi,
26 2007; Lei et al., 2009; Wang et al., 2011) although this interpretation remains debatable.
27
28

29 74 In this paper, we do not intend to discuss the plume debate, but focus on the mantle
30 source heterogeneity of mantle metasomatic origin using bulk-rock major and trace
31 elements and Sr-Nd-Pb-Hf isotopes of the late Cenozoic volcanic rocks from the
32
33

1
2
3 Leizhou Peninsula. These rocks have been relatively poorly studied compared with
4 other Cenozoic volcanic rocks in the Southeast Asia ([Ho et al., 2000](#)), which may
5 provide new perspectives on the mantle source characteristics and mantle evolution
6 histories beneath this area. We have identified two types of mantle metasomatism
7 beneath this region: metasomatism genetically derived from melting of subducted
8 terrigenous sediments (upper continental crust material), and the metasomatism by an
9 incompatible element enriched low-F melt derived from the asthenosphere.
10
11
12
13
14
15
16
17
18
19
20
21
22
23
24
25
26
27
28
29
30
31
32
33
34
35
36
37
38
39
40
41
42
43
44
45
46
47
48
49
50
51
52
53
54
55
56
57
58
59
60

2. Geological setting and samples

The Leizhou Peninsula is located at the geological transition between South China continental margin and the South China Sea Basin (SCSB; [Fig. 1a](#)). Southeast Asia is geologically considered as an assembly of exotic continental terranes fragmented from Gondwana with the amalgamation largely completed during the early Mesozoic ([Lin et al., 1985](#); [Metcalfe, 1990](#); [Tu et al., 1991](#); [Chung et al., 1994](#); [Zou et al., 2000](#)). South China in the Mesozoic was characterized by having an active continental margin with extensive subduction-related granitoid magmatism ([Jahn et al., 1990](#); [Zhou and Li, 2000](#); [Li et al., 2012](#); [Niu et al., 2015](#)). The subduction was predicted to cease at ~ 100 Ma because of trench jam by an exotic micro-continent ([Niu et al., 2015](#)). The South China Sea is thought to open at ~ 32 Ma and spread until ~ 15.5 Ma ([Taylor and Hayes, 1983](#); [Briais et al., 1993](#); [Kido et al., 2001](#)). The intraplate magmatism on the periphery of the SCSB contemporaneous with the SCSB spreading was limited, but resumed extensively after the cessation of the SCSB spreading ([Yan et al., 2006](#); [Huang et al., 2013](#)).

The Ar-Ar and K-Ar dating gives erupting ages of 6.12 to 0.17 Ma for the volcanic

rocks in the Leizhou Peninsula (Ho et al., 2000). Our samples were collected from Huoju, Jiujiang and Tianyang areas (Fig. 1b). These volcanic lavas show layered structures (Fig. 2a), caused by multiple episodes of eruptions (Ho et al., 2000). Porous and ropy structures can be observed at the surface of each lava layer (Fig. 2b). These rocks show intergranular texture, with phenocrysts and microlites of olivine, clinopyroxene and magnetite aggregated between euhedral plagioclase laths (~ 0.5-1 mm; Figs. 2c & d). Spinel peridotite mantle xenoliths and clinopyroxene megacrysts are present in volcanic rocks from Jiujiang and Tianyang (Yu et al., 2006; Huang et al., 2007).

3. Sample preparation and analytical procedures

We crushed fresh rocks to chips of ≤ 5 mm before repeatedly cleaned in Milli-Q water in an ultrasonic bath, dried and grounded into $\geq 200 \mu\text{m}$ powders with an agate mill in a clean environment. Bulk-rock major elements were analyzed at China University of Geosciences, Beijing (CUGB), using a Leeman Prodigy Inductively Coupled Plasma Optical Emission Spectrometer (ICP-OES). Repeated analyses of USGS reference rock standards RCR-1, AGV-2 and national geological standard reference materials GSR-3 give analytical precision better than 1% for most elements except for TiO_2 (~ 1.5%) and P_2O_5 (~ 2.0%). The analytical details are given in Song et al. (2010). See Supplementary Table 1 for major element analytical results for USGS standard AGV-2.

Bulk-rock trace elements were analyzed in the Institute of Oceanology, Chinese Academy of Sciences (IOCAS), using Agilent-7900 inductively coupled plasma mass spectrometer (ICP-MS). Fifty milligrams of each sample were dissolved with acid mix

1
2
3 127 of distilled HCl+3HNO₃ and HF in a high-pressure jacket equipped Teflon beaker for
4 128 15 hours, and then re-dissolved with 20% HNO₃ for 2 hours till complete digestion.
5
6 129 Repeated analyses of USGS reference rock standards AGV-2, W-2, BHVO-2, BCR-2
7
8 130 give analytical precisions better than 5% for most elements. See [Chen et al. \(2017\)](#) for
9 analytical details. See Supplementary Table 1 for trace element analytical results for
10 131 USGS standard AGV-2.
11
12
13
14
15
16

17 133 Bulk-rock Sr-Nd-Pb-Hf isotope ratios were measured using a Nu Plasma MC-ICP-
18
19 134 MS in the IOCAS. About 50 mg of rock powder was dissolved with double distilled
20 HNO₃ + HCl + HF in a high-pressure jacket equipped Teflon beaker at 190°C for 15
21 hours, which was then dried and re-dissolved with 2 ml 3N HNO₃ for 2h. The final
22 sample solution was first loaded onto Sr-spec resin columns to separate Sr and Pb, with
23 the eluted sample solution collected and then loaded onto AG 50W-X8 resin columns
24 to separate REE. The eluted sample solution from AG 50W-X8 resin columns was
25 collected and then loaded onto Ln-spec resin columns to collect Hf. The separated REE
26 solution was dried and re-dissolved with 0.25 N HCl before being loaded onto Ln-spec
27 resin columns to collect Nd. The above streamlined procedure was modified after [Pin](#)
28
29 142 [et al. \(2014\)](#) and [Yang et al. \(2010\)](#). The measured ⁸⁷Sr/⁸⁶Sr, ¹⁴³Nd/¹⁴⁴Nd and ¹⁷⁶Hf/¹⁷⁷Hf
30
31 143 isotope ratios were normalized for instrumental mass fraction using the exponential law
32
33 144 to ⁸⁶Sr/⁸⁸Sr = 0.1194, ¹⁴⁶Nd/¹⁴⁴Nd = 0.7219 and ¹⁷⁹Hf/¹⁷⁷Hf = 0.7325, respectively.
34
35
36 145 International standards of NBS-987, JNd_i-1 and Alfa Hf were used as bracketing
37 standards every five samples to monitor the instrument drift during the analysis of Sr,
38
39 146 Nd and Hf isotopes, respectively. Repeated analysis for NBS-987 gives an average
40
41 147 ⁸⁷Sr/⁸⁶Sr = 0.710245 ± 0.000012 (n = 11, 2σ). Repeated analysis for JNd_i-1 gives an
42
43 148 average ¹⁴³Nd/¹⁴⁴Nd = 0.512094 ± 0.000008 (n = 13, 2σ), and repeated analysis for Alfa
44
45 149 Hf gives an average ¹⁷⁶Hf/¹⁷⁷Hf = 0.282194 ± 0.000007 (n = 7, 2σ). Pb isotope ratios
46
47
48 150
49
50 151
51
52
53
54
55
56
57
58
59
60

were normalized for instrumental mass fraction relative to NBS/SRM 997 $^{203}\text{Tl}/^{205}\text{Tl}$ = 0.41891. The international standard NBS-981 was used to monitor the instrument drift during the analysis of Pb isotopes. Repeated analysis of NBS-981 gives average $^{206}\text{Pb}/^{204}\text{Pb}$ = 16.932 ± 0.001 ($n = 10, 2\sigma$), $^{207}\text{Pb}/^{204}\text{Pb}$ = 15.489 ± 0.003 ($n = 10, 2\sigma$), and $^{208}\text{Pb}/^{204}\text{Pb}$ = 36.684 ± 0.013 ($n = 10, 2\sigma$). See Supplementary Table 2 for the Sr-Nd-Pb-Hf isotopic results of USGS standards of BCR-2 and AGV-2.

4. Geochemistry

4.1 Major element compositions

The analytical data are given in Supplementary Table 1. For comparison, we also compiled major elements, trace elements and Sr-Nd-Pb isotope data of the Cenozoic basaltic rocks in the Hainan Island (Supplementary Table 3; Tu et al., 1991; Flower et al., 1992; Zou and Fan, 2010; Ho et al., 2000; Wang et al., 2011). The volcanic rocks from the Leizhou Peninsula are mainly tholeiitic and show basaltic-andesitic SiO₂ contents of 47.78-61.21 wt.% with Mg[#] of 53-65 (Fig. 3a). The samples from Huoju have highly evolved SiO₂ contents of 54.87-61.21wt.%. The volcanic rocks from the Leizhou Peninsula have comparable Na₂O and K₂O contents with the basaltic rocks from the Hainan Island (Figs. 3b & c). Samples from Jiujiang and Tianyang show apparent higher Al₂O₃ than those from Huoju and Hainan Island (Fig. 3d).

4.2 Trace element compositions

176 Trace element data are given in Supplementary Table 1. These volcanic rocks

1
2
3 177 show varying extents of light rare earth element (LREE) enrichment, with OIB-like
4 178 [La/Yb]_N (chondrite normalized) of 6.0-12.9. They show REE abundances relatively
5 179 less enriched than OIB, with slight positive Eu anomaly. One sample from Tianyang
6 180 (ZC11-02) with negative Ce (Fig. 4a), Zr and Hf anomalies (Fig. 4b) and very high
7 181 Ba/Zr (1.97) and Lu/Hf (0.11) ratios is best explained to reflect significant zircon
8 182 crystallization because Ce⁴⁺ substitute Zr and Hf in zircon (Trail et al., 2012).
9
10
11
12
13
14
15
16
17
18
19
20
21
22
23
24
25
26
27
28
29
30
31
32
33
34
35
36
37
38
39
40
41
42
43
44
45
46
47
48
49
50
51
52
53
54
55
56
57
58
59
60

183 In the primitive-mantle normalized multi-element spider diagram (Fig. 4b), these
184 volcanic rocks are enriched in incompatible elements, and tend to be more enriched in
185 more incompatible elements, except for Nb, Ta, Pb and Sr, which are anomalous. The
186 Huoju samples show varying Nb and Ta anomalies (from slight positive to negative),
187 moderate positive Sr anomaly and prominent positive Pb anomaly. The samples from
188 Jiujiang and Tianyang have positive Nb and Ta anomalies, weak to moderate positive
189 Pb anomaly and significant positive Sr anomaly. The differences in Nb, Ta, Sr and Eu
190 anomalies of these volcanic rocks are more apparent in Fig. 5, with the ratios of
191 [Nb/Th]_N and [Ta/U]_N falling between those of OIB and upper continental crust (UCC),
192 and Sr/Sr* and Eu/Eu* higher than average OIB and most rocks from the Hainan Island.
193 Furthermore, the samples from Huoju have lower [Nb/Th]_N, [Ta/U]_N, Sr/Sr* and Eu/Eu*
194 compared with those from Jiujiang and Tianyang.
195
196

4.3 Sr-Nd-Pb-Hf isotopes

197
198 The Sr, Nd, Pb and Hf isotope data are given in Supplementary Table 2 and shown
199 in Fig. 6. In general, these rocks have more variable Sr-Nd-Pb isotopic compositions
200 than rocks from the Hainan Island, and plot in the field of the Cenozoic basalts from
201 SCSB (Figs. 6a, c & d). They have generally depleted ⁸⁷Sr/⁸⁶Sr (0.702955-0.704888),

1
2
3 202 $^{143}\text{Nd}/^{144}\text{Nd}$ (0.512754-0.512998) and $^{176}\text{Hf}/^{177}\text{Hf}$ (0.282939-0.283124), with ϵ_{Nd} of
4 +2.3 to +7.0 and ϵ_{Hf} of +5.5 to +12.0, respectively. However, they have radiogenic
5
6 203
7 204 $^{207}\text{Pb}/^{204}\text{Pb}$ (15.530-15.666) and $^{208}\text{Pb}/^{204}\text{Pb}$ (38.425-39.077) with intermediate
8
9 205 $^{206}\text{Pb}/^{204}\text{Pb}$ (18.454-18.727).

10
11 206 These rocks in Sr-Nd isotopic space define a negative trend (Fig. 6a), which
12
13 207 extends from the field of the depleted mid-ocean ridge basalts (MORB) to the more
14
15 208 enriched OIB field. The positive Nd-Hf isotopic correlation is subparallel to the
16
17 209 terrestrial array (Vervoort et al., 1999; Fig. 6b). A high-angle trend away from the
18
19 210 Northern Hemisphere Reference Line (NHRL; Hart, 1984) in the $^{207}\text{Pb}/^{204}\text{Pb}$ vs.
21
22 211 $^{206}\text{Pb}/^{204}\text{Pb}$ diagram is significant (Fig. 6c). In the $^{208}\text{Pb}/^{204}\text{Pb}$ vs. $^{206}\text{Pb}/^{204}\text{Pb}$ diagram,
23
24 212 they plot above and subparallel to the NHRL (Fig. 6d), showing a Dupal signature (Hart,
25
26 213 1984). Besides, there are a positive correlation between $^{206}\text{Pb}/^{204}\text{Pb}$ and $^{87}\text{Sr}/^{86}\text{Sr}$ and a
27
28 214 negative correlation between $^{206}\text{Pb}/^{204}\text{Pb}$ and $^{143}\text{Nd}/^{144}\text{Nd}$ (Figs. 6e & f).

29
30 215 The correlations of Sr-Nd-Pb-Hf isotope ratios of the volcanic rocks from the
31
32 216 Leizhou Peninsula are to a first order consistent with two component-mixing in the
33
34 217 mantle source region: an Indian-type depleted mantle component and an isotopically
35
36 218 enriched component. Compared with samples from Jiujiang and Tianyang, the Huoju
37
38 219 samples have higher $^{87}\text{Sr}/^{86}\text{Sr}$ and $^{206}\text{Pb}/^{204}\text{Pb}$ and lower $^{143}\text{Nd}/^{144}\text{Nd}$ and $^{176}\text{Hf}/^{177}\text{Hf}$
39
40 220 (Fig. 6), indicating higher contribution of the isotopically enriched component in the
41
42 221 mantle source region.

43
44 222

45
46 223 **5. Discussion**

47
48 224

49
50 225 **5.1 Effect of fractional crystallization and crustal contamination on magma**
51
52 226 **compositions**

1
2
3 227 Compared with the samples from Jiujiang and Tianyang and the rocks from the
4 228 Hainan Island, the samples from Huoju show relatively lower Mg[#], CaO (Fig. 3e), Ni
5 229 (Fig. 3g) and Cr (Fig. 3h), reflecting their experiencing higher extent of fractional
6 230 crystallization. The rocks from the Leizhou Peninsula show generally lower CaO/Al₂O₃
7 231 relative to the rocks from the Hainan Island, indicating their experiencing higher extent
8 232 of crystallization of clinopyroxenes (Cpx; Fig. 3f). According to the correlations of Mg[#]
9 233 with Cr and Ni, these samples must have experienced olivine and Cpx-dominated
10 234 fractional crystallization (Figs. 3g & h).

11
12
13
14
15 235 Before using bulk-rock trace elements and Sr-Nd-Pb-Hf isotopes to infer source
16 236 compositional characteristics, we need to evaluate the potential contribution of crustal
17 237 contamination in the bulk-rock compositions of these volcanic rocks during their ascent
18 238 to the surface. The continental crust materials are characterized by enriched SiO₂,
19 239 radiogenic Sr isotopes and unradiogenic Nd isotopes. Therefore, involvement of the
20 240 continental crust materials in the basaltic melt can increase both SiO₂ and ⁸⁷Sr/⁸⁶Sr
21 241 values, while decrease ¹⁴³Nd/¹⁴⁴Nd values of the melt. Compared with the samples from
22 242 Jiujiang and Tianyang, the samples from Huoju show generally higher SiO₂ (54.87-
23 243 61.21 wt.%) and ⁸⁷Sr/⁸⁶Sr (0.703882-0.704888) (Fig 7). However, the higher SiO₂ and
24 244 ⁸⁷Sr/⁸⁶Sr features of the Huoju samples should not be caused by crustal contamination,
25 245 and their isotopic compositions were largely inherited from the source materials for the
26 246 following reasons:

27
28 247 (1) simple mixing calculation shows that to generate the Huoju samples with
29 248 54.87-61.21 wt.% SiO₂, as high as ~38-70% UCC materials are needed to
30 249 assimilate with the assumed “primary” basaltic melt. Even if such high extent
31 250 of crustal assimilation was possible, it would generate melts with high
32 251 ⁸⁷Sr/⁸⁶Sr values of ~0.7071-0.7116 (Fig. 7), much higher than the ⁸⁷Sr/⁸⁶Sr

values (0.703882-0.704888) of the Huoju samples;

(2) there are no co-variations between SiO₂ and ⁸⁷Sr/⁸⁶Sr values in the Huoju samples ([Fig. 7](#)), indicating that the SiO₂ and ⁸⁷Sr/⁸⁶Sr variations in the Huoju samples were controlled by different processes, rather than one common process of crustal contamination. The higher SiO₂ contents were caused by high extent of fractional crystallization, while the higher ⁸⁷Sr/⁸⁶Sr values were most likely inherited from the mantle source compositions;

(3) The Sr-Nd-Pb isotope compositions of the volcanic rocks in the Leizhou Peninsula plot in the field of Cenozoic basalts from the SCSB ([Fig. 6](#); [Tu et al., 1992](#); [Yan et al., 2008, 2015](#)). These SCSB basalts were erupted through oceanic crust and experienced little continental crust contamination. Hence, the Sr-Nd-Pb isotope compositions of Cenozoic basalts from the SCSB and intraplate volcanic rocks in the periphery regions of the SCSB must reflect mantle signatures, which has been confirmed by studies of the Cenozoic volcanic rocks from Hainan Island ([Tu et al., 1991](#)), Vietnam ([Hoang et al., 1996](#); [Hoang and Flower, 1998](#)) and Southeast China ([Sun et al., 2017, 2018](#)).

5.2 Explanation of the positive Sr anomaly in the volcanic rocks from the Leizhou Peninsula

The volcanic rocks from the Leizhou Peninsula have a significant positive Sr anomaly ([Fig. 4b](#)). Such positive Sr anomaly has also been observed in Cenozoic basalts from the Hainan Island ([Fig. 8](#)), which was explained to result from the addition of recycled oceanic gabbro in the mantle source region ([Wang et al., 2011](#)), because plagioclase-rich oceanic gabbro has high Sr ([Sobolev et al., 2000](#); [Yaxley and Sobolev,](#)

1
2
3 277 2007; Stroncik and Devey, 2011). Hence, the positive Sr anomaly in the Hainan basalts
4
5 278 was suggested as evidence for the presence of recycled oceanic crust entrained by an
6
7 279 upwelling mantle plume beneath this area (Wang et al., 2011). This explanation is
8
9 280 possible and likely. However, this explanation is not suitable for the volcanic rocks in
10
11 281 the Leizhou Peninsula, as reflected from the distinct correlation trends of Sr/Sr* with
12
13 282 SiO₂, [La/Sm]_N, Nb/U and Zr/Hf between rocks from the Leizhou Peninsula and Hainan
14
15 283 Island (Fig. 8). This is because 1) partial melts from recycled gabbroic oceanic crust
16
17 284 are characterized by both positive Sr anomaly and more silicic composition (Green and
18
19 285 Ringwood, 1968; Wyllie, 1970; Yaxley and Sobolev, 2007). However, the volcanic
20
21 286 rocks from the Leizhou Peninsula show negative correlation between SiO₂ and Sr/Sr*
22
23 287 (Fig. 8a); 2) recycled oceanic crust materials are depleted in incompatible elements with
24
25 288 low [La/Sm]_N (Niu et al., 2002, 2012; Niu and O'Hara, 2003). However, the volcanic
26
27 289 rocks from Jiujiang and Tianyang with higher Sr/Sr* have higher [La/Sm]_N (primitive
28
29 290 mantle normalized) of 2.5-3.3 than the average OIB (~ 2.4; Sun and McDonough, 1989)
30
31 291 (Fig. 7b), reflecting an incompatible element enriched mantle source (Niu and Batiza,
32
33 292 1997). Besides, these samples show Nb/U (38.2-61.3) similar to average OIB (47 ± 10;
34
35 293 Hofmann et al., 1986) and super chondritic Zr/Hf ratios (38.3-43.3; Dupuy et al., 1992;
36
37 294 Niu, 2012) (Figs. 8c & d). As the elements in each ratio pair have similar
38
39 295 incompatibility during mantle melting and magma evolution, these ratios thus largely
40
41 296 reflect the source ratios (Hofmann et al., 1986; Niu and Batiza, 1997). All the above
42
43 297 characteristics suggest that the rocks from the Leizhou Peninsula with a significant
44
45 298 positive Sr anomaly (especially those from Jiujiang & Tianyang) are derived from an
46
47 299 incompatible element enriched mantle source.

56
57 300 The volcanic rocks from Jiujiang and Tianyang show generally depleted Sr-Nd-
58
59 301 Pb-Hf isotope compositions (Fig. 6), indicating their origin from an isotopically

1
2
3 302 depleted asthenospheric mantle. As inferred from MORB, the asthenospheric mantle is
4 303 incompatible element depleted, which is thought to result from continental crust
5 304 extraction in the Earth's early history (Gast, 1968; O'Nions et al., 1979; Allègre et al.,
6 305 1983). However, as inferred above, the mantle source of the Jiujiang and Tianyang
7 306 samples is enriched, not depleted, in incompatible elements. Therefore, there must be a
8 307 process that had re-enriched the incompatible elements in the asthenospheric mantle
9 308 source of these volcanic rocks. Such process must also account for the significant
10 309 positive Sr anomaly observed in these samples because of the positive correlations of
11 310 Sr/Sr* with [La/Sm]_N, Nb/U and Zr/Hf (Fig. 8).

12
13
14
15
16
17
18
19
20
21
22
23
24
25
26 311
27 312 **5.3 Low-F melt metasomatism in the mantle source region**

28
29
30
31 313
32 314 Low-degree (low-F) melt metasomatism enriched in volatiles, alkalis and
33 315 incompatible elements has long been considered significant in forming geochemically
34 316 enriched mantle source (Halliday et al., 1995; Niu et al., 1996, 2002, 2012; Niu and
35 317 O'Hara, 2003; Workman et al., 2004; Tang et al., 2006; Niu, 2005, 2008, 2014; Guo et
36 318 al., 2016; Sun et al., 2017). Such low-F melt may develop within the low velocity zone
37 319 (LVZ) and is inferred to be more enriched in the more incompatible elements (Niu et
38 320 al., 1996, 2002, 2012; Niu and O'Hara, 2003). Furthermore, during ascent through the
39 321 lithosphere, the low-F melt can experience cooling-induced crystallization to form
40 322 metasomatic amphibolite and/or pyroxenite veinlets (Hanson, 1977; Wood, 1979;
41 323 Zanetti et al., 1996; Niu, 2008; Pilet et al., 2008). Indeed, the presence of amphiboles,
42 324 which occurs as interstitial grains in the mantle xenoliths entrained in these volcanic
43 325 rocks indicates the existence of a modal mantle metasomatism (Yu et al., 2006).
44 326 Furthermore, these mantle amphiboles are characterized by enriched incompatible

elements and prominent positive Sr anomaly (Fig. 9; $\text{Sr/Sr}^* = 1.71\text{-}3.96$) (Yu et al., 2006). Although the partition coefficients of Sr/Sr^* ($D_{\text{Sr/Sr}^*} = 2*D_{\text{Sr}}/[D_{\text{Pr}}+D_{\text{Nd}}]$) between amphibole and basaltic melt are experimentally determined to be > 1 ($D_{\text{Sr/Sr}^*} = 1.42$, LaTourrette et al., 1995; also see the compilations in Dalpré and Baker (2000)), crystallization of the low-F melt with $\text{Sr/Sr}^* = 1$ is still inadequate to form amphiboles with Sr/Sr^* of 1.71-3.96. Therefore, it requires the metasomatic low-F melt having $\text{Sr/Sr}^* > 1$ to crystallize the mantle amphiboles with prominent positive Sr anomalies. The volcanic rocks from Jiujiang and Tianyang derived from such low-F melt metasomatized mantle source thus show characteristics of enriched incompatible elements and positive Sr anomalies (Fig. 9).

Because such low-F melt should have high Nd/Sm , U/Pb , Hf/Lu (the element on the numerator is more incompatible than that on the denominator in each ratio pair), it will develop long-time integrated Pb isotopes and unradiogenic Nd and Hf isotopes. However, the samples from Jiujiang and Tianyang with low $^{147}\text{Sm}/^{144}\text{Nd}$ and $^{176}\text{Lu}/^{177}\text{Hf}$ and high $^{238}\text{U}/^{206}\text{Pb}$ have high $^{143}\text{Nd}/^{144}\text{Nd}$ and $^{176}\text{Hf}/^{177}\text{Hf}$ and low $^{206}\text{Pb}/^{204}\text{Pb}$ (Figs. 10b, c, d), which is inconsistent with the characteristics of the low-F melt after long-time decay. Therefore, we support a recent (or “current”) low-F melt metasomatism without enough time for isotope intergrowth, which is consistent with the understanding of the mantle metasomatism beneath eastern China (Niu, 2005, 2014; Guo et al., 2016; Sun et al., 2017, 2018). The positive correlation between $^{87}\text{Rb}/^{86}\text{Sr}$ and $^{87}\text{Sr}/^{86}\text{Sr}$ (Fig. 10a) gives a pseudochron age of 1298 Ma. As the low-F melt metasomatism has been identified to be recent, this age has no geological significance, but is best explained by melting-induced mixing with the pseudochron slope controlled by the compositions of the two endmembers, i.e., a metasomatic low-F melt with relatively low Rb/Sr and depleted Sr isotope composition and another component with

1
2
3 352 high Rb/Sr and enriched Sr isotope composition.
4
5
6 353
7
8 354 **5.4 Recycled UCC material metasomatism in the mantle source region**
9
10 355
11
12 356 The UCC material is characterized by enrichment in LILEs (large ion lithophile
13 elements) and depletion in HFSEs (high field strength elements; e.g. Nb and Ta) with
14 negative Sr and Eu anomalies, higher Pb/Ce than MORB and OIB and enriched Sr-Pb-
15 Nd-Hf isotopes (Hofmann et al., 1986; Rudnick and Gao, 2003; Jackson et al., 2007;
16 Niu and O'Hara, 2009). Therefore, contribution of the UCC material to the
17 asthenospheric mantle or the mantle-derived melt will decrease the HFSE/LILE ratios
18 (e.g. [Nb/Th]_N and [Ta/U]_N), Sr/Sr*, Eu/Eu*, ¹⁴³Nd/¹⁴⁴Nd and ¹⁷⁶Hf/¹⁷⁷Hf, but increase
19 Pb/Ce, ⁸⁷Sr/⁸⁶Sr and ²⁰⁶Pb/²⁰⁴Pb in the melt. The Huoju samples have low [Nb/Th]_N,
20 [Ta/U]_N, Sr/Sr* and Eu/Eu* (Fig. 5) and positive Pb anomaly (Fig. 4) with more
21 enriched Sr-Nd-Pb-Hf isotopes (Fig. 6), which shows apparent crustal signatures.
22 Furthermore, Sr-Pb-Nd-Hf isotope ratios show scattered yet significant correlations
23 with [Nb/Th]_N, [Ta/U]_N, Sr/Sr* and Pb/Ce (See Supplementary Figure 1). With Sr-Pb-
24 Nd-Hf isotopes being more enriched, [Nb/Th]_N, [Ta/U]_N and Sr/Sr* decrease while
25 Pb/Ce increasing, which is most consistent with variable extent of incorporation of
26 UCC material in the volcanic rocks in the Leizhou Peninsula.
27
28 371 As we have discussed above, such crustal signatures in these rocks cannot be
29 attributed to the crustal contamination during melt ascent, and thus they must be
30 inherited from the recycled UCC materials in the mantle source region. The UCC
31 material present in the mantle source region was most likely originated from subducted
32 terrigenous sediments. In Figs. 6c & d, the Pb isotope systematics indeed show trends
33 from a CIR (Central Indian Ridge; Mahoney et al., 1989) MORB mantle component to
34

35
36 372
37 373
38 374
39 375
40 376
41
42
43
44
45
46
47
48
49
50
51
52
53
54
55
56
57
58
59
60

1
2
3 377 a Java terrigenous sediment component ([Plank and Langmuir, 1998](#)). The above
4 inference confirms our previous interpretations that recycled UCC material must have
5 added to the mantle source region of the Cenozoic basalts in Southeast China ([Sun et](#)
6 [al., 2017](#)). The Huoju samples with more enriched Sr-Nd-Pb-Hf isotopes, higher Pb/Ce
7 and lower [Nb/Th]_N, [Ta/U]_N and Sr/Sr^{*} must have higher contributions of recycled
8 UCC materials in the mantle source region.
9
10
11
12
13
14
15
16

17 383 Because clinopyroxene is an important host for incompatible elements in mantle
18 minerals, its elemental and isotopic characteristics have been widely used to study the
19 nature and intensity of the metasomatic event (e.g., [Norman, 1998](#); [Xu et al., 2003](#); [Niu,](#)
20 [2004](#); [Zheng et al., 2006](#); [Tang et al., 2008](#); [Wittig et al., 2009, 2010](#)). Studies on the
21 clinopyroxenes in the mantle xenoliths entrained in the Cenozoic volcanic rocks from
22 the Leizhou peninsula show that some clinopyroxenes have high Pb/Ce with relatively
23 low Sr/Sr^{*} ([Fig. 9; Yu et al., 2006](#)), which is consistent with trace element characteristics
24 of the volcanic rocks from Huoju region and Hainan Island and UCC materials. This
25 further substantiates the existence of recycled UCC material in the mantle source region
26 beneath the Leizhou Peninsula and Hainan Island ([Tu et al., 1991](#)).
27
28
29
30
31
32
33
34
35
36
37
38
39
40
41
42
43
44
45
46
47
48
49
50
51
52
53
54
55
56
57
58
59
60

403 The recycling of UCC material into the asthenospheric mantle must be recent,
404 because 1) ancient (e.g. > 1 Ga) recycled UCC materials with low U/Pb and Th/Pb
405 ratios should have unradiogenic Pb isotope ratios ([Stracke et al., 2003](#)), which is in
406 contrast with the radiogenic Pb isotopes of the Huoju samples; 2) The high angle Pb
407 isotope trend away from the NHRL ([Fig. 6c](#)) that is often observed in volcanic arc
408 magmas (e.g., [Cohen and O’Nions, 1982](#); [Woodhead and Fraster, 1985](#); [Vroon et al.,](#)
409 [1993](#)) is more consistent with a recent recycling of UCC material ([Hart, 1984](#); [Tu, 1991](#)).
410 Trace element modelling shows that ~ 6-10% UCC materials were mixed in the first
411 place with the depleted MORB mantle (DMM) materials. Such UCC material modified

1
2
3 402 mantle source was then mixed by variable extents with the metasomatic low-F melt to
4 403 form the ultimate mantle source of the volcanic rocks in the Leizhou Peninsula ([Fig.](#)
5 404 [11](#)). Subduction of the Pacific plate in the Mesozoic along the present SE China
6 405 coastline prior to opening of the South China Sea may have contributed this recycled
7 406 UCC material as terrigenous sediment into the asthenospheric mantle beneath the
8 407 Leizhou Peninsula ([Fig. 12a; Tu et al., 1991](#)). After the opening of the South China Sea,
9 408 the tectonic setting of the Leizhou Peninsula changed from a subduction zone
10 409 environment to an intraplate environment. The metasomatic agent in the asthenospheric
11 410 mantle beneath the Leizhou Peninsula changed from recycled UCC material to a low-
12 411 F melt derived within the asthenospheric mantle. Such low-F melt is enriched in
13 412 incompatible elements and volatiles, which is buoyant and tends to ascend to
14 413 metasomatize the overlying asthenospheric mantle and the base of the lithosphere ([Fig.](#)
15 414 [12b](#)). The above inference may not be exact, but effectively captures the mantle
16 415 evolution beneath the Leizhou Peninsula in space and time.
17
18
19
20
21
22
23
24
25
26
27
28
29
30
31
32
33
34
35
36
37
38 416
39
40 417 **6. Conclusion**
41
42
43 418
44
45
46
47
48
49
50
51
52
53
54
55
56
57
58
59
60

- 1 419 1) The volcanic rocks in the Leizhou Peninsula show varying elemental and isotopic
2 420 characteristics. The samples from Jiujiang and Tianyang show significant
3 421 primitive-mantle-normalized positive Nb, Ta and Sr anomalies with depleted Sr-
4 422 Nd-Pb-Hf isotope compositions, while some samples from Huoju show significant
5 423 negative Nb and Ta anomalies, positive Pb anomaly and more enriched Sr-Nd-Pb-
6 424 Hf isotope compositions.
- 7 425 2) The positive Sr anomaly in the samples from Jiujiang and Tianyang is not evidence
8 426 for the presence of recycled oceanic gabbro in the mantle source, but is consistent

1
2
3 427 with the incompatible element enrichment of the mantle source materials.
4
5 428 3) A low-F melt mantle metasomatism which is enriched in volatiles and incompatible
6 elements is required to explain the incompatible element enrichment and positive
7
8 429 Sr anomaly in these volcanic rocks. Such mantle metasomatism must take place
9 recently to account for lacking isotope ingrowth in the mantle source regions.
10
11 430
12 431
13
14 432 4) Presence of recycled UCC material in the mantle source region is also required to
15
16 explain the trace element and isotope characteristics of the volcanic rocks from
17
18 433 Huoju. These UCC material, in the form of terrigenous sediments, may be
19
20 434 subducted recently into the upper mantle.
21
22
23
24
25
26 435
27
28 436
29
30 437 **Acknowledgement**
31
32
33 438
34
35 439 We are grateful to the constructive comments of two anonymous reviewers. This
36
37 work was supported by the NSFC-Shandong Joint Fund for Marine Science Research
38
39 440 Centers (U1606401), the National Natural Science Foundation of China (NSFC
40
41 Grants 41776067, 41630968, 41130314, 91014003), Chinese Academy of Sciences
42
43 (Innovation Grant Y42217101L), and grants from Qingdao National Laboratory for
44
45 Marine Science and Technology (2015ASKJ03) and 111 Project (B18048).
46
47
48 446 **References**
49
50
51
52 447
53
54 448 Allègre C. J., Hart S. R. and Minster J. F. (1983) Chemical structure and evolution of
55
56 the mantle and continents determined by inversion of Nd and Sr isotopic data, I.
57
58 449 Theoretical methods. *Earth Planet. Sci. Lett.* **66**, 177–190.
59
60 450
451 Briais A., Patriat P. and Tapponnier P. (1993) Updated interpretation of magnetic

- 1
2
3
4 452 anomalies and seafloor spreading stages in the South China Sea: Implications for
5
6 453 the Tertiary tectonics of Southeast Asia. *J. Geophys. Res.* **98**, 6299–6328.
7
8
9 454 Chauvel C., Hofmann A. W. and Vidal P. (1992) HIMU-EM: the French Polynesian
10
11 455 connection. *Earth Planet. Sci. Lett.* **110**, 99-119.
12
13
14 456 Chen L.-H., Zeng G., Jiang S.-Y., Hofmann A. W., Xu X.-S., and Pan M.-B. (2009)
15
16 457 Sources of Anfengshan basalts: Subducted lower crust in the Sulu UHP belt, China:
17
18 458 *Earth Planet. Sci. Lett.* **286**, 426-435.
19
20
21
22 459 Chen S., Wang X.H., Niu Y.L., Sun P., Duan M., Xiao Y.Y., Guo P.Y., Gong H.M.,
23
24 460 Wang G.D., Xue Q.Q. (2017) Simple and cost-effective methods for precise
25
26 461 analysis of trace element abundances in geological materials with ICP-MS. *Sci.*
27
28 462 *Bull.* **62**, 277-289.
29
30
31
32 463 Chung S.-L., Sun S.-s., Tu K., Chen C.-H. and Lee C.-y. (1994) Late Cenozoic basaltic
33
34 464 volcanism around the Taiwan Strait, SE China: product of lithosphere-
35
36 465 asthenosphere interaction during continental extension. *Chem. Geol.* **112**, 1-20.
37
38
39
40 466 Cohen R. and O'Nions R. (1982) Identification of recycled continental material in the
41
42 467 mantle from Sr, Nd and Pb isotope investigations. *Earth Planet. Sci. Lett.* **61**, 73-
43
44 468 84.
45
46
47
48 469 Dalpé C. and Baker D. R. (2000) Experimental investigation of large-ion-lithophile-
49
50 470 element, high-field-strength-element and rare-earth-element partitioning between
51
52 471 calcic amphibole and basaltic melt: the effects of pressure and oxygen fugacity.
53
54 472 *Contrib. Mineral. Petrol.* **140**, 233-250.
55
56
57 473 Dupuy C., Liotard J. and Dostal J. (1992) Zr/Hf fractionation in intraplate basaltic
58
59
60

- 1
2
3
4 474 rocks: carbonate metasomatism in the mantle source. *Geochim. Cosmochim. Acta*
5
6 475 **56**, 2417-2423.
7
8
9 476 Ekström G. and Dziewonski A. M. (1998) The unique anisotropy of the Pacific upper
10
11 477 mantle. *Nature* **394**, 168.
12
13
14 478 Farley K. (1995) Rapid cycling of subducted sediments into the Samoan mantle plume.
15
16
17 479 *Geology* **23**, 531-534.
18
19
20 480 Flower M. F., Zhang M., Chen C., Tu K. and Xie G. (1992) Magmatism in the south
21
22 481 China basin: 2. Post-spreading Quaternary basalts from Hainan Island, south China.
23
24
25 482 *Chem. Geol.* **97**(1), 65-87.
26
27
28 483 Gast P. W. (1968) Trace element fractionation and the origin of tholeiitic and alkaline
29
30 484 magma types, *Geochim. Cosmochim. Acta* **32**, 1055 – 1086.
31
32
33 485 Green T. H. and Ringwood A. E. (1968) Genesis of the calc-alkaline igneous rock suite,
34
35 486 *Contrib. Mineral. Petrol.* **18**, 105-162.
36
37
38 487 Guo P., Niu Y., Sun P., Ye L., Liu J., Zhang Y., Feng Y. X. and Zhao J. X. (2016) The
39
40 488 origin of Cenozoic basalts from central Inner Mongolia, East China: The
41
42 489 consequence of recent mantle metasomatism genetically associated with
43
44 490 seismically observed paleo-Pacific slab in the mantle transition zone. *Lithos* **240**-
45
46
47 491 **243**, 104-118.
48
49
50
51 492 Halliday A. N., Lee D.-C., Tommasini S., Davies G. R., Paslick C. R., Fitton J. G. and
52
53 493 James D. E. (1995) Incompatible trace elements in OIB and MORB and source
54
55 494 enrichment in the sub-oceanic mantle. *Earth Planet. Sci. Lett.* **133**, 379-395.
56
57
58 495 Hanson G. N. (1977) Geochemical evolution of the suboceanic mantle. *J. Geol. Soc.*
59
60

- 1
2
3
4 496 134(2), 235-253.
5
6 497 Hart S. R. (1984) A large-scale isotope anomaly in the Southern Hemisphere mantle.
7
8 498 *Nature* **309**, 753-757.
9
10 499 Hart S. R. (1988) Heterogeneous mantle domains: signatures, genesis and mixing
11
12 500 chronologies. *Earth Planet. Sci. Lett.* **90**, 273-296.
13
14
15
16
17 501 Ho K., Chen J. and Juang W. (2000) Geochronology and geochemistry of late Cenozoic
18
19 basalts from the Leiqiong area, southern China. *J. Asian Earth Sci.* **18**(3), 307-324.
20
21
22 503 Hoang N., Flower M. F. J. and Carlson R. W. (1996) Major, trace element, and isotopic
23
24 compositions of Vietnamese basalts: Interaction of hydrous EM1-rich
25
26 asthenosphere with thinned Eurasian lithosphere. *Geochim. Cosmochim. Acta* **60**,
27
28
29 506 4329-4351.
30
31
32 507 Hoang N. and Flower M. (1998) Petrogenesis of Cenozoic Basalts from Vietnam:
33
34
35 Implication for Origins of a 'Diffuse Igneous Province'. *J. Petrol.* **39**(3), 369-395.
36
37
38 509 Huang X.-L., Xu Y.-G., Lo C.-H. Wang R.-C. and Lin C.-Y. (2007) Exsolution lamellae
39
40 in a clinopyroxene megacryst aggregate from Cenozoic basalt, Leizhou Peninsula,
41
42
43 511 South China: petrography and chemical evolution. *Contrib. Mineral. Petrol.* **154**,
44
45
46 512 691-705.
47
48
49 513 Huang X.-L., Niu Y., Xu Y.-G., Ma J.-L., Qiu H.-N. and Zhong, J.-W. (2013)
50
51
52
53
54
55
56
57
58
59
60 514 Geochronology and geochemistry of Cenozoic basalts from eastern Guangdong, SE
China: constraints on the lithosphere evolution beneath the northern margin of the
South China Sea. *Contrib. Mineral. Petrol.* **165**, 437-455.
517 Hofmann A. W. and White W. M. (1982) Mantle plumes from ancient oceanic crust.

- 1
2
3
4 518 *Earth Planet. Sci. Lett.* **57**, 421-436.
5
6 519 Hofmann A., Jochum K., Seufert M. and White W. (1986) Nb and Pb in oceanic basalts:
7
8 520 new constraints on mantle evolution. *Earth Planet. Sci. Lett.* **79**, 33-45.
9
10 521 Jackson M. G., Hart S. R., Koppers A. A. P., Staudigel H., Konter J., Blusztajn J., Kurz
11
12 522 M. and Russel J. A. (2007) The return of subducted continental crust in Samoan
13
14 523 lavas. *Nature* **448**(7154), 684-687.
15
16
17 524 Jahn B. M., Zhou X. H. and Li J. L. (1990) Formation and tectonic evolution of
18
19 525 southeast China: isotopic and geochemical constraints. *Tectonophysics* **183**, 145-
20
21 526 160.
22
23
24 527 Johnson M. C. and Plank T. (2000) Dehydration and melting experiments constrain the
25
26 528 fate of subducted sediments. *Geochem. Geophys. Geosyst.* **1**(12).
27
28
29 529 Kido Y., Suyehiro K. and Kinoshita H. (2001) Rifting to spreading process along the
30
31 530 northern continental margin of the South China Sea. *Marine Geophysical
32 Research* **22**(1), 1-15.
33
34
35 532 LaTourrette T., Hervig R. L. and Holloway J. R. (1995) Trace element partitioning
36
37 533 between amphibole, phlogopite, and basanite melt. *Earth Planet. Sci. Lett.* **135**, 13-
38
39 534 30.
40
41
42 535 Lebedev S. and Nolet G. (2003) Upper mantle beneath Southeast Asia from S velocity
43
44 536 tomography. *J. Geophys. Res.* **108**, 2048.
45
46
47 537 Lei J., Zhao D., Steinberger B., Wu B., Shen F. and Li Z. (2009) New seismic
48
49 538 constraints on the upper mantle structure of the Hainan plume. *Phys. Earth Planet
50 In.* **173**, 33-50.
51
52
53
54
55
56
57
58
59
60

- 1
2
3
4 540 Li Z. X., Li X. H., Chung S. L., Lo C., Xu X. and Li W. (2012) Magmatic switch-on and
5
6 switch-off along South China continental margin since the Permian: transition from
7
8 an Andean-type to a western Pacific type. *Tectonophysics* **523–535**, 271–290.
9
10
11 543 Lin J. L., Fuller M. and Zhang W. Y. (1985) Preliminary Phanerozoic polar wander
12
13 paths for the North and South China blocks. *Nature* **313**, 444-449.
14
15
16 545 Liu J. Q., Ren Z-Y., Nichols A., Song M., Qian S., Zhang Y. and Zhao P. (2015)
17
18 Petrogenesis of Late Cenozoic Basalts from North Hainan Island: Constraints from
19
20 Melt Inclusions and Their Host Olivines. *Geochim. Cosmochim. Acta.* **152**, 89–121.
21
22
23 547 Mahoney J., Natland J., White W., Poreda R., Bloomer S., Fisher R. and Baxter A.
24
25
26
27 (1989) Isotopic and geochemical provinces of the western Indian Ocean spreading
28 centers. *J. Geophys. Res.* **94**, 4033-4052.
29
30
31 551 Metcalfe I. (1990) Allochthonous terrane processes in Southeast Asia. *Philos. Trans. R. Soc. London* **331**, 625-640.
32
33
34
35
36
37 553 Niu Y. (2004). Bulk-rock major and trace element compositions of abyssal peridotites:
38
39 implications for mantle melting, melt extraction and post-melting processes beneath
40
41 mid-ocean ridges. *J. Petrol.* **45**(12), 2423-2458.
42
43
44
45 556 Niu Y. (2005) Generation and evolution of basaltic magmas: some basic concepts and
46
47 a new view on the origin of Mesozoic–Cenozoic basaltic volcanism in eastern
48
49
50 558 China. *Geological Journal of China Universities* **11**, 9-46.
51
52
53
54 559 Niu Y. (2008) The origin of alkaline lavas. *Science* **320**, 883-884.
55
56
57 560 Niu, Y. (2012). Earth processes cause Zr–Hf and Nb–Ta fractionations, but why and
58 how? *RSC Advances* **2**, 3587-3591.
59
60

- 1
2
3
4 562 Niu Y. (2014) Geological understanding of plate tectonics: Basic concepts, illustrations,
5
6 563 examples and new perspectives. *Global Tectonics and Metallogeny* **10**, 23-46.
7
8
9 564 Niu Y. and Batiza R. (1997) Trace element evidence from seamounts for recycled
10
11 565 oceanic crust in the Eastern Pacific mantle. *Earth Planet. Sci. Lett.* **148**, 471-483.
12
13
14 566 Niu Y. and O'Hara M. J. (2003) Origin of ocean island basalts: A new perspective from
15
16 567 petrology, geochemistry, and mineral physics considerations. *J. Geophys. Res.* **108**,
17
18 568 2209.
19
20
21
22 569 Niu Y. and O'Hara M. J. (2009) MORB mantle hosts the missing Eu (Sr, Nb, Ta and
23
24 570 Ti) in the continental crust: new perspectives on crustal growth, crust-mantle
25
26 571 differentiation and chemical structure of oceanic upper mantle. *Lithos* **112**, 1-17.
27
28
29
30 572 Niu Y., Waggoner D. G., Sinton J. M. and Mahoney J. J. (1996) Mantle source
31
32 573 heterogeneity and melting processes beneath seafloor spreading centers, the East
33
34 574 Pacific Rise, 18–19 S. *J. Geophys. Res.* **101**, 27711-27733.
35
36
37
38 575 Niu Y., Collerson K. D., Batiza R., Wendt J. I. and Regelous M. (1999) Origin of
39
40 576 enriched-type mid-ocean ridge basalt at ridges far from mantle plumes: The East
41
42 577 Pacific Rise at 11° 20' N. *J. Geophys. Res.* **104**(B4), 7067-7087.
43
44
45
46 578 Niu Y., Regelous M., Wendt I. J., Batiza R. and O'Hara. (2002) Geochemistry of near-
47
48 579 EPR seamounts: importance of source vs. process and the origin of enriched mantle
49
50 580 component. *Earth Planet. Sci. Lett.* **199**, 327-345.
51
52
53
54 581 Niu Y., Wilson M., Humphreys E. R. and O'Hara M. J. (2012) A trace element
55
56 582 perspective on the source of ocean island basalts (OIB) and fate of subducted ocean
57
58 583 crust (SOC) and mantle lithosphere (SML). *Episodes* **35**, 310.

- 1
2
3
4 584 Niu Y., Liu Y., Xue Q., Shao F., Chen S., Duan M., Guo P., Gong H., Hu Y., Hu Z.,
5
6 585 Kong J., Li J., Liu J., Sun P., Sun W., Ye L., Xiao Y. and Zhang Y. (2015) Exotic
7
8 586 origin of the Chinese continental shelf: new insights into the tectonic evolution of
9
10 the western Pacific and eastern China since the Mesozoic. *Sci. Bull.* **60**, 1598-1616.
11
12 587 Norman M. D. (1998) Melting and metasomatism in the continental lithosphere: laser
13
14 588 ablation ICPMS analysis of minerals in spinel lherzolites from eastern Australia.
15
16 589 *Contrib. Mineral. Petrol.* **130**, 240-255.
17
18
19 590 O'Nions R. K., Evensen N. M. and Hamilton P. J. (1979) Geochemical modeling of
20
21 mantle differentiation and crustal growth. *J. Geophys. Res.* **84**, 6091–6101.
22
23 591 Pilet S., Baker M. B. and Stolper E. M. (2008) Metasomatized lithosphere and the origin
24
25 592 of alkaline lavas. *Science* **320**, 916-919.
26
27
28 593 Pin C., Gannoun A. and Dupont A. (2014) Rapid, simultaneous separation of Sr, Pb,
29
30 594 and Nd by extraction chromatography prior to isotope ratios determination by TIMS
31
32 595 and MC-ICP-MS. *Journal of Analytical Atomic Spectrometry* **29**, 1858-1870.
33
34
35 596 Plank T. and Langmuir C. H. (1998) The chemical composition of subducting sediment
36
37 597 and its consequences for the crust and mantle. *Chem. Geol.* **145**, 325-394.
38
39
40 598 Rudnick R. L. and Gao S. (2003) Composition of the continental crust. *Treatise on*
41
42 599
43
44 600 *geochemistry* **3**, 1-64.
45
46
47 601 Salters V.J. and Stracke, A. (2004) Composition of the depleted mantle. *Geochem.*
48
49 602
50
51 603 *Geophys. Geosyst.* **5**.
52
53
54 604 Sobolev A. V., Hofmann A. W. and Nikogosian I. K. (2000) Recycled oceanic crust
55
56 605 observed in ‘ghost plagioclase’within the source of Mauna Loa lavas. *Nature* **404**,

- 1
2
3
4 606 986-990.
5
6 607 Song S., Su L., Li X., Zhang G., Niu Y. and Zhang L. (2010) Tracing the 850-Ma
7 continental flood basalts from a piece of subducted continental crust in the North
8
9 608 Qaidam UHPM belt, NW China. *Precam. Res.* **183**, 805-816.
10
11 609
12
13 610 Stracke A., Bizimis M. and Salters V. J. (2003) Recycling oceanic crust: quantitative
14 constraints. *Geochem. Geophys. Geosyst.* **4**.
15
16 611
17
18 612 Stroncik N. A. and Devey C. W. (2011) Recycled gabbro signature in hotspot magmas
19 unveiled by plume–ridge interactions. *Nature Geoscience* **4**, 393.
20
21 613
22
23 614 Sun S. and McDonough W. F. (1989) Chemical and isotopic systematics of oceanic
24 basalts: implications for mantle composition and processes. *Geological Society,*
25
26 615
27
28 616 *London, Special Publications* **42**, 313-345.
29
30
31 617 Sun P., Niu Y., Guo P., Ye L., Liu J. and Feng Y. (2017) Elemental and Sr–Nd–Pb
32 isotope geochemistry of the Cenozoic basalts in Southeast China: Insights into their
33
34 618 mantle sources and melting processes. *Lithos* **272–273**, 16-30.
35
36
37 619
38
39 620 Sun P., Niu Y., Guo P., Cui H., Ye L. and Liu J. (2018) The evolution and ascent paths
40 of mantle xenolith-bearing magma. Observations and insights from Cenozoic
41
42 621 basalts in Southeast China. *Lithos* **310–311**, 171-181.
43
44
45 622
46
47 623 Tang Y.J., Zhang H.F. and Ying J.F. (2006) Asthenosphere-lithospheric mantle
48 interaction in an extensional regime: Implication from the geochemistry of
49
50 624 Cenozoic basalts from Taihang Mountains, North China Craton. *Chem. Geol.* **233**,
51
52 625
53
54 626 309-327.
55
56
57 627 Tang Y.J., Zhang H.F., Ying J.F., Zhang J. and Liu X.M. (2008) Refertilization of
58
59
60

- 1
2
3
4 628 ancient lithospheric mantle beneath the central North China Craton: Evidence from
5
6 629 petrology and geochemistry of peridotite xenoliths. *Lithos* **101**, 435-452.
7
8
9 630 Taylor B. and Hayes D. E. (1983) Origin and history of the South China Sea basin. In:
10
11 631 Dennis E, Hayes D E, eds. The Tectonic and Geologic Evolution of South Eastern
12
13 632 Asian seas and islands. *AGU Geophys Monogr*, 23–56.
14
15
16
17 633 Trail D., Watson E. B. and Tailby N. D. (2012) Ce and Eu anomalies in zircon as
18
19 proxies for the oxidation state of magmas. *Geochim. Cosmochim. Acta* **97**, 70-87.
20
21
22 635 Tu K., Flower M. F., Carlson R. W., Zhang M. and Xie G. (1991) Sr, Nd, and Pb
23
24 636 isotopic compositions of Hainan basalts (south China): implications for a
25
26 637 subcontinental lithosphere Dupal source. *Geology* **19**, 567-569.
27
28
29
30 638 Tu K., Flower M. F., Carlson R. W., Xie G., Chen C. and Zhang M. (1992) Magmatism
31
32 639 in the South China Basin. *Chem. Geol.* **97**(1), 47-63.
33
34
35 640 Vervoort J. D., Patchett P. J., Blichert-Toft J. and Albarède F. (1999) Relationships
36
37 641 between Lu–Hf and Sm–Nd isotopic systems in the global sedimentary system.
38
39
40 642 *Earth Planet. Sci. Lett.* **168**, 79-99.
41
42
43 643 Vroon P., Bergen M. V., White W. and Varekamp J. (1993) Sr-Nd-Pb isotope
44
45 644 systematics of the Banda Arc, Indonesia: Combined subduction and assimilation of
46
47 645 continental material. *J.Geophys. Res.* **98**, 22349-22366.
48
49
50 646 Wang X., Li Z., Li X., Li J., Liu Y., Long W., Zhou J. and Wang F. (2011) Temperature,
51
52 647 pressure, and composition of the mantle source region of Late Cenozoic basalts in
53
54 648 Hainan Island, SE Asia: a consequence of a young thermal mantle plume close to
55
56 649 subduction zones? *J. Petrol.* **53**, 177-233.
57
58
59
60

- 1
2
3
4 650 Wang X., Li Z., Li X., Li J., Xu. Y. and Li X. (2013) Identification of an ancient mantle
5 reservoir and young recycled materials in the source region of a young mantle
6 plume: Implications for potential linkages between plume and plate tectonics. *Earth*
7
8 652 *Planet. Sci. Lett.* **377**, 248–259.
9
10 653
11
12 654 Weaver B. L. (1991) The origin of ocean island basalt end-member compositions: trace
13 element and isotopic constraints. *Earth Planet. Sci. Lett.* **104**, 381-397.
14
15 655
16
17 656 Willbold M. and Stracke A. (2006) Trace element composition of mantle end-members:
18
19 657 Implications for recycling of oceanic and upper and lower continental crust.
20
21 658 *Geochem. Geophys. Geosyst.* **7**.
22
23
24 659 Wittig N., Pearson D. G., Downes H. and Baker J. A. (2009) The U, Th and Pb
25 elemental and isotope compositions of mantle clinopyroxenes and their grain
26 boundary contamination derived from leaching and digestion experiments.
27
28 660
29 661
30 662 *Geochim. Cosmochim. Acta* **73**, 469-488.
31
32
33
34
35
36
37
38 663 Wittig N., Pearson D. G., Duggen S., Baker J. A. and Hoernle K. (2010) Tracing the
39 metasomatic and magmatic evolution of continental mantle roots with Sr, Nd, Hf
40
41 664 and and Pb isotopes: A case study of Middle Atlas (Morocco) peridotite xenoliths.
42
43 665
44
45 666 *Geochim. Cosmochim. Acta* **74**, 1417-1435.
46
47
48 667 Wood D. A. (1979) A variably veined suboceanic upper mantle—Genetic significance
49
50 668 for mid-ocean ridge basalts from geochemical evidence. *Geology* **7**, 499-503.
51
52
53 669 Woodhead J. D. and Fraser D. G. (1985) Pb, Sr and 10Be isotopic studies of volcanic
54
55 rocks from the Northern Mariana Islands. Implications for magma genesis and
56
57 670 crustal recycling in the Western Pacific. *Geochim. Cosmochim. Acta* **49**, 1925-1930.
58
59
60

- 1
2
3
4 672 Workman R. K., Hart S. R., Jackson M., Regelous M., Farley K. A., Blusztajn J., Kurz
5
6 673 M. and Staudigel H. (2004) Recycled metasomatized lithosphere as the origin of
7
8 674 the Enriched Mantle II (EM2) end-member: Evidence from the Samoan Volcanic
9
10 675 Chain. *Geochem. Geophys. Geosyst.* **5**.
11
12 676 Wyllie P. J. (1970) Ultramafic rocks and upper mantle, *Mineral. Soc. Am. Spec. Pap.*
13
14 677 **3**, 3-32.
15
16
17 678 Xu X., O'Reilly S. Y., Griffin W. and Zhou X. (2003) Enrichment of upper mantle
18
19 679 peridotite: petrological, trace element and isotopic evidence in xenoliths from SE
20
21 680 China. *Chem. Geol.* **198**, 163-188.
22
23
24
25
26
27 681 Xu Y., Sun M., Yan W., Liu Y., Huang X. and Chen X. (2002) Xenolith evidence for
28
29 682 polybaric melting and stratification of the upper mantle beneath South China. *J.*
30
31 683 *Asian Earth Sci.* **20**, 937-954.
32
33
34
35 684 Yaxley G. M. and Sobolev A. V. (2007) High-pressure partial melting of gabbro and
36
37 685 its role in the Hawaiian magma source. *Contrib. Mineral. Petrol.* **154**, 371-383.
38
39
40 686 Yan P., Deng H., Liu H., Zhang Z. and Jiang Y. (2006) The temporal and spatial
41
42 687 distribution of volcanism in the South China Sea region. *J. Asian Earth Sci.* **27**(5),
43
44 688 647-659.
45
46
47
48 689 Yan Q. and Shi X. (2007) Hainan mantle plume and the formation and evolution of the
49
50 690 South China Sea. *Geological Journal of China Universities* **13**, 311-322.
51
52
53 691 Yan Q., Shi X., Wang K., Bu W. and Xiao L. (2008) Major element, trace element, and
54
55 692 Sr, Nd and Pb isotope studies of Cenozoic basalts from the South China Sea.
56
57
58 693 *Science in China Series D: Earth Sciences* **51**, 550-566.
59
60

- 1
2
3
4 694 Yan Q., Castillo P., Shi X., Wang L., Liao L. and Ren J. (2015) Geochemistry and
5 petrogenesis of volcanic rocks from Daimao Seamount (South China Sea) and their
6 tectonic implications. *Lithos* **218**, 117-126.
7
8
9
10
11 697 Yang Y., Zhang H., Chu Z., Xie L. and Wu F. (2010) Combined chemical separation
12 of Lu, Hf, Rb, Sr, Sm and Nd from a single rock digest and precise and accurate
13 isotope determinations of Lu–Hf, Rb–Sr and Sm–Nd isotope systems using Multi-
14 Collector ICP-MS and TIMS. *Int. J. Mass Spectrom.* **290**, 120-126.
15
16
17
18
19
20 701 Yu J., O'Reilly S. Y., Zhang M., Griffin W. and Xu X. (2006) Roles of melting and
21 metasomatism in the formation of the lithospheric mantle beneath the Leizhou
22 Peninsula, South China. *J. Petrol.* **47**, 355-383.
23
24
25
26
27
28 704 Zanetti A., Vannucci R., Bottazzi P., Oberti R. and Ottolini L. (1996) Infiltration
29 metasomatism at Lherz as monitored by systematic ion-microprobe investigations
30 close to a hornblendite vein. *Chem. Geol.* **134**(1), 113-133.
31
32
33
34
35
36
37
38 707 Zeng G., Chen L.-H., Hu S.-L., Xu X.-S., and Yang L.-F. (2013) Genesis of Cenozoic
39 low-Ca alkaline basalts in the Nanjing basaltic field, eastern China: The case for
40 mantle xenolith-magma interaction: *Geochem. Geophys. Geosyst.* **14**, 1660-1677.
41
42
43
44
45
46 710 Zhang M., Tu K., Xie G., and Flower M. F. (1996) Subduction-modified subcontinental
47 mantle in South China: Trace element and isotope evidence in basalts from Hainan
48 Island. *Chinese Journal of Geochemistry* **15**(1), 1-19.
49
50
51
52
53
54 713 Zhao D. (2004) Global tomographic images of mantle plumes and subducting slabs:
55 insight into deep Earth dynamics. *Phys. Earth Planet In.* **146**, 3-34.
56
57
58
59
60 715 Zheng J., Griffin W. L., O'Reilly S. Y., Yang J., Li T., Zhang M., Zhang R. Y. and Liou

- 1
2
3
4 716 J. G. (2006) Mineral chemistry of peridotites from Paleozoic, Mesozoic and
5
6 717 Cenozoic lithosphere: constraints on mantle evolution beneath eastern China. *J.*
7
8 718 *Petrol.* **47**, 2233-2256.
9
10
11 719 Zindler A. and Hart S. (1986) Chemical geodynamics. *Annual review of earth and*
12
13 720 *planetary sciences* **14**, 493-571.
14
15
16 721 Zhou X. M. and Li W. X. (2000) Origin of Late Mesozoic igneous rocks of southeastern
17
18 722 China: implications for lithosphere subduction and underplating of mafic magma.
19
20
21 723 *Tectonophysics* **326**, 269–287.
22
23
24 724 Zou H., Zindler A., Xu X. and Qi Q. (2000) Major, trace element, and Nd, Sr and Pb
25
26 725 isotope studies of Cenozoic basalts in SE China: mantle sources, regional variations,
27
28 726 and tectonic significance. *Chem. Geol.* **171**, 33-47.
29
30
31 727 Zou H. and Fan Q. (2010) U-Th isotopes in Hainan basalts: Implications for sub-
32
33 728 asthenospheric origin of EM2 mantle endmember and the dynamics of melting
34
35 729 beneath Hainan Island. *Lithos* **116**(1), 145-152.
36
37
38
39
40
41
42 730
43 731 **Figure captions**
44
45 732 **Fig. 1.** (a) Distribution of the Cenozoic intraplate volcanism in Southeast Asia (after
46
47 733 Wang et al. (2011)). (b) Distribution of the Cenozoic intraplate volcanism in the
48
49 734 Leizhou Peninsula and Hainan Island and sampling locations of the late Cenozoic
50
51 735 volcanic rocks in the Leizhou Peninsula.
52
53
54
55
56 736
57
58 737 **Fig. 2.** (a) Layered structures of the volcanic lavas in the Leizhou Peninsula. (b) Porous
59
60 738 and ropy structures at the surface of lava layers. (c-d) Photomicrographs showing

1
2
3 739 intergranular textures, with phenocrysts and microlites of olivine, clinopyroxene and
4 740 magnetite aggregated between euhedral plagioclase laths.
5
6
7 741
8
9
10 742 **Fig. 3.** TAS diagram (a) and selected Mg[#] variation diagrams (b-h). These volcanic
11 rocks have experienced varying extent of fractional crystallization with the liquidus
12 minerals dominated by olivine and clinopyroxene. The volcanic rocks from Huoju are
13 more evolved with higher SiO₂ and lower Mg[#] than those from Jiujiang and Tianyang.
14
15 744 For comparison, the compiled major element compositions and Cr and Ni contents of
16 Cenozoic basaltic rocks from the Hainan Island are also plotted (Tu et al., 1991; Flower
17 et al., 1992; Zou and Fan, 2010; Ho et al., 2000; Wang et al., 2011).
18
19 745
20
21 746
22
23 747
24
25 748
26
27 749
28
29 750 **Fig. 4.** (a) Chondrite-normalized REE patterns of the volcanic rocks from the Leizhou
30 Peninsula. (b) Primitive mantle-normalized multiple incompatible element abundances
31 of these rocks. For comparison, average compositions of present-day OIB (Sun and
32 McDonough, 1989) and upper continental crust (UCC) (Rudnick and Gao, 2003) are
33 plotted. The sample ZC11-02 with negative Ce anomaly also has negative Zr and Hf
34 anomalies as the result of excess zircon crystallization.
35
36 751
37
38 752
39
40 753
41
42 754
43
44 755
45
46 756
47
48 757 **Fig. 5.** Distinct [Nb/Th]_N and [Ta/U]_N (a) (primitive mantle normalized Nb/Th and Ta/U
49 ratios to show the Nb and Ta anomalies) and Sr/Sr* and Eu/Eu* (b) (Sr/Sr* =
50 2*Sr_{PM}/[Pr_{PM} + Nd_{PM}] and Eu/Eu* = 2*Eu_{PM}/[Sm_{PM} + Gd_{PM}] to show the Sr and Eu
51 anomalies) between the samples from Huoju and Jiujiang and Tianyang. For
52 comparison, the compositions of Cenozoic basalts from the Hainan Island (Tu et al.,
53 1991; Flower et al., 1992; Zou and Fan, 2010; Ho et al., 2000; Wang et al., 2011) and
54 the average compositions of present-day OIB, both normal (N-type) and enriched (E-
55
56
57
58
59
60

1
2
3 764 type) MORB ([Sun and McDonough, 1989](#)) and UCC ([Rudnick and Gao, 2003](#)) are also
4 765 plotted.
5
6 766
7
8
9

10 767 **Fig. 6.** Sr-Nd-Pb-Hf isotope co-variations of the volcanic rocks from the Leizhou
11 Peninsula. The terrestrial array in the Nd-Hf isotopic space is from [Vervoort et al.](#)
12
13 768 ([1999](#)). Northern Hemisphere Reference Line (NHRL) is from [Hart \(1984\)](#). The Sr-Nd-
14
15 769 Pb isotope compositions of Cenozoic basalts from the Hainan Island ([Tu et al., 1991](#);
16
17 770 [Flower et al., 1992; Zou and Fan, 2010; Ho et al., 2000; Wang et al., 2011](#)) and the
18
19 771 South China Sea Basin (SCSB; [Tu et al., 1992; Yan et al., 2008, 2015](#)), the Pb isotope
20
21 772 compositions of the Central Indian Ridge (CIR) MORB ([Mahoney et al., 1989](#)) and
22
23 773 average Java trench sediment that is largely mature continent derived ([Plank and](#)
24
25 774 [Langmuir, 1998](#)) are also plotted for comparison.
26
27
28
29

30 776
31
32
33 777 **Fig. 7.** Modelling of crustal contamination in the SiO₂ vs. ⁸⁷Sr/⁸⁶Sr diagram. The sample
34 from Jiujiang with lowest SiO₂ (47.78 wt. %) was assumed as the basaltic melt
35 unaffected by crustal contaminations. UCC material with 66.6 wt.% SiO₂, 327 ppm Sr
36
37 779 ([Rudnick and Gao, 2003](#)) and ⁸⁷Sr/⁸⁶Sr value of 0.7173 ([Plank and Langmuir, 1998](#)) is
38 modelled to mix with the basaltic melt by variable extents. The modelling results show
39
40 780 that the volcanic rocks in the Leizhou Peninsula are apparently off the mixing trend. To
41
42 781 generate the Huoju samples with 54.87-61.21 wt.% SiO₂, as high as ~38-70% UCC
43
44 782 materials are needed to assimilate with the basaltic melt, which would generate melts
45
46 783 with high ⁸⁷Sr/⁸⁶Sr values of ~0.7071-0.7116, much higher than the ⁸⁷Sr/⁸⁶Sr values
47
48 784 (0.703882-0.704888) of the Huoju samples.
49
50
51
52
53
54
55
56
57
58
59
60

785 787 **Fig. 8.** In contrast with the positive correlation between Sr/Sr* and SiO₂ and negative
788

1
2
3 789 correlations between Sr/Sr* and [La/Sm]_N, Nb/U and Zr/Hf in the Cenozoic volcanic
4 790 rocks in the Hainan Island, the samples from the Leizhou Peninsula have negative
5 791 correlation of Sr/Sr* with SiO₂, and positive correlations of Sr/Sr* with [La/Sm]_N, Nb/U
6 792 and Zr/Hf. Hence, the positive Sr anomalies in the volcanic rocks from the Leizhou
7 793 Peninsula cannot be explained by the involvement of the recycled oceanic crust
8 794 materials in the mantle source region. The positive Sr anomalies (Sr/Sr* > 1) of the
9 795 volcanic rocks from the Leizhou peninsula are consistent with the incompatible element
10 796 enrichment in the mantle source (See text for details).
11
12
13
14
15
16
17
18
19
20
21
22
23
24
25
26
27
28
29
30
31
32
33
34
35
36
37
38
39
40
41
42
43
44
45
46
47
48
49
50
51
52
53
54
55
56
57
58
59
60

797
798 **Fig. 9.** Distinct Pb/Ce and Sr/Sr* trends between Jiujiang/Tianyang and Huoju rock
799 suites. For comparison, the compositions of Cenozoic basalts from the Hainan Island
800 are also plotted (Tu et al., 1991; Flower et al., 1992; Zou and Fan, 2010; Ho et al., 2000;
801 Wang et al., 2011). The Jiujiang and Tianyang samples show low Pb/Ce but high Sr/Sr*,
802 which is similar to the amphiboles in the mantle xenoliths (Yu et al., 2006) and is
803 consistent with a low-F melt mantle metasomatism. The Huoju samples and rocks from
804 the Hainan Island show high Pb/Ce and relative low Sr/Sr*, which is similar to the
805 clinopyroxenes in the mantle xenoliths (Yu et al., 2006) and indicates a mantle
806 metasomatism by recycled UCC materials.
807
808

809 **Fig. 10.** Correlations of Sr-Nd-Pb-Hf isotope ratios with their respective
810 parent/daughter ratios (⁸⁷Rb/⁸⁶Sr, ¹⁴⁷Sm/¹⁴⁴Nd, ²³⁸U/²⁰⁴Pb and ¹⁷⁶Lu/¹⁷⁷Hf). The positive
811 correlation between Rb/Sr and ⁸⁷Sr/⁸⁶Sr gives a pseudochron age of 1298 Ma. This age
812 has no geological significance, but is best explained by melting-induced mixing with
813 the pseudochron slope controlled by the compositions of the two endmembers, i.e., a
low-F melt metasomatized asthenospheric mantle material with high Sr content, low

1
2
3 814 Rb/Sr and depleted Sr isotope composition and a recycled UCC material with high
4
5 815 Rb/Sr and enriched Sr isotope composition. The samples from Jiujiang and Tianyang
6
7 816 with low $^{147}\text{Sm}/^{144}\text{Nd}$ and $^{176}\text{Lu}/^{177}\text{Hf}$ and high $^{238}\text{U}/^{206}\text{Pb}$ have high $^{143}\text{Nd}/^{144}\text{Nd}$ and
8
9 817 $^{176}\text{Hf}/^{177}\text{Hf}$ and low $^{206}\text{Pb}/^{204}\text{Pb}$, which is consistent with the characteristics of a recent
10
11 818 (or “current”) low-F melt metasomatism without enough time for isotope intergrowth.
12
13 819 Sample ZC11-02 show the same characteristics with other Jiujiang/Tianyang samples
14
15 820 except for its low Zr-Hf-Ce due to excess zircon fractionation (see Fig. 4).
16
17 821
18
19
20
21
22 822 **Fig. 11.** Trace element modelling of the multiple metasomatic events in the mantle
23
24 source region of the volcanic rocks in the Leizhou Peninsula. Sr-Nd-Pb-Hf isotopes are
25
26 not used in these modellings because the recent metasomatic low-F melts should have
27
28 indistinguishable depleted Sr-Nd-Pb-Hf isotopes with the depleted MORB mantle
29
30 (DMM). The average La/Yb, Lu/Hf, Ta/U and Nb/Th ratios of the recycled upper
31
32 continental crust (UCC) materials are calculated using recommended UCC
33
34 compositions from Rudnick and Gao (2003). The average values of the above element
35
36 ratios of DMM are calculated using recommended DMM compositions from Salters
37
38 and Stracke (2004). The low-F melt component is assumed to be represented by an
39
40 incompatible elements most enriched sample from Jiujiang and Tianyang (JJ11-01).
41
42 The modelling results show that ~6%-10% recycled UCC materials were mixed with
43
44 the DMM in the first place. Such recycled UCC material modified mantle was then
45
46 further metasomatized by the low-F melt by variable extents to generate the ultimate
47
48 mantle source of the volcanic rocks in the Leizhou Peninsula.
49
50
51
52
53
54
55
56 836
57
58 837 **Fig. 12.** (a) The paleo-Pacific plate subducted along the present Southeast China
59 coastline in the Mesozoic until exotic terranes (represented by the basement of
60

1
2
3 continental shelf of East and South China Seas) jammed the trench and ceased the
4 subduction activity at ~ 100 Ma ([Niu et al., 2015](#)). UCC material subducted as terrestrial
5 sediment can melt and metasomatize the overlying asthenosphere in the mantle wedge
6 ([Johnson and Plank, 2000](#)). (b) After subduction cessation, the Leizhou Peninsula was
7 in an intraplate environment. The asthenospheric mantle beneath Leizhou Peninsula
8 experienced a low-F melt metasomatism. Such low-F melt enriched in incompatible
9 elements and volatiles tended to rise (green arrows) due to buoyancy to metasomatize
10 the overlying asthenospheric mantle that had been pre-modified by a recycling UCC
11 material. The low-F melt can also metasomatize the overlying lithospheric mantle by
12 crystallizing hydrous minerals (e.g. amphibole) and forming garnet pyroxenite,
13 hornblende-pyroxenite and hornblendite veins in the lithospheric mantle ([Niu et al.,](#)
14 [2002, 2012; Niu and O'Hara, 2003; Niu, 2005](#)). Decompressional melting (red arrows)
15 of such a multiply metasomatized asthenospheric mantle formed the late Cenozoic
16 volcanisms we studied.

Fig. 1

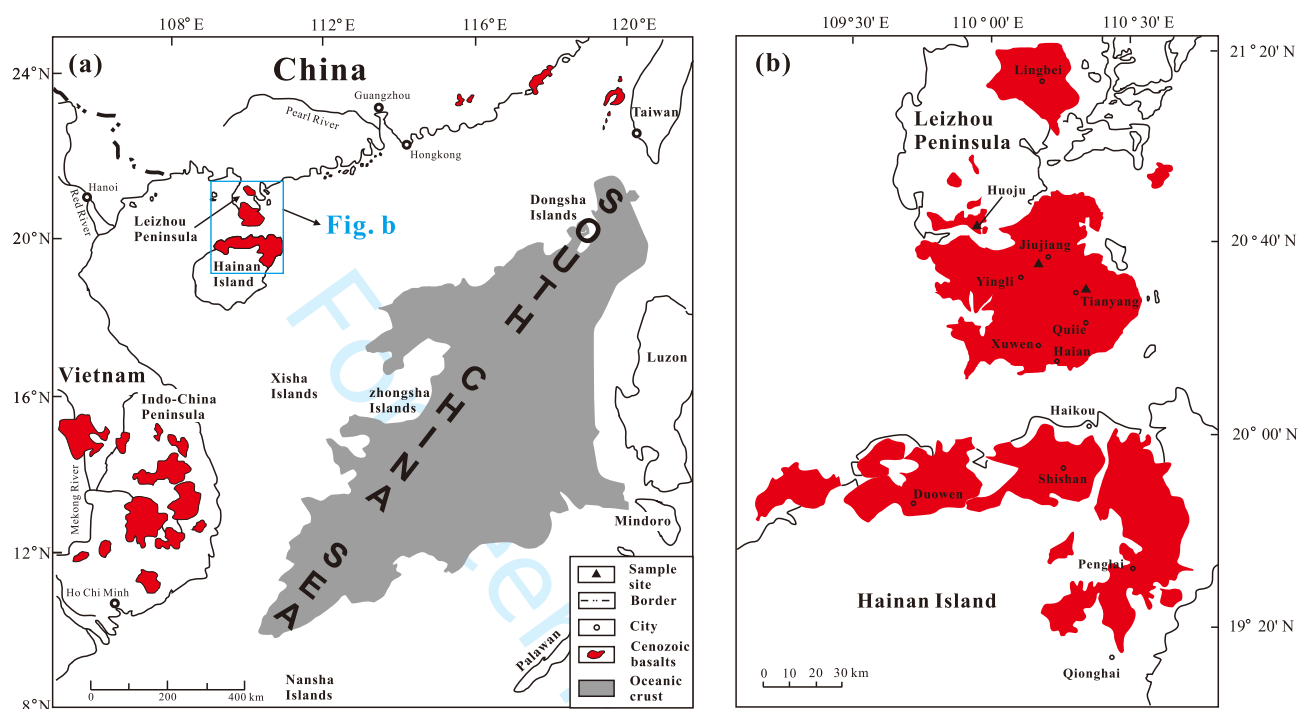


Fig. 2



1

2

3

4

5

6

7

8

9

10

11

12

13

14

15

16

17

18

19

20

21

22

23

24

25

26

27

28

29

30

31

32

33

34

35

36

37

38

39

40

41

42

43

44

45

46

47

48

49

50

51

52

53

54

55

56

57

58

59

60

Fig. 3

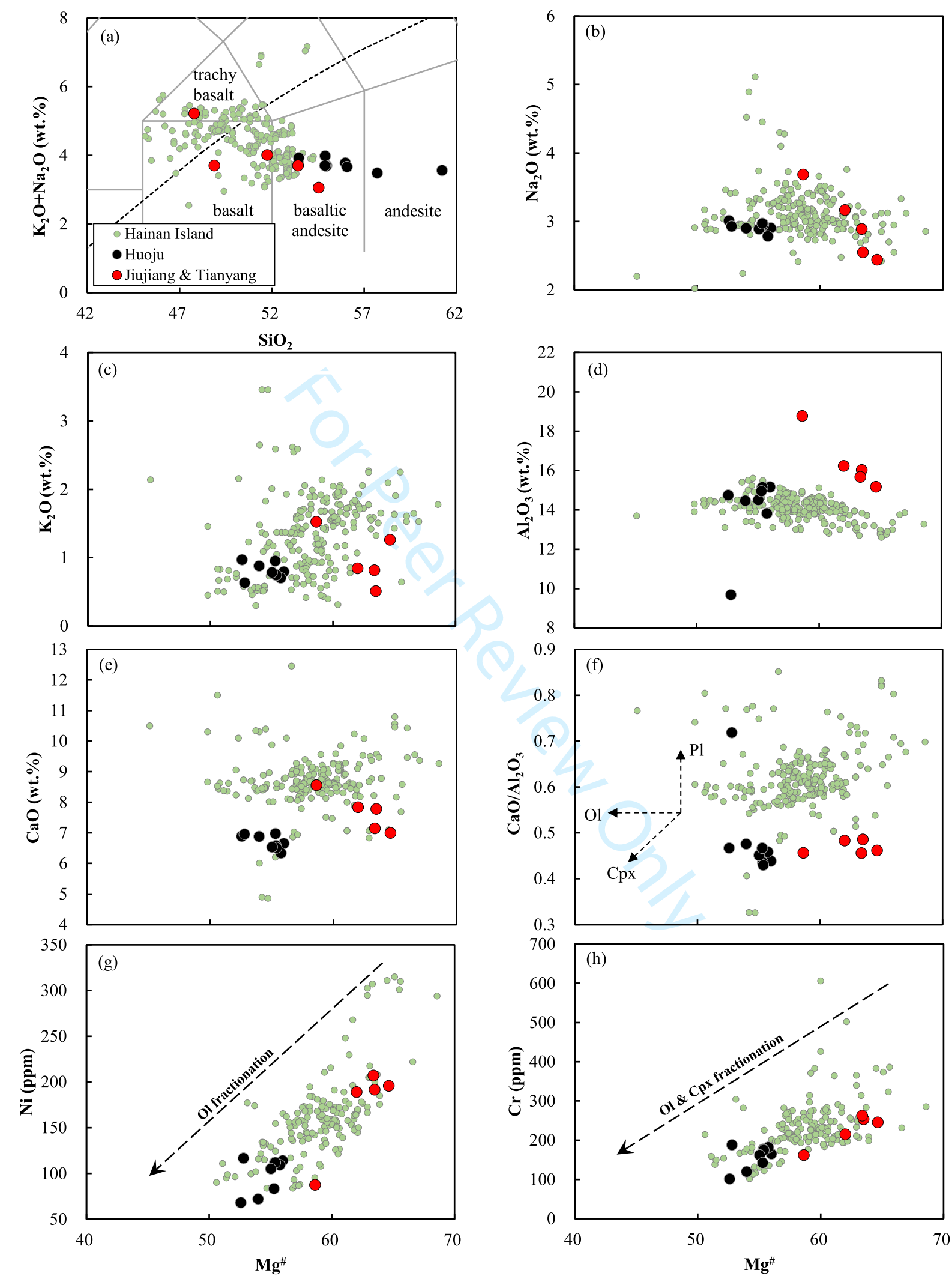


Fig. 4

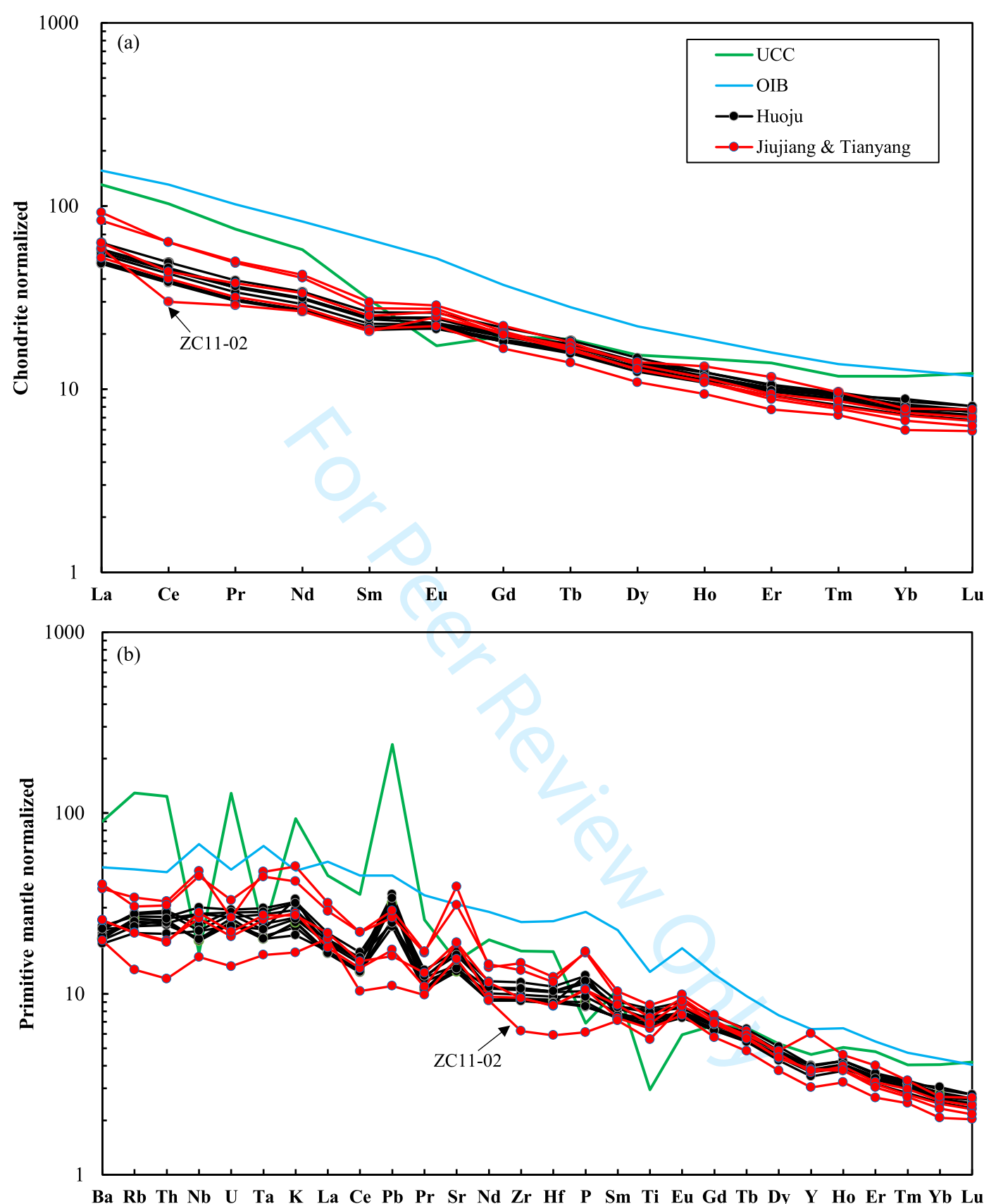


Fig. 5

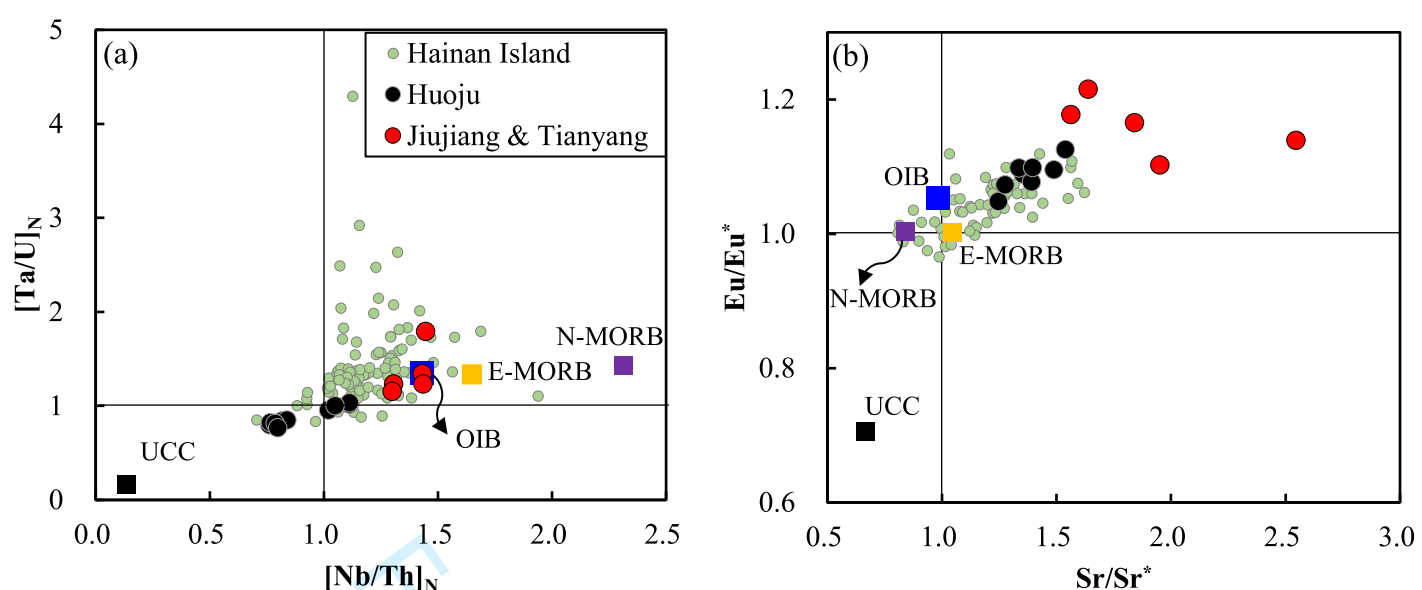


Fig. 6

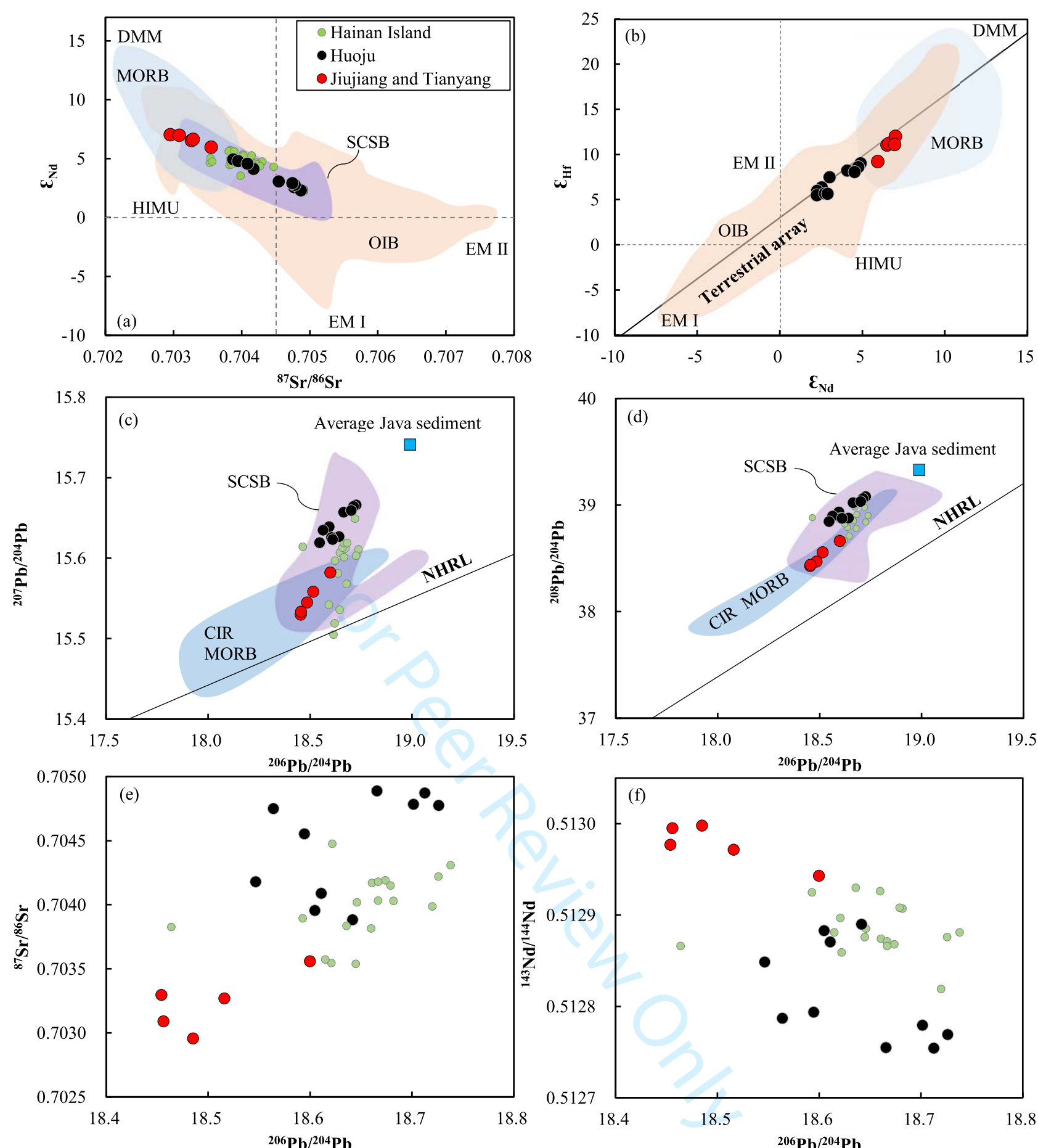


Fig. 7

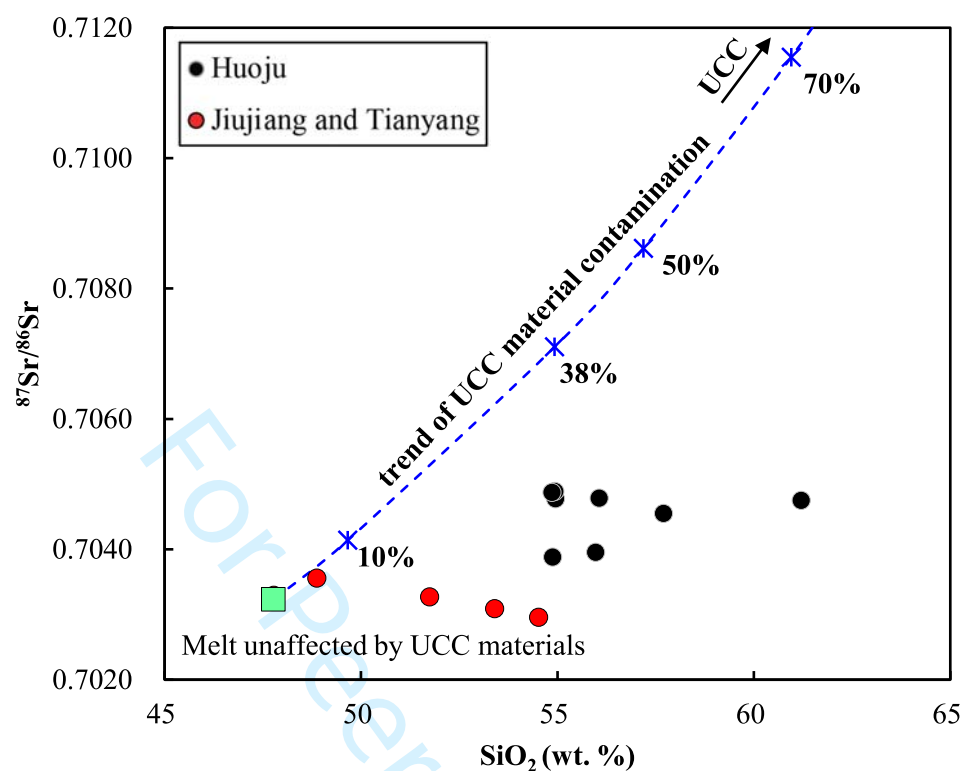
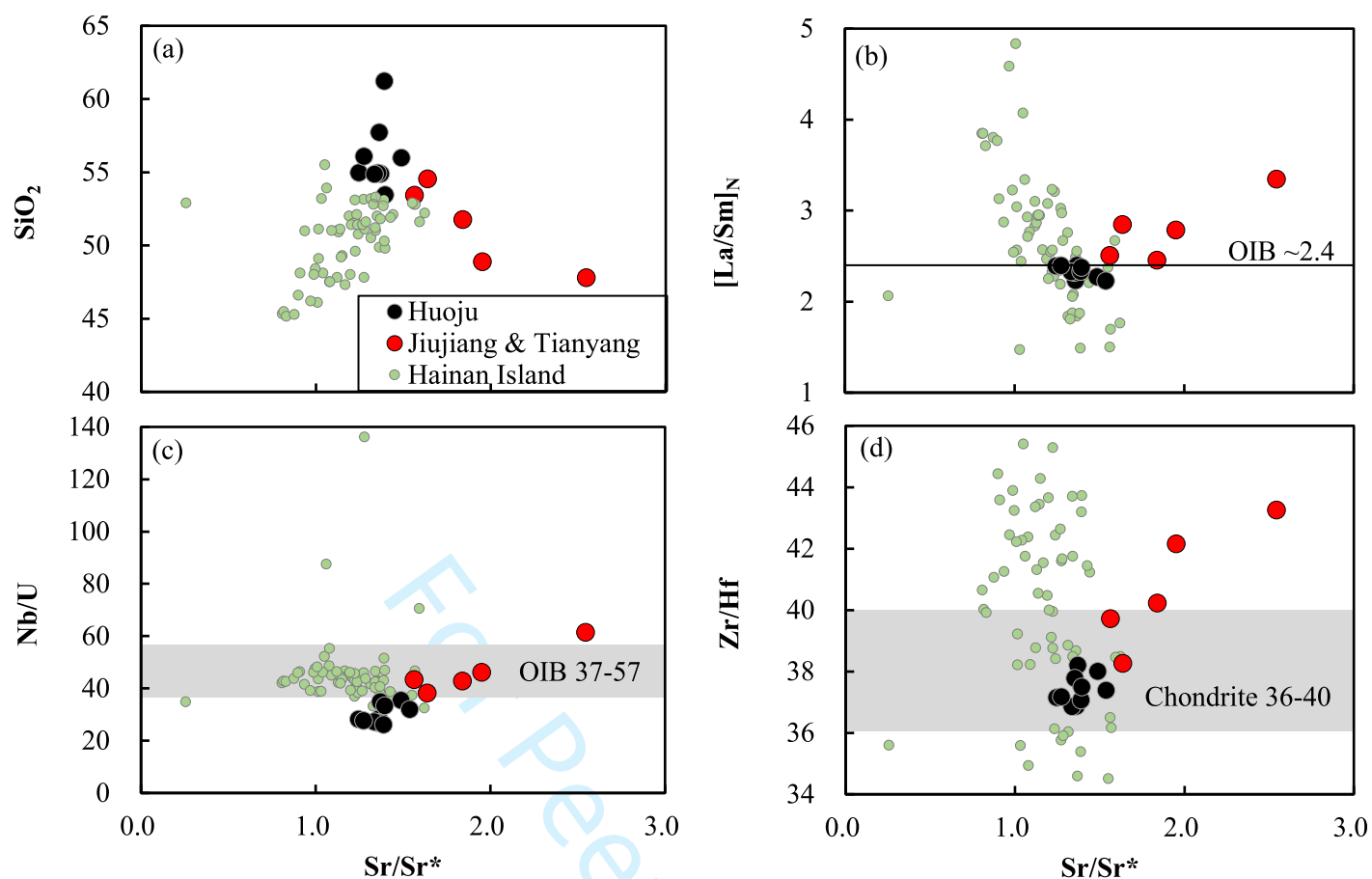


Fig. 8



1
2
3
4
5
6

Fig. 9

7
8
9
10
11
12
13
14
15
16
17
18
19
20
21
22
23
24
25
26
27
28
29
30
31
32
33
34
35
36
37
38
39
40
41
42
43
44
45
46
47
48
49
50
51
52
53
54
55
56
57
58
59
60

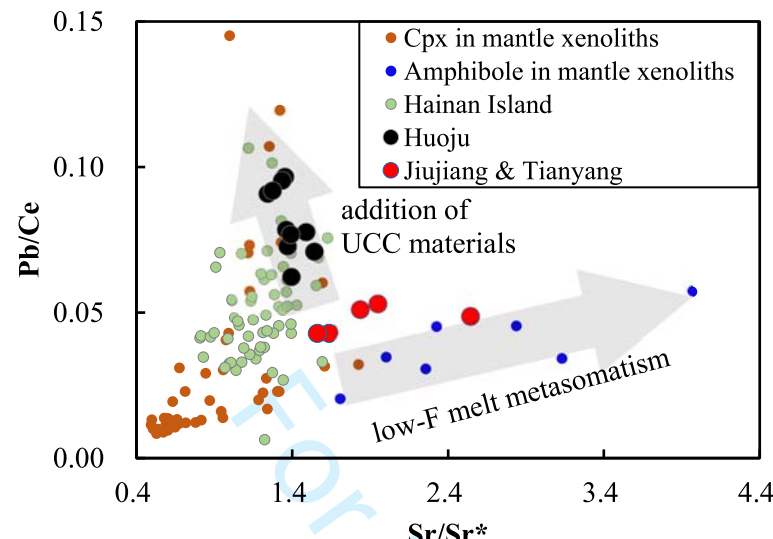


Fig. 10

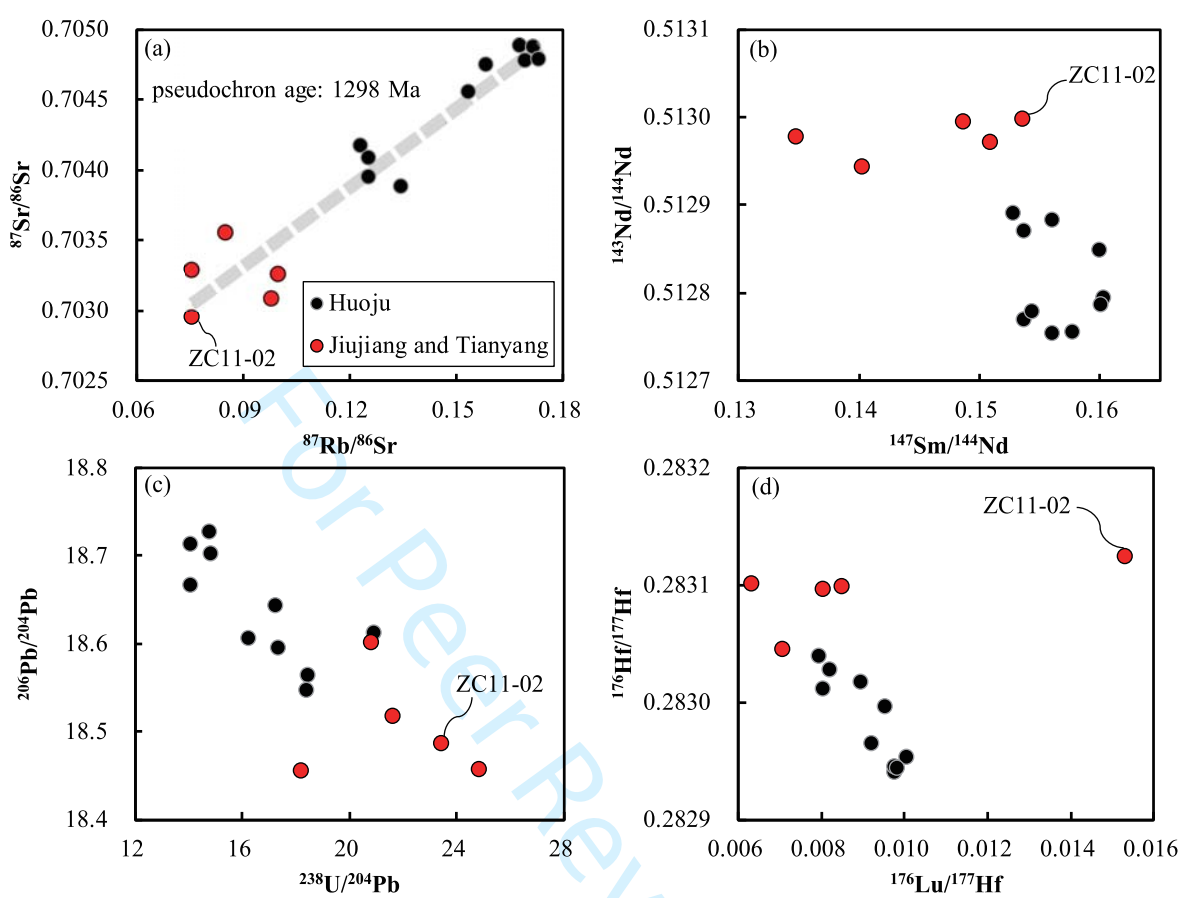


Fig. 11

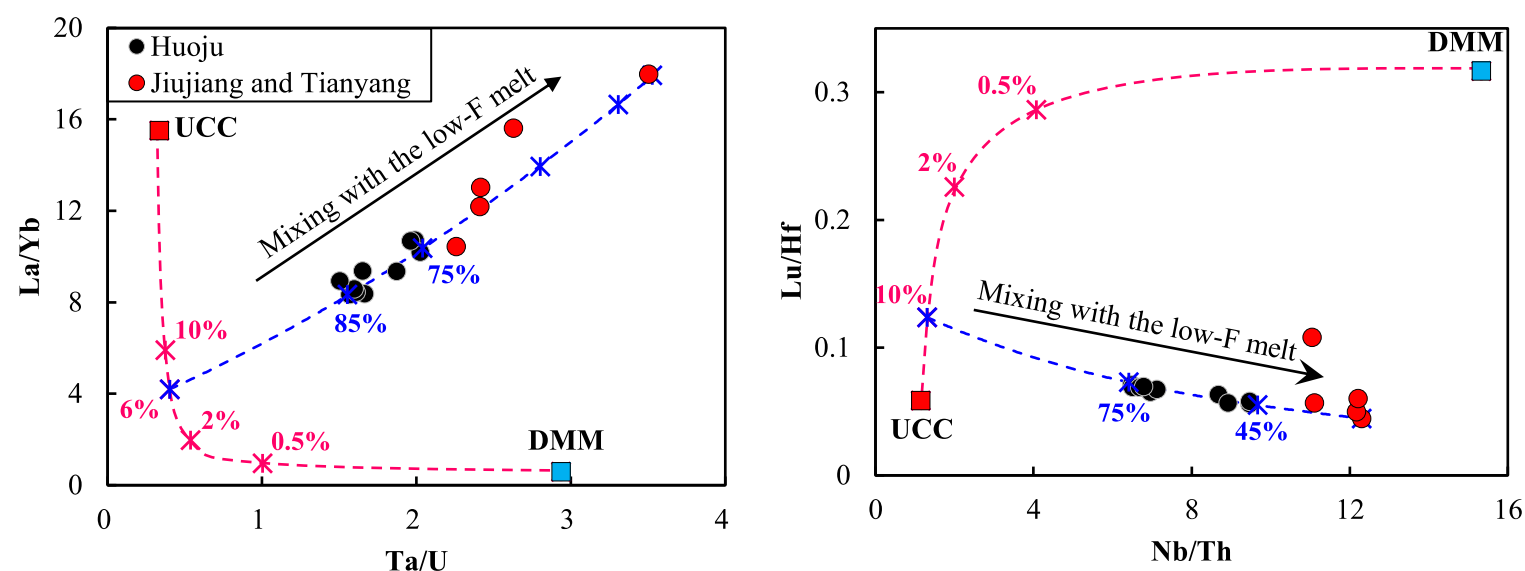
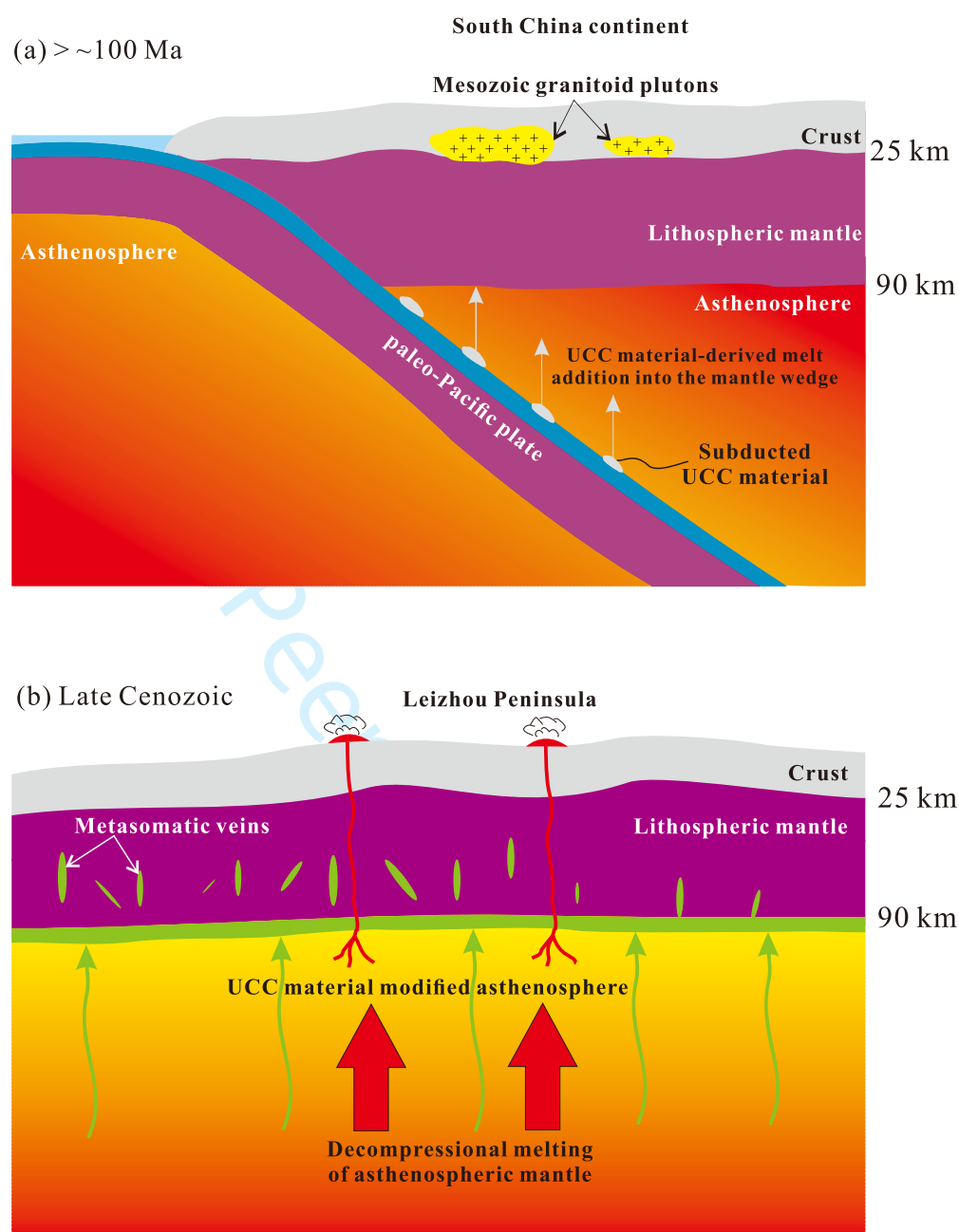
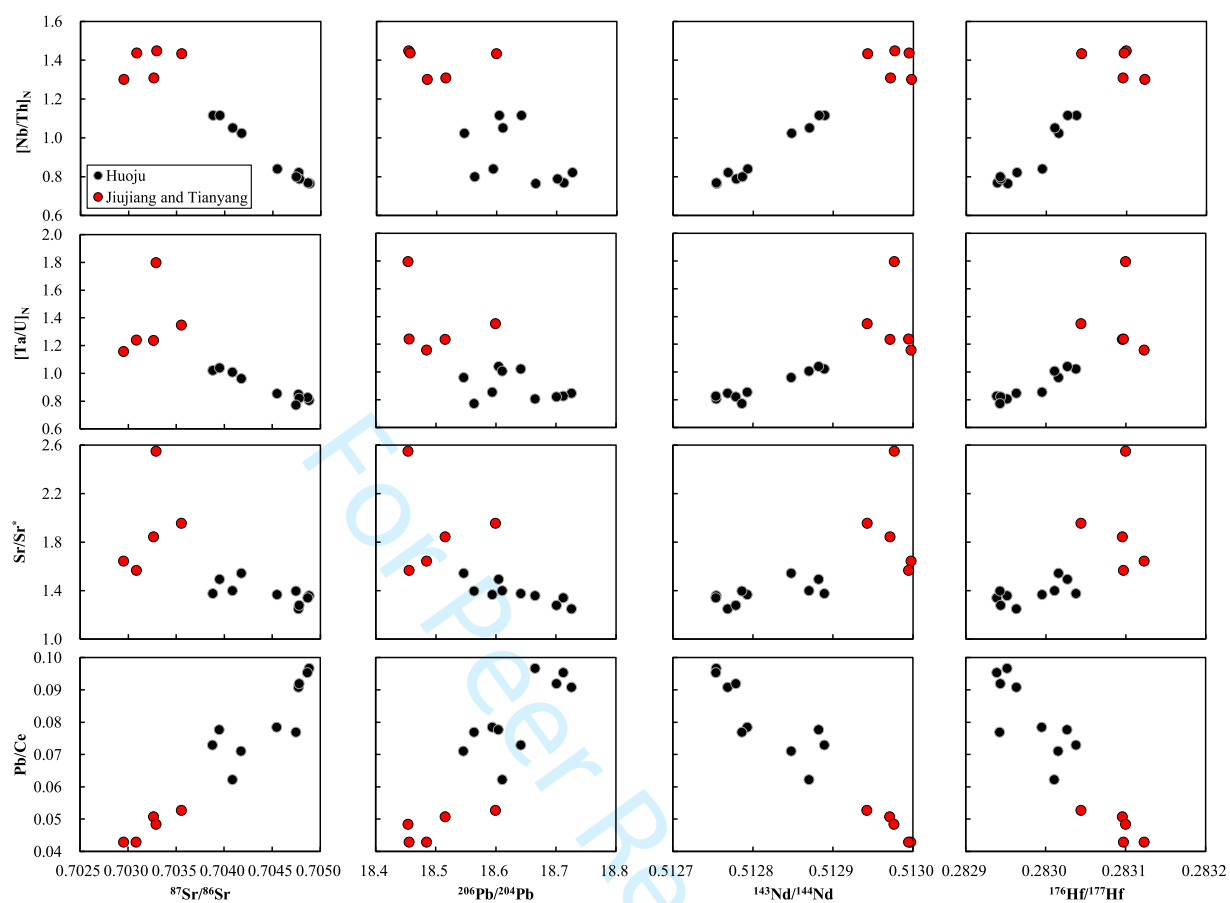


Fig. 12





Supplementary Figure 1 Significant correlations of Sr-Nd-Pb-Hf isotope ratios with $[Nb/Th]_N$, $[Ta/U]_N$, Sr/Sr^* and Pb/Ce ratios, suggesting that the isotopically enriched component has low $[Nb/Th]_N$, $[Ta/U]_N$ and Sr/Sr^* and high Pb/Ce , which is consistent with the contribution of recycled UCC materials in the mantle source regions.

Supplementary Table 1 Major and trace element compositions of the analyzed USGS standard AGV-2 and the volcanic rocks from Leizhou Peninsula

Sample	AGV-2	Hujia										Jiujiang & Tianyang				
		HJ11-01	HJ11-03	HJ11-06	HJ11-07	HJ11-09	HJ11-11	HJ11-12	HJ11-13	HJ11-14	HJ11-15	JJ11-01	TY11-01	ZC11-01	ZC11-02	ZC11-03
Lat.		20.77	20.77	20.77	20.77	20.77	20.77	20.77	20.77	20.77	20.77	20.59	20.52	20.52	20.52	20.52
Long.		109.95	109.95	109.95	109.95	109.95	109.95	109.95	109.95	109.95	109.95	110.17	110.31	110.31	110.31	110.31
ICP-OES analyses (wt.%)																
SiO ₂	59.48	54.96	54.88	57.71	54.94	55.98	54.87	56.06	61.21	53.45	47.78	51.75	48.88	54.53	53.41	
TiO ₂	1.07	1.63	1.86	1.51	1.53	1.76	1.55	1.59	1.53	1.83	1.83	1.54	1.94	1.27	1.52	
Al ₂ O ₃	17.31	15.16	14.75	13.82	15.11	14.47	15.15	14.50	9.68	14.95	18.77	16.23	15.17	16.03	15.67	
TFe ₂ O ₃	6.72	10.06	10.27	9.88	10.56	9.78	10.52	10.26	10.32	10.44	9.95	10.01	10.71	9.05	9.45	
MnO	0.10	0.11	0.10	0.10	0.11	0.10	0.11	0.11	0.11	0.09	0.13	0.11	0.12	0.11	0.10	
MgO	1.79	5.81	5.17	5.65	5.94	5.21	5.93	5.70	5.24	5.86	6.41	7.43	8.90	7.15	7.43	
CaO	5.08	6.65	6.89	6.34	6.58	6.88	6.51	6.54	6.96	6.98	8.56	7.84	7.00	7.79	7.14	
Na ₂ O	4.20	2.91	3.01	2.78	2.94	2.90	2.96	2.89	2.93	2.97	3.69	3.17	2.44	2.55	2.89	
K ₂ O	2.95	0.80	0.97	0.70	0.75	0.88	0.74	0.78	0.64	0.95	1.53	0.84	1.26	0.51	0.82	
P ₂ O ₅	0.51	0.23	0.27	0.18	0.19	0.25	0.20	0.21	0.19	0.26	0.37	0.23	0.37	0.13	0.23	
LOI	0.41	1.07	1.18	0.66	0.72	1.15	0.83	0.72	0.53	1.62	0.41	0.27	2.70	0.27	0.75	
Total	99.62	99.37	99.37	99.35	99.36	99.36	99.36	99.36	99.34	99.39	99.43	99.41	99.49	99.38	99.41	
Mg# ^a	37.18	55.98	52.58	55.74	55.33	53.98	55.37	55.02	52.79	55.29	58.63	62.01	64.65	63.49	63.38	
ICP-MS analyses (ppm)																
Sc	12.4	17.5	17.5	18.1	18	17.8	18	17.8	18.2	17.4	18.2	17.8	18.8	17.7	17.9	
V	115	128	144	132	129	144	128	130	124	141	139	154	129	154	125	
Cr	15	165	102	182	177	120	175	162	188	175	143	162	215	246	253	
Mn	726	1018	952	971	1001	979	999	989	1038	945	826	1070	973	1158	1050	
Co	14.3	39.1	36.7	39.3	39.3	36.5	38.5	38.2	39	39.3	38	37.4	42.4	47.7	42.3	
Ni	17	114	68	109	112	72	112	105	117	98	83	87	189	196	192	
Cu	45	44	34	42	41	33	41	43	41	34	36	52	72	52	53	
Zn	87	112	107	106	107	105	108	108	103	103	102	87	90	99	90	
Ga	18.7	19	19.3	18.7	18.7	18.9	18.4	18.3	18.4	18.2	18.5	19.5	17.5	17.9	16.3	
Rb	62.0	17.7	17	15	16.5	15.8	16.6	17.5	15.9	13.8	15	21.6	13.9	19.3	8.6	
Sr	639	303	365	283	284	363	279	292	290	324	345	827	400	653	329	
Y	17.8	18.1	18.3	17.2	17.3	17.3	17.1	18.1	16.8	15.9	16.9	17.5	13.8	16.7	28	
Zr	220	117	130	106	104	121	103	111	103	102	120	166	106	151	70	
Nb	13.2	17	21	14.5	14	19.7	14	15.9	14.3	15.9	19.7	34	18.6	32	11.4	
Cs	1.125	0.3	0.22	0.172	0.23	0.24	0.25	0.24	0.21	0.147	0.144	0.134	0.21	0.13	0.157	
Ba	1100	158	166	138	143	150	141	160	145	132	160	266	178	282	138	
La	36.4	13.6	14.9	11.5	11.7	13.3	11.6	12.9	11.8	11.5	13.8	21.9	12.4	19.7	13.9	
Ce	66.0	27.8	30.1	23.3	23.7	27.2	23.6	26.2	23.9	23.5	28.1	38.8	24.6	39	18.4	
Pr	7.64	3.4	3.73	2.88	2.93	3.41	2.92	3.22	2.94	2.92	3.46	4.64	3.02	4.74	2.72	
Nd	28.6	14.5	15.9	12.5	12.5	14.6	12.5	13.6	12.4	12.7	14.7	18.9	13.1	19.7	12.4	
Sm	5.11	3.69	4.02	3.32	3.26	3.78	3.22	3.48	3.29	3.35	3.75	4.23	3.26	4.58	3.16	
Eu	1.46	1.33	1.51	1.27	1.25	1.42	1.25	1.31	1.24	1.31	1.4	1.59	1.28	1.66	1.44	
Gd	4.35	4.08	4.45	3.84	3.78	4.16	3.74	3.97	3.74	3.73	4.04	4.25	3.42	4.56	4.16	
Tb	0.606	0.662	0.690	0.616	0.6	0.647	0.608	0.636	0.593	0.586	0.637	0.623	0.522	0.674	0.6	
Dy	3.21	3.59	3.77	3.36	3.39	3.51	3.36	3.54	3.29	3.16	3.49	3.25	2.77	3.44	3.57	
Ho	0.632	0.701	0.699	0.666	0.668	0.669	0.659	0.697	0.637	0.615	0.664	0.623	0.532	0.653	0.754	
Er	1.69	1.75	1.73	1.67	1.68	1.63	1.65	1.74	1.60	1.52	1.63	1.51	1.28	1.56	1.93	
Tm	0.251	0.245	0.239	0.231	0.233	0.221	0.234	0.236	0.226	0.209	0.22	0.205	0.184	0.22	0.245	
Yb	1.58	1.46	1.39	1.37	1.4	1.3	1.37	1.50	1.33	1.23	1.29	1.22	1.02	1.26	1.33	
Lu	0.244	0.205	0.19	0.193	0.196	0.184	0.193	0.205	0.192	0.173	0.181					

1
2
3
4
5
6
7
8**Supplementary Table 2** Sr, Nd, Pb and Hf isotope data of the USGS standards and the volcanic rocks in Leizhou Peninsula

Sample	$^{87}\text{Sr}/^{86}\text{Sr}$ ($\pm 2\sigma$)	$^{143}\text{Nd}/^{144}\text{Nd}$ ($\pm 2\sigma$)	εNd	$^{206}\text{Pb}/^{204}\text{Pb}$	$^{207}\text{Pb}/^{204}\text{Pb}$	$^{208}\text{Pb}/^{204}\text{Pb}$	$^{176}\text{Hf}/^{177}\text{Hf}$ ($\pm 2\sigma$)	εHf
<i>USGS standards</i>								
AGV-2	0.703980 \pm 8	0.512771 \pm 8		18.845	15.613	38.527	0.282938 \pm 5	
BCR-2	0.705010 \pm 7	0.512612 \pm 9		18.752	15.622	38.712	0.282840 \pm 5	
<i>Huoju</i>								
HJ11-01	0.704775 \pm 8	0.512769 \pm 8	2.6	18.727	15.666	39.077	0.282964 \pm 9	6.3
HJ11-03	0.703882 \pm 14	0.512890 \pm 9	4.9	18.642	15.627	38.877	0.283039 \pm 8	9.0
HJ11-06	0.704551 \pm 8	0.512794 \pm 9	3.0	18.595	15.639	38.934	0.282996 \pm 8	7.5
HJ11-07	0.704888 \pm 7	0.512755 \pm 10	2.3	18.666	15.657	39.019	0.282952 \pm 6	5.9
HJ11-09	0.703954 \pm 8	0.512883 \pm 10	4.8	18.605	15.626	38.876	0.283027 \pm 6	8.6
HJ11-11	0.704871 \pm 8	0.512754 \pm 8	2.3	18.713	15.664	39.058	0.282939 \pm 5	5.5
HJ11-12	0.704783 \pm 7	0.512779 \pm 7	2.8	18.702	15.659	39.031	0.282944 \pm 6	5.6
HJ11-13	0.704749 \pm 9	0.512787 \pm 7	2.9	18.564	15.635	38.894	0.282943 \pm 7	5.6
HJ11-14	0.704179 \pm 6	0.512849 \pm 9	4.1	18.547	15.619	38.842	0.283016 \pm 5	8.2
HJ11-15	0.704088 \pm 8	0.512871 \pm 9	4.5	18.611	15.623	38.874	0.283011 \pm 6	8.0
<i>Jiujiang & Tianyang</i>								
TY11-01	0.703267 \pm 6	0.512972 \pm 7	6.5	18.516	15.558	38.555	0.283096 \pm 5	11.0
JJ11-01	0.703295 \pm 8	0.512977 \pm 9	6.6	18.454	15.530	38.425	0.283100 \pm 6	11.1
ZC11-01	0.703557 \pm 7	0.512943 \pm 8	6.0	18.600	15.582	38.661	0.283045 \pm 6	9.2
ZC11-02	0.702955 \pm 7	0.512998 \pm 11	7.0	18.485	15.545	38.469	0.283124 \pm 6	12.0
ZC11-03	0.703088 \pm 8	0.512995 \pm 8	8.0	18.456	15.533	38.438	0.283098 \pm 7	11.1

$\varepsilon\text{Nd} = (^{143}\text{Nd}/^{144}\text{Nd}_{\text{sample}}/^{143}\text{Nd}/^{144}\text{Nd}_{\text{CHUR}} - 1) \times 10000$, $^{143}\text{Nd}/^{144}\text{Nd}_{\text{CHUR}} = 0.512638$ (Bouvier et al., 2008).

$\varepsilon\text{Hf} = (^{176}\text{Hf}/^{177}\text{Hf}_{\text{sample}}/^{176}\text{Hf}/^{177}\text{Hf}_{\text{CHUR}} - 1) \times 10000$, $^{176}\text{Hf}/^{177}\text{Hf}_{\text{CHUR}} = 0.282772$ (Blichert-Toft and Albarède, 1997).

50

51

52

53

54

55

56

57

58

59

60

Supplementary Table 3 Compiled bulk-rock compositional data for the Cenozoic volcanic rocks in the Hainan Island

Locality		Hainan Island (Tu et al., 1991 & Flower et al., 1992)													
Sample		HN1	HN2	HN3	HN12	HN27	HN64	HN97	HN98	HN99	HN28	HN32	HN33	HN62	HN54
Rock Type		AB	AB	AB	AB	AB	BS	AB	AB	AB	OT	OT	OT	OT	OT
Major elements (wt. %)															
SiO ₂	48.20	49.41	48.89	47.01	47.35	45.71	47.32	47.30	47.27	51.53	50.51	49.87	47.88	49.28	
TiO ₂	2.22	2.39	2.28	2.48	2.61	2.73	2.65	2.81	2.80	2.56	2.63	2.56	2.58	2.31	
Al ₂ O ₃	13.30	13.19	13.35	14.46	13.74	13.26	12.94	13.89	13.85	14.50	14.37	14.03	13.97	13.91	
TFe ₂ O ₃	12.45	12.17	12.50	12.65	12.52	12.56	12.36	12.64	12.70	11.39	11.13	11.28	11.69	11.57	
MnO	0.16	0.15	0.17	0.17	0.18	0.17	0.16	0.17	0.17	0.15	0.15	0.15	0.15	0.15	
MgO	9.06	9.60	9.19	7.59	9.04	9.06	9.16	8.19	8.06	7.40	6.97	7.55	8.45	7.94	
CaO	6.83	7.10	7.07	9.10	10.09	9.53	8.77	7.47	7.51	9.40	9.21	9.18	8.76	8.63	
Na ₂ O	3.07	3.08	3.05	2.41	2.87	3.22	3.23	3.66	3.39	3.41	3.42	3.28	2.79	2.99	
K ₂ O	2.27	2.10	2.25	1.78	1.72	2.06	1.42	1.67	1.82	2.06	2.14	2.06	1.90	1.73	
P ₂ O ₅	0.84	0.76	0.83	0.73	0.64	0.72	0.59	0.70	0.68	0.53	0.60	0.54	0.59	0.51	
Total	98.41	99.94	99.58	98.38	100.76	99.02	98.62	98.51	98.25	102.93	101.12	100.49	98.76	99.02	
Mg#	62.9	64.5	62.9	58.2	62.5	62.4	63.1	59.9	59.4	57.7	59.1	60.6	60.3	61.3	
Trace elements (ppm)															
Sc	17.7	18.8	16.8	21.1	23.9	16.8	18.3	16.8	19.4	23.2	21.1	22.0	17.0	14.3	
V	133	140	133	186	221	189	185	153	145	196	206	198	184	178	
Cr	365	383	340	207	252	257	206	228	230	275	260	273	183	201	
Co	53.0	57.6	58.6	55.4	65.5	54.8	57.6	50.6	53.4	56.2	59.0	53.2	48.8	53.6	
Ni	303	311	295	195	177	178	218	216	211	121	108	127	158	158	
Cu	39.9	41.2	37.5	53.6	60.7	54.6	42.3	47.4	43.2	65.3	66.0	63.7	51.6	50.9	
Zn	150	140	145	125	116	123	123	136	124	119	114	111	121	122	
Rb	47.9	44.7	42.9	38.8	37.0	40.6	41.4	53.5	62.4	42.9	46.5	45.4	41.1	34.9	
Sr	922	685	929	762	685	776	712	832	772	613	617	609	598	533	
Y	29.2	26.4	28.1	30.6	29.1	27.9	26.1	27.4	28.6	25.3	27.4	26.5	27.5	25.1	
Zr	332	288	309	250	277	249	257	298	288	222	234	225	241	206	
Nb	69.6	59.7	66.1	69.6	63.9	57.5	55.2	64.2	61.5	44.2	47.1	43.4	48.0	39.8	
Ba	567	485	571	765	488	479	501	571	573	457	500	481	395	340	
La	48.1	40.0	45.1	50.1	47.8	42.5	33.0	42.8	41.0	31.5	32.7	31.4	34.9	29.1	
Ce	104.9	76.3	91.5	101.5	103.3	83.9	33.0	42.8	41.0	67.3	65.8	63.1	69.8	58.4	
Nd	47.3	40.5	44.0	39.2	43.4	41.7	34.4	42.8	39.8	30.8	29.6	27.0	36.1	30.3	
Sm	9.10	8.10	8.97	7.92	7.89	8.72	7.69	8.54	8.52	6.64	6.90	6.86	8.02	7.08	
Eu	3.30	2.60	2.95	2.78	2.78	2.94	2.56	2.86	2.90	2.43	2.37	2.27	2.65	2.34	
Tb	0.91	0.76	0.74	0.77	0.88	0.87	0.75	0.77	0.73	0.79	0.62	0.62	0.84	0.77	
Yb	1.69	1.51	1.35	1.82	1.80	1.67	1.11	1.41	1.45	1.59	1.31	1.35	1.66	1.54	
Lu	0.18	0.19	0.21	0.23	0.29	0.23	0.16	0.21	0.20	0.23	0.24	0.25	0.21	0.22	
Hf	7.75	6.10	6.39	6.01	6.75	5.85	5.55	6.43	6.56	5.74	5.18	5.13	5.33	4.80	
Ta	5.43	4.10	4.69	4.89	4.98	3.86	3.65	4.94	4.61	3.19	2.92	2.72	5.04	2.45	
Th	5.76	4.16	6.01	6.18	5.81	5.28	4.42	5.52	5.44	4.23	4.61	4.56	4.63	4.00	
U	1.38	1.17	1.38	0.95	1.47	1.50	1.08	1.38	1.30	0.66	1.09	1.25	1.30	1.09	
[La/Sm] _N	3.42	3.19	3.25	4.09	3.92	3.15	2.77	3.24	3.11	3.07	3.06	2.96	2.81	2.66	
[Nb/Th] _N	1.42	1.69	1.29	1.32	1.29	1.28	1.47	1.37	1.33	1.23	1.20	1.12	1.22	1.17	
[Ta/U] _N	2.02	1.79	1.74	2.64	1.74	1.32	1.73	1.83	1.82	2.48	1.37	1.11	1.99	1.15	
Nb/U	50.43	51.03	47.90	73.26	43.47	38.32	51.11	46.52	47.31	66.97	43.21	34.72	36.92	36.51	
Zr/Hf	42.89	47.13	48.29	41.63	41.08	42.60	46.36	46.31	43.84	38.59	45.12	43.86	45.29	42.92	
Sr-Nd-Pb isotopes															
⁸⁷ Sr/ ⁸⁶ Sr	0.703833				0.704170			0.703537	0.703544	0.703571		0.704017	0.704019		
¹⁴³ Nd/ ¹⁴⁴ Nd	0.512891				0.512874			0.512876	0.512897	0.512881		0.512885	0.512912		
²⁰⁶ Pb/ ²⁰⁴ Pb					18.661			18.645	18.621	18.615		18.646			
²⁰⁷ Pb/ ²⁰⁴ Pb					15.610			15.536	15.519	15.505		15.607			
²⁰⁸ Pb/ ²⁰⁴ Pb					38.87			38.71	38.6						

Supplementary Table 3 Continued

Locality		Hainan Island (Tu et al., 1991 & Flower et al., 1992)													
Sample		HN55	HN57	HN69	HN87	HN22	HN76	HN77	HN23	HN35	HN36	HN37	HN41	HN95	HN96
Rock Type		OT	OT	OT	OT	OT	OT	OT	OT	OT	OT	OT	OT	OT	OT
Major elements (wt. %)															
SiO ₂	49.48	49.86	50.01	50.41	49.89	50.79	50.20	52.59	52.17	52.86	52.40	52.53	52.20	52.66	
TiO ₂	2.24	2.23	2.29	2.31	2.44	2.33	2.31	2.19	2.16	2.23	2.22	2.01	2.03	2.14	
Al ₂ O ₃	14.11	14.24	14.50	14.54	15.01	14.68	14.58	14.85	14.84	15.27	15.50	14.62	14.44	14.68	
TFe ₂ O ₃	11.37	11.30	12.07	11.81	11.40	12.02	11.88	11.14	11.00	11.58	11.48	10.83	11.76	11.66	
MnO	0.15	0.14	0.15	0.15	0.14	0.15	0.15	0.14	0.14	0.14	0.14	0.14	0.14	0.15	
MgO	7.96	7.95	6.94	7.74	6.53	6.94	7.13	6.33	6.77	6.35	5.87	7.15	6.91	6.95	
CaO	8.46	8.25	8.62	8.57	9.15	8.65	8.58	8.96	9.08	8.53	8.40	8.61	8.40	8.38	
Na ₂ O	3.09	3.07	3.46	3.46	3.04	3.53	3.51	3.29	3.27	3.25	3.30	3.09	3.07	3.23	
K ₂ O	1.66	1.62	1.60	1.59	1.46	1.62	1.71	1.43	1.35	1.37	1.37	1.51	1.41	1.46	
P ₂ O ₅	0.47	0.52	0.50	0.49	0.43	0.53	0.51	0.42	0.37	0.37	0.37	0.38	0.33	0.32	
Total	98.99	99.18	100.15	101.08	99.49	101.26	100.56	101.34	101.15	101.96	101.05	100.86	100.71	101.64	
Mg#	61.8	61.9	57.0	60.3	57.1	57.2	58.2	56.8	58.6	55.8	54.2	60.3	57.5	57.8	
Trace elements (ppm)															
Sc	19.9	17.4	22.2	21.3	24.5	24.1	21.0	18.9	22.4	19.9	21.2	24.1	16.0	20.9	
V	165	162	237	159	196	193	173	170	195	162	168	173	148	151	
Cr	217	212	227	233	263	230	224	230	269	136	102	278	204	199	
Co	64.4	52.5	60.2	53.9	49.7	56.3	52.1	51.2	56.6	62.6	60.1	56.1	57.4	62.2	
Ni	159	165	152	172	87	159	173	84	95	135	122	126	158	157	
Cu	51.5	52.9	58.0	66.8	52.6	52.6	55.0	67.2	54.2	53.7	55.4	51.0	54.1	56.3	
Zn	120	112	126	118	119	125	118	113	113	122	118	113	124	131	
Rb	28.0	32.3	35.1	33.9	22.6	29.1	36.8	26.5	27.5	25.3	26.0	30.7	29.7	29.0	
Sr	513	487	554	547	554	579	552	456	476	446	455	446	438	442	
Y	24.0	23.1	26.2	25.5	25.2	27.1	25.7	22.6	23.5	24.3	24.9	22.7	22.9	23.8	
Zr	199	191	200	201	213	211	200	176	179	170	171	160	164	169	
Nb	36.1	35.3	37.3	37.6	34.6	38.7	37.9	28.5	27.9	25.6	25.1	28.4	25.6	27.0	
Ba	348	350	338	322	376	320	319	274	262	225	227	296	259	272	
La	27.4	25.2	26.2	26.5	24.6	26.8	26.9	20.1	20.2	16.4	16.3	20.5	18.0	18.8	
Ce	55.9	50.6	52.9	52.8	54.3	53.7	53.9	44.2	43.5	33.9	34.7	40.5	37.7	40.2	
Nd	28.9	26.2	30.2	31.2	27.5	29.8	28.3	22.8	21.6	21.2	19.1	20.7	18.6	19.6	
Sm	6.63	5.95	6.83	6.49	6.10	6.73	6.64	5.69	5.55	5.25	5.31	5.54	5.00	5.23	
Eu	2.23	1.99	2.33	2.30	2.29	2.34	2.36	1.92	1.90	1.85	1.87	1.92	1.73	1.81	
Tb	0.80	0.66	0.80	0.79	0.81	0.84	0.83	0.66	0.67	0.69	0.65	0.66	0.56	0.62	
Yb	1.67	1.36	1.62	1.56	1.47	1.44	1.65	1.43	1.44	1.41	1.57	1.56	1.30	1.50	
Lu	0.21	0.19	0.24	0.19	0.21	0.24	0.20	0.24	0.20	0.22	0.20	0.21	0.19	0.18	
Hf	4.62	4.11	4.51	4.63	5.30	4.57	4.79	4.05	3.92	3.81	3.72	3.88	3.57	3.51	
Ta	2.30	2.23	2.16	2.14	2.37	2.34	2.33	1.98	1.75	1.56	1.59	1.55	1.49	1.64	
Th	3.80	3.63	3.11	3.22	3.29	3.21	3.36	2.93	2.88	2.27	2.31	2.95	2.90	2.83	
U	0.98	0.68	0.87	0.81	1.04	0.95	1.06	0.79	0.84	0.72	0.75	0.85	0.67	0.81	
[La/Sm] _N	2.67	2.74	2.48	2.64	2.61	2.57	2.62	2.29	2.35	2.02	1.98	2.39	2.33	2.32	
[Nb/Th] _N	1.12	1.14	1.41	1.37	1.24	1.42	1.33	1.14	1.14	1.33	1.28	1.13	1.04	1.12	
[Ta/U] _N	1.20	1.68	1.27	1.35	1.17	1.26	1.13	1.28	1.07	1.11	1.09	0.93	1.14	1.04	
Nb/U	36.84	51.91	42.87	46.42	33.27	40.74	35.75	36.08	33.21	35.56	33.47	33.41	38.21	33.33	
Zr/Hf	43.12	46.35	44.30	43.30	40.09	46.24	41.82	43.48	45.71	44.72	45.83	41.26	46.05	48.12	
Sr-Nd-Pb isotopes															
⁸⁷ Sr/ ⁸⁶ Sr	0.704190				0.703824	0.703833	0.703814			0.704032		0.703985	0.704178		
¹⁴³ Nd/ ¹⁴⁴ Nd	0.512868				0.512866	0.512930	0.512926			0.512871		0.512819	0.512866		
²⁰⁶ Pb/ ²⁰⁴ Pb	18.674				18.464	18.636	18.660			18.667		18.720	18.667		
²⁰⁷ Pb/ ²⁰⁴ Pb	15.612				15.614	15.581	15.613			15.601		15.649	15.619		
²⁰⁸ Pb															

Supplementary Table 3 Continued

Locality		Hainan Island (Tu et al., 1991 & Flower et al., 1992)												
Sample	HN83	HN40	HN68	HN75	HN90	HN5	HN6	HN8	HN34	HN91	HN10	HN13	HN17	HN19
Rock Type	OT	OT	OT	OT	OT	QT	QT	QT	QT	QT	QT	QT	QT	QT
Major elements (wt. %)														
SiO ₂	51.93	52.26	52.89	52.28	52.88	54.77	53.55	54.24	52.20	52.56	51.22	52.12	52.21	49.10
TiO ₂	2.18	2.14	1.96	1.96	1.91	1.99	1.81	1.60	1.77	1.84	1.95	1.75	1.77	1.87
Al ₂ O ₃	14.63	15.13	14.14	14.75	14.44	14.42	14.27	14.83	14.66	14.35	14.06	14.23	14.16	14.63
TFe ₂ O ₃	11.50	11.42	11.29	11.76	11.15	11.60	11.67	11.69	12.09	10.99	11.40	11.24	11.15	9.57
MnO	0.14	0.14	0.14	0.14	0.14	0.15	0.17	0.14	0.15	0.13	0.15	0.16	0.14	0.29
MgO	7.29	6.53	7.06	6.94	7.39	6.82	8.07	6.95	7.11	6.81	6.94	7.27	6.70	5.41
CaO	8.51	8.47	8.49	8.30	8.36	8.44	8.58	8.67	8.59	8.32	8.57	8.62	8.13	12.45
Na ₂ O	3.38	3.34	2.90	3.08	3.03	3.09	3.00	3.04	2.89	3.01	2.80	2.99	2.89	2.88
K ₂ O	1.41	1.24	1.12	1.02	1.16	0.91	0.78	0.93	0.83	0.93	0.61	0.70	0.72	0.53
P ₂ O ₅	0.42	0.36	0.32	0.33	0.29	0.23	0.25	0.25	0.23	0.26	0.28	0.24	0.25	0.28
Total	101.40	101.03	100.32	100.55	100.76	102.42	102.16	102.35	100.51	99.21	97.98	99.32	98.13	97.02
Mg#	59.4	56.8	59.1	57.7	60.3	57.6	61.4	57.7	57.5	58.8	58.4	60.1	58.2	56.6
Trace elements (ppm)														
Sc	21.8	20.2	18.3	20.9	22.6	23.4	20.9	21.1	25.1	21.8	19.5	25.0	20.3	25.5
V	161	155	163	163	144	138	141	138	165	152	147	140	128	149
Cr	224	146	297	243	230	215	291	208	218	207	193	248	254	237
Co	52.3	60.1	57.1	54.8	67.5	57.2	66.6	58.6	59.1	54.5	61.6	61.8	48.5	64.7
Ni	151	136	146	173	172	172	230	137	158	181	184	170	168	150
Cu	55.6	44.1	57.7	63.9	58.1	68.5	75.0	59.6	67.2	66.1	68.5	52.7	70.4	70.3
Zn	113	117	123	130	118	118	118	116	123	119	120	112	110	124
Rb	28.0	22.0	23.9	20.1	19.4	19.8	17.4	23.5	16.0	17.1	11.3	14.7	13.0	10.6
Sr	498	442	375	401	367	337	329	311	306	337	365	319	322	346
Y	23.9	24.4	22.4	24.2	21.3	22.8	21.5	20.2	21.2	22.4	20.7	21.6	22.2	23.0
Zr	182	164	146	152	143	150	120	120	121	134	130	112	117	126
Nb	31.2	23.1	20.7	24.4	20.4	22.2	21.1	16.8	16.9	18.7	19.0	18.7	18.9	21.1
Ba	272	214	153	160	127	148	186	169	127	124	135	168	186	216
La	22.2	16.2	15.0	17.5	15.1	12.8	13.5	13.0	11.8	12.3	12.7	13.0	12.9	15.4
Ce	42.9	33.5	31.3	34.8	32.3	28.2	26.9	27.5	25.3	26.8	25.5	27.3	30.1	32.7
Nd	20.8	17.9	17.3	20.4	18.2	15.5	14.4	14.5	14.1	12.6	15.2	13.5	16.8	16.3
Sm	5.99	5.06	4.78	5.36	4.77	4.10	4.15	3.84	3.83	4.47	4.24	3.79	4.00	4.40
Eu	2.04	1.84	1.76	1.93	1.78	1.71	1.51	1.46	1.39	1.61	1.63	1.53	1.60	1.75
Tb	0.79	0.59	0.72	0.79	0.67	0.70	0.79	0.57	0.85	0.69	0.73	0.62	0.69	0.73
Yb	1.23	1.44	1.50	1.61	1.41	1.77	1.38	1.57	1.50	1.17	1.56	1.75	1.66	1.50
Lu	0.18	0.21	0.18	0.21	0.22	0.20	0.19	0.19	0.22	0.17	0.18	0.19	0.18	0.21
Hf	4.13	4.10	3.40	3.89	3.62	4.20	2.71	3.16	2.67	3.04	3.65	3.17	3.36	3.58
Ta	1.91	1.38	1.17	1.31	1.35	1.60	1.42	1.11	0.85	1.12	1.42	1.03	1.16	1.30
Th	2.65	1.40	2.29	2.44	2.18	1.67	1.90	2.05	1.73	1.89	1.42	1.75	1.80	1.91
U	0.90	0.64	0.64	0.60	0.68	0.60	0.35	0.68	0.40	0.65	0.42	0.59	0.44	0.44
[La/Sm] _N	2.40	2.07	2.03	2.11	2.05	2.02	2.10	2.19	1.99	1.78	1.94	2.22	2.08	2.26
[Nb/Th] _N	1.38	1.94	1.06	1.18	1.10	1.56	1.31	0.96	1.15	1.16	1.57	1.26	1.23	1.30
[Ta/U] _N	1.09	1.10	0.94	1.12	1.02	1.37	2.08	0.84	1.09	0.88	1.73	0.89	1.35	1.51
Nb/U	34.67	36.09	32.34	40.67	30.00	37.00	60.29	24.71	42.25	28.77	45.24	31.69	42.95	47.95
Zr/Hf	44.00	39.90	42.91	39.02	39.36	35.76	44.35	37.97	45.32	43.91	35.67	35.24	34.70	35.25
Sr-Nd-Pb isotopes														
⁸⁷ Sr/ ⁸⁶ Sr	0.703893	0.704028			0.704149					0.704308	0.704220			0.704474
¹⁴³ Nd/ ¹⁴⁴ Nd	0.512925	0.512907			0.512908					0.512881	0.512876			0.512859
²⁰⁶ Pb/ ²⁰⁴ Pb	18.593	18.682			18.679					18.738	18.726			18.622
²⁰⁷ Pb/ ²⁰⁴ Pb	15.542	15.619			15.568					15.611	15.603			15.597
²⁰⁸ Pb/ ²⁰⁴ Pb	38.69	38.91			38.78					38.90	38.84			

Supplementary Table 3 Continued

Locality													
Sample	HN9	HN11	HN14	HN15	HN16	HN18	HN92	HN93	HN94	HN7	HN20	HN21	HN25
Rock Type	QT	QT	QT	QT	OT	OT							
Major elements (wt. %)													
SiO ₂	54.08	52.34	53.20	51.59	51.85	51.25	52.42	52.09	51.71	53.65	51.72	50.67	51.22
TiO ₂	1.59	2.02	1.86	1.89	1.81	1.83	1.81	1.81	1.73	2.06	2.36	2.41	2.41
Al ₂ O ₃	14.82	14.52	14.54	14.25	14.21	14.41	14.16	14.21	14.40	14.11	14.53	14.88	14.85
TFe ₂ O ₃	14.90	11.84	10.40	11.28	10.95	11.26	10.96	11.09	11.56	11.52	11.29	11.43	11.15
MnO	0.15	0.19	0.12	0.16	0.16	0.14	0.13	0.13	0.14	0.23	0.14	0.14	0.14
MgO	7.09	6.57	6.56	6.08	6.58	7.16	7.06	6.94	6.79	6.98	6.42	6.64	6.48
CaO	8.72	8.77	8.13	8.47	9.27	8.40	8.30	8.28	8.51	8.74	8.43	9.15	8.95
Na ₂ O	3.02	3.14	2.98	2.97	2.98	2.82	3.01	3.02	2.74	3.13	2.99	3.20	3.38
K ₂ O	0.89	0.97	0.72	1.05	0.67	0.59	0.92	0.94	0.61	0.94	1.56	1.59	1.69
P ₂ O ₅	0.25	0.27	0.29	0.34	0.26	0.25	0.25	0.22	0.19	0.29	0.41	0.43	0.42
Total	105.51	100.64	98.80	98.09	98.73	98.11	99.02	98.74	98.38	101.66	99.86	100.55	100.70
Mg#	57.9	56.0	59.4	55.4	58.0	59.5	59.8	59.1	57.6	58.2	57.0	57.4	57.3
Trace elements (ppm)													
Sc	21.9	22.1	23.3	18.0	22.0	23.8	23.0	19.0	24.2	21.6	21.0	19.2	21.2
V	142	145	145	131	136	143	145	142	133	140	193	196	198
Cr	211	202	226	225	246	233	233	314	205	241	282	261	271
Co	66.4	58.5	45.5	55.7	52.6	51.9	53.0	50.5	48.9	61.4	59.6	52.9	56.0
Ni	144	165	173	155	161	171	176	170	135	184	87	88	87
Cu	61.2	67.8	90.8	94.7	66.1	66.9	64.7	65.5	50.0	83.2	37.6	52.5	49.3
Zn	111	125	107	125	112	116	116	113	120	114	118	117	120
Rb	21.4	19.3	15.4	22.3	13.4	9.2	16.5	18.9	11.8	20.9	34.4	25.6	27.7
Sr	214	380	318	330	341	322	329	330	336	320	517	549	525
Y	18.9	21.0	21.8	29.0	22.7	21.9	21.1	21.3	18.4	23.9	24.6	25.2	24.7
Zr	117	140	118	165	120	122	131	133	124	139	202	210	205
Nb	17.6	19.5	19.2	24.6	20.6	20.9	18.6	17.0	16.8	24.6	33.3	34.4	34.1
Ba	160	152	177	262	192	183	129	127	133	206	336	378	369
Locality													
Sample	HN26	HN29	HN30	HN31	HN38	HN39	HN42	HN44	HN45	HN46	HN47	HN48	HN49
Rock Type	OT	AB	OT	OT	OT	OT	OT	OT	OT	OT	OT	OT	OT
Major elements (wt. %)													
SiO ₂	51.94	46.49	49.49	50.26	53.05	51.53	52.66	48.98	48.87	49.42	50.38	49.62	48.71
TiO ₂	2.11	2.66	2.42	2.51	2.21	2.23	2.20	2.69	2.44	2.43	2.53	2.46	2.42
Al ₂ O ₃	14.94	13.59	13.87	14.07	15.49	15.61	15.23	14.31	14.03	14.27	14.30	14.45	14.05
TFe ₂ O ₃	11.08	13.11	11.43	11.24	11.38	11.58	11.17	11.58	11.30	11.06	11.22	11.15	11.51
MnO	0.15	0.18	0.14	0.14	0.14	0.14	0.14	0.15	0.15	0.14	0.14	0.14	0.15
MgO	6.80	9.12	8.10	7.49	6.14	6.03	5.81	7.58	7.18	6.95	7.31	7.35	8.00
CaO	8.57	10.23	9.24	9.25	8.61	8.59	8.47	9.59	9.08	9.06	9.27	9.24	8.60
Na ₂ O	3.18	2.48	3.12	3.36	3.45	3.28	3.26	2.97	2.86	3.02	3.30	3.01	2.97
K ₂ O	1.20	1.44	1.93	2.03	1.37	1.16	1.34	1.92	1.81	1.83	2.05	1.78	1.80
P ₂ O ₅	0.38	0.63	0.47	0.52	0.35	0.35	0.37	0.65	0.56	0.55	0.52	0.55	0.55
Total	100.37	99.92	100.21	100.88	102.19	100.51	100.65	100.44	98.29	98.73	101.00	99.75	98.77
Mg#	58.6	61.7	62.1	60.5	55.4	54.6	54.5	60.2	59.5	59.2	60.0	60.4	61.6
Trace elements (ppm)													
Sc	23.4	24.5	20.0	20.2	19.6	21.2	20.8	23.2	18.4	17.2	22.1	17.1	18.4
V	154	246	193	199	161	170	162	175	161	171	172	178	163
Cr	258	271	502	283	123	132	117	189	233	371	426	210	233
Co	62.2	64.7	62.9	55.2	60.4	60.0	53.1	52.8	51.4	51.0	55.1	57.6	52.9
Ni	142	196	145	122	124	133	115	153	146	177	159	156	153
Cu	63.4	56.0	60.5	62.3	54.4	48.8	60.5	54.1	55.7	52.2	49.7	51.6	52.6
Zn	119	128	116	114	119	121	118	119	116	114	113	117	120
Rb	20.1	27.4	39.9	43.9	25.0	18.7	25.1	40.7	38.3	38.7	36.3	36.7	37.2
Sr	456	720	597	504	448	453	440	654	580	573	574	611	567
Y	24.3	29.9	23.7	26.1	23.9	23.4	25.1	27.6	25.5	27.3	25.9	26.2	25.7
Zr	181	278	214	222	172	1							

Supplementary Table 3 Continued

Locality													
Sample	HN50	HN51	HN52	HN53	HN56	HN58	HN59	HN60	HN61	HN65	HN66	HN67	HN70
Rock Type	OT	OT	OT	OT	OT	OT	OT	OT	OT	OT	OT	OT	OT
Major elements (wt. %)													
SiO ₂	49.10	48.82	49.50	49.03	53.05	48.36	48.96	49.10	48.55	53.11	48.82	49.50	49.03
TiO ₂	2.41	2.40	2.44	2.37	2.27	2.31	2.33	2.41	2.39	2.00	2.40	2.44	2.37
Al ₂ O ₃	14.17	13.98	14.34	13.95	14.42	13.72	14.03	14.04	13.94	14.54	13.98	14.34	13.95
TFe ₂ O ₃	11.40	11.24	11.43	11.49	10.83	11.54	11.53	11.86	11.50	10.71	11.24	11.43	11.49
MnO	0.14	0.15	0.14	0.14	0.12	0.15	0.15	0.15	0.15	0.14	0.15	0.14	0.14
MgO	8.02	7.48	7.29	8.06	6.82	8.84	7.86	8.44	8.45	6.71	7.48	7.29	8.06
CaO	8.42	9.04	8.72	8.21	8.87	8.78	7.06	8.56	8.67	8.66	9.04	8.72	8.21
Na ₂ O	2.89	2.99	3.13	2.89	3.18	2.81	2.98	2.97	2.78	2.96	2.99	3.13	2.89
K ₂ O	1.80	1.77	1.87	1.84	1.68	1.65	1.72	1.75	1.77	1.22	1.77	1.87	1.84
P ₂ O ₅	0.53	0.56	0.55	0.54	0.48	0.51	0.53	0.53	0.54	0.32	0.56	0.55	0.54
Total	98.88	98.43	99.41	98.52	101.73	98.67	97.16	99.82	98.75	100.38	98.43	99.41	98.52
Mg#	61.9	60.6	59.5	61.8	59.3	63.9	61.1	62.1	62.9	59.2	60.6	59.5	61.8
Trace elements (ppm)													
Sc	21.8	16.3	19.1	14.8	18.5	15.4	19.7	21.6	17.9	22.4	20.1	23.0	19.1
V	170	165	177	167	176	158	159	158	164	163	165	166	184
Cr	194	202	383	194	209	208	364	206	210	245	232	244	223
Co	49.4	54.2	55.5	53.9	50.9	53.7	54.0	50.7	52.2	51.9	52.5	51.4	54.3
Ni	150	149	159	163	162	185	171	169	173	129	142	133	147
Cu	53.6	53.2	52.6	54.3	51.3	51.9	50.8	53.1	51.7	47.0	45.1	52.1	61.6
Zn	115	114	122	120	119	110	113	113	113	109	113	112	118
Rb	39.8	36.4	35.0	36.6	34.8	34.4	36.2	36.7	38.7	25.0	24.9	25.8	21.0
Sr	579	561	547	528	516	547	565	558	811	407	397	394	469
Y	26.0	25.0	25.8	26.0	25.7	25.3	25.3	25.0	26.1	23.2	23.3	23.5	24.8
Zr	217	216	219	221	204	207	201	210	206	152	151	150	177
Nb	41.9	42.2	41.7	43.5	37.1	38.9	39.0	41.0	41.5	23.0	22.4	23.1	28.2
Ba	391	375	383	357	328	368	364	410	405	210	173	179	254
Locality													
Sample	HN71	HN72	HN73	HN74	HN78	HN79	HN80	HN81	HN82	HN84	HN85	HN86	HN88
Rock Type	OT	OT	OT	OT	OT	OT	OT	OT	OT	OT	OT	OT	OT
SiO ₂	53.05	48.36	48.96	49.10	48.55	53.11	50.71	52.53	50.76	50.79	50.86	50.82	50.50
TiO ₂	2.27	2.31	2.33	2.41	2.39	2.00	2.28	2.27	2.31	2.28	2.30	2.30	2.31
Al ₂ O ₃	14.42	13.72	14.03	14.04	13.94	14.54	14.46	14.44	14.62	14.57	14.69	14.35	14.34
TFe ₂ O ₃	10.83	11.54	11.53	11.86	11.50	10.71	11.74	11.73	11.76	11.64	11.60	11.84	11.72
MnO	0.12	0.15	0.15	0.15	0.15	0.14	0.15	0.15	0.15	0.15	0.15	0.14	0.15
MgO	6.82	8.84	7.86	8.44	8.45	6.71	7.62	7.53	7.60	7.63	7.54	7.83	7.62
CaO	8.87	8.78	7.06	8.56	8.67	8.66	8.64	8.58	8.59	8.56	8.62	8.53	8.58
Na ₂ O	3.18	2.81	2.98	2.97	2.78	2.96	3.48	3.45	3.49	3.43	3.52	3.52	3.44
K ₂ O	1.68	1.65	1.72	1.75	1.77	1.22	1.54	1.55	1.57	1.55	1.59	1.56	1.60
P ₂ O ₅	0.48	0.51	0.53	0.53	0.54	0.32	0.48	0.47	0.49	0.45	0.50	0.47	0.51
Total	101.73	98.67	97.16	99.82	98.75	100.38	101.11	102.71	101.34	101.05	101.37	101.36	100.77
Mg#	59.3	63.9	61.1	62.1	62.9	59.2	60.0	59.8	59.9	60.2	60.0	60.4	60.1
Trace elements (ppm)													
Sc	25.6	18.2	23.2	18.9	21.9	18.1	15.9	19.6	22.3	23.6	23.7	19.6	22.7
V	162	152	156	151	162	160	159	157	160	156	164	161	164
Cr	236	198	209	211	233	274	606	231	228	228	216	229	232
Co	56.8	53.1	53.9	52.4	52.6	52.7	50.4	49.1	54.3	55.2	53.8	51.7	61.0
Ni	179	176	179	170	166	159	157	153	155	158	154	166	169
Cu	61.6	61.4	62.6	55.6	65.2	54.5	57.2	57.9	74.6	66.2	71.5	61.9	53.6
Zn	122	117	116	119	117	116	109	116	114	117	115	117	116
Rb	22.6	20.9	22.2	20.4	30.4	30.1	29.1	30.1	30.5	31.1	30.3	30.1	31.6
Sr	404	396	401	396	547	538	533	542	548	539	549	555	552
Y	23.3	23.0	24.4	21.6	25.2	25.4	24.4	25.6	25.9	26.4	25.4	26.6	25.0
Zr	157	152	155	152	199	196	193	197	203	198	201	200	199
Nb	23.1	22.6	22.9	22.5	36.7</td								

Supplementary Table 3 Continued

Locality		Hainan Island (Zou & Fan, 2010)								
Sample	HN9901	HN9902	106B1	HN9907	HN9908	HN9910	HN9911	HN9912	HN9914	119B1
Rock Type	OT	OT	OT	OT	AOB	AOB	AOB	AOB	OT	QT
Major elements (wt. %)										
SiO ₂	51.74	50.77	50.99	49.10	45.32	45.47	45.14	45.27	49.87	53.14
TiO ₂	2.34	2.37	2.27	2.30	2.81	2.76	2.76	2.75	2.17	1.62
Al ₂ O ₃	14.32	15.12	14.33	13.36	12.83	12.98	12.99	12.76	13.86	14.36
TFe ₂ O ₃	10.64	10.42	10.97	11.42	12.79	12.67	11.52	12.63	10.41	10.07
MnO	0.15	0.25	0.14	0.27	0.20	0.31	0.19	0.20	0.15	0.14
MgO	6.53	6.81	7.47	9.63	10.29	10.17	9.90	10.29	9.08	6.80
CaO	8.92	9.24	9.28	9.46	10.57	10.80	10.43	10.46	9.37	8.53
Na ₂ O	3.41	2.82	2.71	2.55	2.85	2.42	2.95	3.12	3.12	3.03
K ₂ O	1.68	1.46	1.38	1.53	1.64	1.43	1.61	1.63	1.53	1.00
P ₂ O ₅	0.47	0.47	0.47	0.48	0.86	0.82	0.75	0.79	0.42	0.23
Total	100.19	99.73	100.02	100.11	100.15	99.84	98.24	99.88	99.97	98.93
Mg#	59.0	60.0	61.0	66.0	65.0	65.0	66.0	65.0	67.0	61.0
Trace elements (ppm)										
Rb	35.6	30.0	28.8	32.4	36.5	35.0	35.2	38.8	30.0	23.6
Sr	546	559	489	557	817	820	769	811	525	318
Y	23.4	23.3	25.5	22.7	30.0	29.8	28.6	29.1	21.2	18.8
Zr	188	189	198	191	309	309	289	294	152	108
Nb	33.6	33.7	41.1	46.1	84.1	83.9	77.1	79.1	33.8	16.4
Ba	396	423	351	396	573	574	535	536	353	216
La	24.9	24.9	29.5	33.3	64.8	64.1	58.9	59.4	22.3	14.0
Ce	49.4	49.6	57.6	65.2	125.7	125.5	114.8	116.5	43.4	27.5
Pr	6.2	6.26	7.38	7.83	14.79	14.71	13.55	13.58	5.4	3.44
Nd	26.9	27.1	30.8	32.0	57.2	57.0	52.3	52.2	23.0	15.2
Sm	6.94	6.83	6.64	7.07	10.89	10.77	10.26	10.10	5.79	4.14
Eu	2.34	2.36	2.11	2.33	3.35	3.37	3.15	3.24	2.05	1.48
Gd	6.79	6.85	6.44	6.52	9.12	9.15	8.85	8.65	5.95	4.56
Tb	1.03	1.01	0.96	0.97	1.28	1.29	1.24	1.23	0.88	0.73
Dy	5.52	5.51	5.22	5.25	6.96	6.94	6.65	6.53	4.87	4.18
Ho	0.98	0.96	0.91	0.94	1.23	1.21	1.18	1.16	0.86	0.78
Er	2.26	2.20	2.19	2.23	2.97	2.87	2.77	2.72	2.07	1.89
Yb	1.61	1.53	1.78	1.66	2.17	2.15	2.04	2.06	1.46	1.44
Lu	0.22	0.22	0.26	0.24	0.32	0.32	0.30	0.31	0.22	0.21
Hf	4.85	4.92	4.80	4.87	7.60	7.72	7.24	7.16	3.93	3.02
Ta	2.04	2.04	2.44	2.80	5.20	5.25	4.77	4.79	2.05	0.98
Pb	3.03	3.53	4.06	3.53	5.19	5.27	3.98	4.84	2.48	2.79
Th	3.87	3.90	4.29	4.70	8.36	8.29	7.63	7.76	3.38	2.73
U	0.91	0.88	0.99	1.19	2.00	1.96	1.81	1.81	0.79	0.59
[La/Sm] _N	2.32	2.36	2.87	3.04	3.85	3.85	3.71	3.80	2.49	2.19
[Nb/Th] _N	1.02	1.02	1.13	1.15	1.18	1.19	1.19	1.20	1.17	0.71
[Ta/U] _N	1.15	1.19	1.26	1.21	1.33	1.37	1.35	1.36	1.33	0.85
Sr/Sr*	1.22	1.24	0.94	1.02	0.81	0.81	0.83	0.88	1.36	1.27
Nb/U	36.93	38.30	41.47	38.75	42.04	42.81	42.57	43.67	42.76	27.80
Zr/Hf	38.76	38.41	41.25	39.22	40.66	40.03	39.92	41.06	38.68	35.76
Pb/Ce	0.06	0.07	0.07	0.05	0.04	0.04	0.03	0.04	0.06	0.10
Sr-Nd-Pb isotopes										
⁸⁷ Sr/ ⁸⁶ Sr	0.703853	0.703919		0.70418	0.70423	0.704273		0.704182		
¹⁴³ Nd/ ¹⁴⁴ Nd	0.512868	0.512884		0.512848	0.512869	0.512861		0.512862		
²⁰⁶ Pb/ ²⁰⁴ Pb	18.631			18.655	18.692	18.696		18.705		
²⁰⁷ Pb/ ²⁰⁴ Pb	15.605			15.633	15.647	15.63		15.622		
²⁰⁸ Pb/ ²⁰⁴ Pb	38.846			38.874	38.881	38.872		38.853		

Supplementary Table 3 Continued

Locality		Hainan Island (Ho et al., 2000)								
Sample	HK04	HK11A	HK14	HK16	HK17	HK22	HK24A	HK25	HK27	HK28
Rock Type	AOB	AOB	AOB	OT	QT	OT	AOB	OT	QT	QT
Major elements (wt. %)										
SiO ₂	48.15	47.84	47.54	51.28	52.90	51.45	47.92	49.58	50.75	52.52
TiO ₂	2.28	2.26	3.13	1.89	1.59	1.94	2.27	2.02	1.98	1.74
Al ₂ O ₃	12.75	13.28	13.88	14.77	14.48	14.04	13.76	13.83	13.56	14.64
TFe ₂ O ₃	11.46	11.82	12.02	10.71	11.00	10.83	11.39	11.29	10.59	11.02
MnO	0.15	0.15	0.15	0.14	0.14	0.13	0.15	0.15	0.14	0.14
MgO	8.79	10.42	7.56	6.76	6.39	7.19	9.17	7.94	6.96	5.81
CaO	7.69	9.27	8.88	8.92	9.56	8.18	9.56	9.58	9.10	8.44
Na ₂ O	3.12	2.86	3.49	3.26	3.09	3.76	3.33	3.13	2.98	3.09
K ₂ O	2.25	1.78	1.97	1.18	0.55	1.71	1.65	1.32	1.07	0.71
P ₂ O ₅	0.78	0.45	0.67	0.35	0.19	0.43	0.42	0.37	0.24	0.24
Total	99.24	100.12	99.28	99.77	99.89	99.66	99.64	99.21	99.28	99.38
L.O.I.	1.81	-	-	0.51	-	-	-	-	1.91	1.04
Mg#	65.5	68.6	60.9	61.0	59.0	62.2	66.6	63.5	62.0	56.6
Trace elements (ppm)										
Sc	15.5	17.6	16.9	17.4	20.2	16.0	21.8	21.2	20.9	21.3
V	120	155	171	127	129	126	183	165	149	142
Cr	323	285	191	203	176	197	231	247	213	140
Co	50.0	64.0	55.0	60.0	52.0	55.0	55.0	52.0	50.0	51.0
Ni	301	294	139	189	110	150	222	200	164	117
Cu	27.0	54.0	53.0	55.0	59.0	54.0	53.0	57.0	63.0	56.0
Zn	137	112	126	120	108	121	109	112	105	111
Rb	50.0	41.0	43.0	24.0	12.0	33.0	32.0	21.0	24.0	13.0
Sr	840	520	661	438	259	554	609	443	341	321
Y	17.9	24.9	29.1	21.2	18.8	20.0	23.1	21.9	21.2	20.8
Zr	279	179	254	141	99	188	192	161	134	128
Nb	72.6	41.4	55.6	26.5	11.9	49.0	49.0	29.8	24.8	17.9
Ba	546	407	573	250	93	457	379	277	217	171
La	41.5	27.6	34.8	17.3	6.6	28.8	27.0	18.8	12.7	11.3
Ce	81.6	53.4	63.9	33.6	17.2	49.2	49.0	36.7	26.7	24.9
Nd	46.1	31.9	41.5	21.0	11.3	28.1	29.5	22.1	15.5	15.1
Sm	8.90	6.60	9.00	5.00	3.40	6.00	6.20	5.10	4.10	4.10
Eu	2.71	2.06	2.85	1.68	1.25	2.07	2.05	1.79	1.52	1.47
Tb	0.96	0.84	1.04	0.72	0.61	0.77	0.79	0.75	0.67	0.65
Yb	1.69	1.52	1.65	1.48	1.45	1.28	1.58	1.56	1.55	1.54
Lu	0.26	0.23	0.24	0.22	0.21	0.19	0.22	0.23	0.22	0.23
Hf	6.26	4.42	5.74	3.44	2.61	4.22	4.08	3.46	3.06	2.91
Th	6.10	4.52	5.14	2.72	1.17	4.41	3.78	2.99	2.10	1.70
U	1.49	0.98	1.15	0.77	0.32	0.70	0.80	0.83	0.58	0.51
[La/Sm] _N	3.01	2.70	2.50	2.24	1.25	3.10	2.81	2.38	2.00	1.78
[Nb/Th] _N	1.40	1.08	1.27	1.15	1.20	1.31	1.52	1.17	1.39	1.24
Nb/U	48.72	42.24	48.35	34.42	37.19	70.00	61.25	35.90	42.76	35.10
Zr/Hf	44.57	40.50	44.25	40.99	37.93	44.55	47.06	46.53	43.79	43.99

Supplementary Table 3 Continued

Locality		Hainan Island (Wang et al., 2011)											
Sample	08HN-2A	08HN-2B	08HN-3	08HN-4A	08HN-4B	08HN-4C	08HN-4D	08HN-4G	08HN-5A	08HN-5B	08HN-5C	08HN-5D	08HN-5E
Rock Type	AB	AB	OT	QT	QT	QT	OT						
Major elements (wt. %)													
SiO ₂	47.50	47.80	47.30	52.10	52.00	52.00	50.50	52.00	51.20	51.10	51.00	50.90	51.10
TiO ₂	2.98	2.85	2.70	1.98	1.91	2.12	1.83	2.02	1.91	1.99	1.96	1.99	1.98
Al ₂ O ₃	13.00	13.20	12.70	13.80	13.60	14.00	12.90	13.90	13.70	13.90	14.00	13.90	13.90
TFe ₂ O ₃	13.20	13.00	13.50	11.60	11.80	11.60	12.00	11.60	12.30	11.90	11.90	12.00	11.80
MnO	0.14	0.14	0.14	0.12	0.13	0.13	0.15	0.13	0.13	0.14	0.14	0.14	0.14
MgO	9.68	9.29	10.60	7.79	8.13	7.25	10.40	7.47	7.85	7.75	7.99	7.83	7.76
CaO	7.89	8.00	8.22	8.60	8.47	8.79	8.58	8.49	8.92	8.56	8.63	8.60	8.76
Na ₂ O	3.40	3.32	2.69	2.94	2.89	2.96	2.70	3.09	2.91	3.15	3.08	3.16	3.16
K ₂ O	1.52	1.64	1.59	0.81	0.82	0.85	0.64	0.95	0.73	1.11	1.01	1.11	1.07
P ₂ O ₅	0.67	0.69	0.49	0.24	0.23	0.32	0.28	0.28	0.30	0.36	0.35	0.36	0.36
Total	99.98	99.93	99.93	99.98	99.97	100.01	99.98	99.93	99.95	99.95	100.05	99.99	100.03
L.O.I.	0.73	0.72	0.85	0.60	0.76	0.89	0.68	0.20	1.29	0.71	0.92	0.68	0.67
Mg#	61.7	61.1	63.3	59.7	60.2	57.8	65.6	58.5	58.4	58.9	59.6	59.0	59.1
Trace elements (ppm)													
Sc	17.9	16.8	20.0		20.4	21.4	21.0				20.8	20.1	20.9
V	156	144	159		142	154	142				150	154	175
Cr	284	248	314		273	207	386				214	196	209
Co	50.5	47.0	55.9		43.7	40.5	49.5				41.6	43.3	43.2
Ni	268	248	307		191	168	310				156	162	162
Cu	47.8	41.2	51.4		60.6	66.4	53.3				56.6	57.7	58.4
Zn	140	125	120		113	114	104				105	109	108
Rb	50.0	50.1	26.4		15.8	13.4	6.4				15.9	21.9	17.7
Sr	764	906	587		318	382	388				391	429	431
Y	23.0	23.2	20.3		17.1	19.9	16.6				19.0	20.5	20.2
Zr	264	260	189		106	138	115				126	138	135
Nb	61.2	58.8	41.7		18.1	27.0	23.9				29.6	31.2	31.0
Ba	626	870	424		185	221	231				284	339	335
La	39.7	40.3	26.7		12.4	18.0	17.4				21.0	22.7	22.6
Ce	81.8	82.0	55.1		25.6	36.3	34.6				41.6	45.2	45.0
Pr	10.2	10.2	7.11		3.27	4.5	4.22				5	5.43	5.49
Nd	41.0	41.2	29.7		14.2	19.1	17.2				20.2	22.1	21.7
Sm	8.76	8.62	6.72		3.86	4.71	4.08				4.80	5.12	4.96
Eu	2.87	2.85	2.26		1.44	1.75	1.52				1.70	1.78	1.70
Gd	7.94	7.57	6.35		4.25	5.13	4.33				5.15	5.29	5.25
Tb	1.10	1.05	0.90		0.69	0.77	0.68				0.83	0.82	0.83
Dy	5.52	5.40	4.49		3.83	4.11	3.68				4.38	4.44	4.46
Ho	0.93	0.90	0.78		0.69	0.74	0.65				0.76	0.82	0.80
Er	2.22	2.12	1.86		1.78	1.86	1.58				1.96	2.01	1.97
Tm	0.27	0.27	0.24		0.22	0.24	0.21				0.26	0.26	0.27
Yb	1.53	1.56	1.42		1.31	1.39	1.23				1.49	1.51	1.53
Lu	0.21	0.22	0.21		0.19	0.20	0.18				0.21	0.22	0.22
Hf	6.23	6.25	4.55		2.76	3.41	2.96				3.25	3.34	3.33
Ta	4.18	3.98	2.81		1.13	1.57	1.50				1.84	1.74	1.80
Pb	2.69	2.40	1.88		5.45	1.34	1.57				1.61	4.43	2.43
Th	5.20	5.20	3.65		1.85	2.80	2.61				3.51	3.04	3.39
U	1.26	1.28	0.90		0.43	0.59	0.57				0.74	0.65	0.69
[La/Sm] _N	2.93	3.02	2.57		2.08	2.47	2.76				2.87	2.83	2.94
[Nb/Th] _N	1.38	1.33	1.34		1.15	1.13	1.08				1.05	1.14	1.08
[Ta/U] _N	1.70	1.59	1.61		1.36	1.35	1.34				1.38	1.27	1.33
Sr/Sr*	1.08	1.27	1.17		1.35	1.19	1.31				1.12	1.13	1.14
Nb/U	48.57	45.94	46.59		42.49	45.45	41.78				45.75	42.16	44.67
Zr/Hf	42.38	41.60	41.54		38.41	40.47	38.85				38.77	41.32	40.54
Pb/Ce	0.03	0.03	0.03		0.21	0.04	0.05				0.11	0.04	0.05

Supplementary Table 3 Continued

Locality													
Sample	08HN-5F	08HN-5G	08HN-5H	08HN-5I	08HN-5J	08HN-5K	08HN-6A	08HN-6B	08HN-6C	08HN-6D	08HN-6F	08HN-7A	08HN-7B
Rock Type	QT	OT	OT	QT	OT	OT	QT						
Major elements (wt. %)													
SiO ₂	52.10	51.20	51.00	51.50	51.00	51.10	53.20	52.90	52.90	53.30	52.90	52.80	53.10
TiO ₂	1.93	2.00	1.97	1.96	1.89	2.22	1.81	1.78	1.80	1.84	1.78	1.77	1.66
Al ₂ O ₃	13.90	13.90	14.00	13.90	13.90	13.90	14.40	14.30	14.40	14.50	14.20	14.50	14.50
TFe ₂ O ₃	11.80	11.80	11.90	12.10	12.00	12.70	12.30	12.40	12.30	12.00	12.70	12.60	12.00
MnO	0.14	0.14	0.13	0.14	0.15	0.13	0.12	0.14	0.14	0.12	0.13	0.13	0.13
MgO	7.36	7.61	7.81	7.56	8.63	6.86	5.91	5.84	5.94	5.93	5.94	5.86	6.26
CaO	8.63	8.63	8.55	8.77	8.44	8.40	8.36	8.63	8.62	8.24	8.43	8.53	8.71
Na ₂ O	3.03	3.20	3.15	2.96	2.88	3.19	3.06	2.88	2.87	3.04	3.00	3.17	2.96
K ₂ O	0.80	1.11	1.10	0.75	0.86	1.09	0.69	0.83	0.81	0.72	0.67	0.51	0.46
P ₂ O ₅	0.28	0.37	0.36	0.31	0.33	0.35	0.23	0.22	0.22	0.23	0.23	0.19	0.16
Total	99.96	99.95	99.97	99.94	100.07	99.95	100.08	99.93	100.00	99.92	99.97	100.06	99.93
L.O.I.	0.98	0.71	1.02	0.74	2.03	0.01	0.53	0.79	0.67	0.80	0.71	0.49	0.17
Mg#	57.8	58.7	59.0	57.9	61.4	54.3	51.4	50.8	51.5	52.1	50.7	50.6	53.4
Trace elements (ppm)													
Sc	20.9			22.3	20.5	22.0	20.3		21.4	20.2			22.2
V	146			152	140	161	141		144	136			142
Cr	200			196	214	171	138		150	154			167
Co	41.9			40.2	45.0	41.5	38.9		41.0	39.4			41.6
Ni	152			145	176	134	95		99	97			100
Cu	64.3			60.6	59.6	65.0	53.4		55.6	40.4			51.9
Zn	109			109	108	123	111		112	116			109
Rb	12.1			14.3	11.6	23.5	9.0		12.4	9.9			6.4
Sr	350			387	380	367	310		327	325			268
Y	19.7			20.3	19.4	22.1	17.0		16.6	17.3			17.4
Zr	116			124	125	146	111		110	117			91
Nb	20.7			25.0	28.5	28.6	14.6		14.6	15.7			9.7
Ba	205			228	292	239	145		136	151			82
La	15.7			18.0	20.4	20.1	11.3		11.3	11.7			8.2
Ce	31.8			36.4	40.8	40.8	24.2		24.7	25.7			17.6
Pr	3.98			4.59	4.98	5.12	3.23		3.3	3.36			2.56
Nd	16.9			18.4	20.3	21.3	14.4		14.5	14.6			12.2
Sm	4.46			4.57	4.77	5.07	3.97		3.97	4.04			3.56
Eu	1.57			1.68	1.64	1.70	1.46		1.48	1.53			1.36
Gd	4.81			5.05	4.87	5.49	4.32		4.27	4.43			4.1
Tb	0.78			0.80	0.77	0.89	0.72		0.71	0.70			0.68
Dy	4.27			4.30	4.16	4.74	3.91		3.79	3.75			3.81
Ho	0.78			0.77	0.77	0.87	0.72		0.69	0.67			0.71
Er	1.92			1.96	1.90	2.14	1.79		1.73	1.62			1.77
Tm	0.26			0.27	0.25	0.28	0.24		0.23	0.23			0.23
Yb	1.50			1.54	1.52	1.70	1.39		1.33	1.29			1.38
Lu	0.22			0.22	0.23	0.24	0.21		0.19	0.20			0.20
Hf	3.21			3.17	3.27	3.82	3.08		2.93	3.04			2.56
Ta	1.28			1.50	1.70	1.80	0.96		0.91	0.93			0.61
Pb	1.56			1.57	1.54	2.22	1.26		1.51	1.69			1.24
Th	2.38			2.78	3.15	3.13	1.55		1.54	1.60			0.98
U	0.51			0.57	0.63	0.66	0.35		0.38	0.37			0.23
[La/Sm] _N	2.28			2.55	2.76	2.56	1.84		1.84	1.87			1.49
[Nb/Th] _N	1.02			1.06	1.06	1.07	1.11		1.11	1.15			1.16
[Ta/U] _N	1.30			1.35	1.38	1.40	1.40		1.24	1.29			1.39
Sr/Sr*	1.23			1.21	1.09	1.01	1.32		1.37	1.34			1.39
Nb/U	40.99			43.86	45.02	43.53	41.60		38.83	42.43			43.07
Zr/Hf	36.14			39.12	38.23	38.22	36.04		37.54	38.49			35.39
Pb/Ce	0.05			0.04	0.04	0.05	0.05		0.06	0.07			0.07

Supplementary Table 3 Continued

Locality		Hainan Island (Wang et al., 2011)												
Sample		08HN-7D	08HN-7E	08HN-8A	08HN-8B	08HN-9A	08HN-9B	08HN-9C	08HN-10A	08HN-10B	08HN-10C	08HN-11A	08HN-11B	08HN-12A
Rock Type	QT	QT	OT	AB	QT	QT	QT	QT	QT	QT	QT	QT	QT	OT
Major elements (wt. %)														
SiO ₂	53.30	53.20	49.60	49.90	52.50	52.90	52.90	52.20	52.80	52.80	52.70	52.80	51.10	
TiO ₂	1.64	1.66	2.25	2.36	1.71	1.74	1.75	1.92	1.91	1.96	1.98	1.99	1.90	
Al ₂ O ₃	14.50	14.50	12.80	13.40	14.30	14.50	14.50	13.50	13.70	13.90	13.80	13.90	14.00	
TFe ₂ O ₃	11.90	12.10	12.70	12.30	13.20	12.70	11.80	11.70	11.80	11.40	11.40	11.20	11.30	
MnO	0.13	0.13	0.17	0.13	0.13	0.13	0.13	0.12	0.13	0.13	0.13	0.12	0.10	
MgO	6.18	6.43	8.96	7.61	5.97	6.05	6.00	7.05	7.19	7.15	6.77	6.78	7.09	
CaO	8.69	8.36	8.31	8.61	8.66	8.38	8.73	9.27	8.26	8.40	9.04	8.97	8.88	
Na ₂ O	2.94	2.90	3.24	3.47	2.91	2.89	3.41	2.97	3.00	3.08	2.88	2.90	3.56	
K ₂ O	0.53	0.52	1.50	1.71	0.45	0.50	0.58	0.71	0.91	0.97	1.10	1.11	1.63	
P ₂ O ₅	0.16	0.17	0.44	0.48	0.17	0.18	0.18	0.26	0.26	0.26	0.27	0.27	0.39	
Total	99.97	99.97	99.97	99.97	100.01	99.97	99.97	99.70	99.96	100.05	100.07	100.04	99.95	
L.O.I.	0.01	0.21	-0.18	0.18	0.27	0.23	0.20	0.87	0.02	-0.16	0.53	0.34	1.61	
Mg#	53.3	53.8	60.8	57.6	49.8	51.1	52.7	57.0	57.3	58.0	56.7	57.2	58.0	
Trace elements (ppm)														
Sc	21.3	22.1			21.0			20.0	19.4		19.6		16.6	
V	133	170			140			144	151		145		131	
Cr	170	248			159			206	217		204		202	
Co	43.2	58.7			42.9			42.0	41.7		41.0		44.1	
Ni	102	165			111			156	156		138		144	
Cu	51.0	47.9			45.0			55.8	57.2		53.3		54.9	
Zn	107	128			111			111	111		106		118	
Rb	7.1	22.0			7.2			13.9	13.9		17.2		20.2	
Sr	209	558			198			433	348		373		525	
Y	16.4	21.3			44.6			19.5	18.8		19.4		16.3	
Zr	90	199			94			122	122		128		170	
Nb	10.1	37.3			11.3			15.6	15.9		16.6		39.6	
Ba	94	524			114			146	143		159		443	
La	8.4	25.4			37.3			12.4	12.3		12.6		25.2	
Ce	18.5	50.7			82.2			27.5	27.0		27.6		48.7	
Pr	2.71	6.4			10.9			3.66	3.59		3.7		5.9	
Nd	12.7	27.1			45.5			16.3	16.0		16.4		23.7	
Sm	3.71	6.40			11.70			4.55	4.40		4.36		5.48	
Eu	1.44	2.26			4.18			1.63	1.59		1.60		2.00	
Gd	4.15	6.35			11.6			4.79	4.74		4.71		5.56	
Tb	0.68	0.90			1.93			0.76	0.75		0.78		0.81	
Dy	3.72	4.61			9.99			4.23	4.11		4.22		3.89	
Ho	0.70	0.80			1.75			0.77	0.77		0.75		0.63	
Er	1.72	1.86			4.12			1.88	1.93		1.88		1.46	
Tm	0.23	0.23			0.56			0.26	0.26		0.25		0.18	
Yb	1.34	1.36			3.12			1.45	1.47		1.48		1.02	
Lu	0.20	0.19			0.43			0.21	0.21		0.21		0.14	
Hf	2.54	4.98			2.64			3.17	3.32		3.46		4.08	
Ta	0.63	2.24			0.71			0.96	1.01		1.04		2.44	
Pb	0.89	0.32			1.17			2.08	2.20		2.05		2.09	
Th	1.04	3.32			1.06			1.98	2.02		2.21		4.13	
U	0.26	0.86			0.32			0.48	0.48		0.53		0.29	
[La/Sm] _N	1.47	2.56			2.06			1.76	1.81		1.87		2.97	
[Nb/Th] _N	1.14	1.32			1.25			0.93	0.93		0.88		1.13	
[Ta/U] _N	1.24	1.33			1.13			1.02	1.08		1.01		4.29	
Sr/Sr*	1.03	1.22			0.26			1.62	1.33		1.39		1.28	
Nb/U	38.85	43.22			34.88			32.43	33.13		31.32		136.08	
Zr/Hf	35.59	39.96			35.61			38.49	36.75		36.99		41.67	
Pb/Ce	0.05	0.01			0.01			0.08	0.08		0.07		0.04	

Supplementary Table 3 Continued

Hainan Island (Wang et al., 2011)													
Locality	08HN-12B	08HN-13A	08HN-13B	08HN-14A	08HN-14B	08HN-15A	08HN-15B	08HN-16A	08HN-16B	08HN-16C	08HN-17A	08HN-17B	08HN-18A
Sample	OT	OT	OT	OT	OT	QT	QT	AB	AB	AB	OT	AB	QT
Rock Type	OT	OT	OT	OT	OT	QT	QT	AB	AB	AB	OT	AB	QT
Major elements (wt. %)													
SiO ₂	51.10	51.60	51.70	53.90	53.80	52.80	52.90	51.40	51.30	51.40	55.70	55.50	52.80
TiO ₂	1.96	1.67	1.67	1.71	1.71	1.65	1.59	2.06	2.09	2.04	1.54	1.53	1.63
Al ₂ O ₃	13.90	14.40	14.40	14.80	14.60	14.30	14.30	14.20	14.20	14.10	15.00	14.90	14.20
TFe ₂ O ₃	11.90	11.70	11.80	10.40	10.40	12.30	12.30	11.30	11.40	11.30	9.10	9.04	12.50
MnO	0.12	0.12	0.13	0.10	0.10	0.13	0.13	0.11	0.11	0.11	0.09	0.09	0.13
MgO	7.32	7.09	6.98	5.54	5.83	6.66	6.64	6.69	6.80	6.79	4.89	4.96	6.56
CaO	7.79	8.19	8.10	6.01	6.20	8.43	8.50	6.86	7.03	6.94	4.90	4.86	8.48
Na ₂ O	3.73	3.56	3.56	4.52	4.45	3.01	2.99	4.30	4.10	4.28	4.89	5.11	2.96
K ₂ O	1.68	1.36	1.35	2.65	2.59	0.58	0.58	2.62	2.55	2.59	3.46	3.46	0.56
P ₂ O ₅	0.39	0.29	0.29	0.44	0.43	0.17	0.16	0.48	0.48	0.47	0.49	0.47	0.18
Total	99.89	99.99	99.98	100.07	100.11	100.04	100.10	100.02	100.07	100.03	100.06	99.92	100.00
L.O.I.	-0.62	-0.17	-0.01	-0.28	-0.47	-0.32	-0.41	-0.46	-0.26	-0.54	0.20	-0.01	0.52
Mg#	57.4	57.2	56.5	54.0	55.3	54.4	54.4	56.7	56.8	57.1	54.2	54.7	53.6
Trace elements (ppm)													
Sc	18.8		12.9			21.7		18.4			14.6		9.5
V	128		100			143		133			135		86
Cr	267		178			190		173			171		116
Co	46.0		35.8			45.5		41.5			39.5		29.1
Ni	166		116			130		144			103		84
Cu	52.6		33.1			62.0		55.5			48.6		42.3
Zn	118		140			114		128			144		152
Rb	20.0		35.3			8.4		17.4			39.2		56.5
Sr	532		672			293		416			680		742
Y	15.1		14.6			16.1		18.8			16.1		14.1
Zr	135		291			94		148			275		440
Nb	31.1		57.8			11.2		26.7			55.6		79.8
Ba	365		644			106		218			533		711
La	19.2		39.6			8.2		17.9			33.5		49.6
Ce	38.5		73.8			18.3		37.4			66.6		92.6
Pr	4.8		9.24			2.5		4.8			7.99		10.6
Nd	19.3		36.0			11.8		20.9			31.3		38.7
Sm	4.65		7.67			3.54		5.14			6.75		7.88
Eu	1.62		2.62			1.34		1.77			2.28		2.57
Gd	4.45		6.89			3.9		5.14			5.99		6.78
Tb	0.68		0.92			0.64		0.82			0.84		0.90
Dy	3.43		4.08			3.45		4.18			3.98		3.84
Ho	0.57		0.60			0.65		0.76			0.61		0.55
Er	1.38		1.30			1.66		1.78			1.39		1.09
Tm	0.17		0.16			0.22		0.23			0.17		0.12
Yb	0.99		0.79			1.24		1.34			0.95		0.68
Lu	0.14		0.11			0.19		0.20			0.13		0.09
Hf	3.51		6.97			2.57		3.70			6.48		9.69
Ta	1.85		3.77			0.71		1.68			3.60		5.47
Pb	1.27		3.37			1.26		2.37			2.91		4.36
Th	2.95		5.88			1.18		2.77			5.44		8.63
U	0.44		0.66			0.27		0.68			1.31		1.53
[La/Sm] _N	2.67		3.34			1.50		2.25			3.21		4.07
[Nb/Th] _N	1.24		1.16			1.12		1.13			1.20		1.09
[Ta/U] _N	2.15		2.92			1.36		1.27			1.41		1.83
Sr/Sr*	1.59		1.06			1.56		1.20			1.24		1.05
Nb/U	70.52		87.44			41.95		39.32			42.44		52.16
Zr/Hf	38.46		41.75			36.50		40.00			42.44		45.41
Pb/Ce	0.03		0.05			0.07		0.06			0.04		0.05

Supplementary Table 3 Continued

Locality	Hainan Island (Wang et al., 2011)												
Sample	08HN-18B	08HN-18C	08HN-18D	08HN-19A	08HN-19B	08HN-19C	08HN-19D	08HN-20A	08HN-20B	08HN-21A	08HN-21B	08HN-21C	08HN-21D
Rock Type	QT	QT	QT	AB	AB	AB	AB	OT	OT	OT	OT	OT	QT
Major elements (wt. %)													
SiO ₂	52.80	52.90	52.80	48.10	48.10	48.40	48.40	51.00	51.10	52.10	51.90	52.20	52.20
TiO ₂	1.59	1.61	1.62	3.19	3.15	3.16	3.19	2.41	2.43	1.92	1.85	1.95	1.96
Al ₂ O ₃	14.30	14.20	14.30	13.10	13.00	13.00	13.30	13.60	13.60	14.30	14.20	14.20	14.20
TFe ₂ O ₃	12.40	12.50	12.40	12.90	12.80	12.80	12.80	12.20	12.20	11.80	12.00	12.00	12.00
MnO	0.13	0.13	0.13	0.16	0.14	0.14	0.16	0.13	0.12	0.13	0.13	0.13	0.13
MgO	6.71	6.62	6.66	8.22	8.22	8.04	7.82	7.46	7.37	6.90	7.05	6.61	6.67
CaO	8.47	8.40	8.46	8.60	8.63	8.68	8.52	8.13	8.06	8.11	8.08	8.02	8.02
Na ₂ O	2.95	2.95	2.96	3.19	3.34	3.27	3.30	3.37	3.31	3.27	3.30	3.34	3.32
K ₂ O	0.52	0.56	0.51	1.91	1.89	1.89	1.95	1.35	1.36	1.22	1.18	1.22	1.17
P ₂ O ₅	0.17	0.17	0.17	0.66	0.65	0.65	0.68	0.41	0.41	0.32	0.31	0.33	0.33
Total	100.04	100.04	100.02	100.03	99.92	100.03	100.11	100.06	99.96	100.06	100.00	100.00	100.01
L.O.I.	0.36	0.33	0.41	-0.39	-0.51	-0.41	-0.41	-0.40	-0.40	-0.22	-0.30	-0.54	-0.26
Mg#	54.4	53.9	54.2	58.4	58.5	58.1	57.4	57.4	57.1	56.3	56.5	54.8	55.1
Trace elements (ppm)													
Sc	21.5			19.5		19.1		18.7		18.6		18.5	
V	134			194		177		159		152		140	
Cr	181			229		220		217		197		197	
Co	44.7			49.3		47.6		44.5		46.0		43.9	
Ni	134			144		138		141		162		156	
Cu	76.4			62.9		57.0		62.0		53.0		50.7	
Zn	116			147		139		124		127		117	
Rb	7.4			31.9		30.8		16.9		20.2		19.2	
Sr	286			665		626		486		458		434	
Y	14.8			26.8		28.5		26.2		18.1		17.8	
Zr	92			257		243		172		141		138	
Nb	12.1			48.0		46.2		28.7		25.7		24.6	
Ba	111			636		616		220		215		208	
La	8.5			33.3		33.7		18.3		16.5		16.3	
Ce	18.7			69.0		67.3		37.3		34.4		33.5	
Pr	2.49			8.96		8.84		4.97		4.44		4.27	
Nd	11.2			38.1		37.3		22.1		19.0		18.1	
Sm	3.26			8.82		8.57		5.76		4.84		4.58	
Eu	1.26			2.80		2.85		2.12		1.68		1.72	
Gd	3.69			8.36		8.56		6.09		4.9		4.76	
Tb	0.60			1.22		1.24		0.94		0.75		0.72	
Dy	3.30			6.01		6.10		4.83		3.98		3.78	
Ho	0.61			1.05		1.02		0.84		0.69		0.66	
Er	1.55			2.32		2.40		2.01		1.70		1.62	
Tm	0.21			0.28		0.29		0.25		0.23		0.22	
Yb	1.18			1.62		1.60		1.32		1.31		1.23	
Lu	0.17			0.22		0.23		0.19		0.19		0.17	
Hf	2.53			6.08		5.62		4.12		3.42		3.33	
Ta	0.78			3.14		2.98		1.76		1.56		1.49	
Pb	3.52			2.08		2.18		1.00		2.66		1.76	
Th	1.25			4.59		4.34		2.28		2.61		2.42	
U	0.26			1.04		0.97		0.62		0.69		0.64	
[La/Sm] _N	1.69			2.44		2.54		2.05		2.20		2.30	
[Nb/Th] _N	1.14			1.23		1.25		1.48		1.16		1.20	
[Ta/U] _N	1.54			1.55		1.57		1.46		1.16		1.20	
Sr/Sr*	1.57			1.04		1.00		1.34		1.44		1.43	
Nb/U	46.72			46.15		47.43		46.52		37.41		38.74	
Zr/Hf	36.17			42.27		43.24		41.75		41.23		41.44	
Pb/Ce	0.19			0.03		0.03		0.03		0.08		0.05	

Supplementary Table 3 Continued

Locality													
Sample	08HN-21E	08HN-22A	08HN-22B	08HN-22C	08HN-22D	08HN-23A	08HN-23B	08HN-24A	08HN-24B	08HN-24C	08HN-24D	08HN-25A	08HN-25B
Rock Type	QT	OT	AB	AB	AB	AB	OT	AB	AB	OT	AB	OT	OT
Major elements (wt. %)													
SiO ₂	53.10	49.30	49.30	49.50	46.60	49.40	49.20	48.00	47.80	50.60	48.00	49.80	50.00
TiO ₂	2.10	2.51	2.50	2.58	2.64	2.60	2.55	2.43	2.41	2.05	2.33	2.10	2.11
Al ₂ O ₃	14.10	13.40	13.30	13.50	12.90	13.50	13.30	13.00	13.10	14.20	13.20	13.70	13.80
TFe ₂ O ₃	11.50	12.00	11.90	11.80	13.20	12.00	12.00	12.30	12.60	12.00	12.30	12.40	12.60
MnO	0.12	0.14	0.14	0.13	0.16	0.14	0.14	0.14	0.15	0.13	0.15	0.15	0.14
MgO	5.92	8.28	8.25	7.52	9.25	7.80	8.31	9.55	9.78	7.85	9.80	8.18	8.12
CaO	8.13	9.03	9.05	9.15	9.85	8.99	9.05	9.50	9.37	8.57	9.47	8.92	8.61
Na ₂ O	3.42	3.01	3.15	3.27	3.05	3.18	2.94	2.98	2.85	2.86	2.73	3.00	3.05
K ₂ O	1.23	1.92	1.91	1.99	1.67	1.92	1.96	1.59	1.55	1.26	1.51	1.43	1.28
P ₂ O ₅	0.36	0.49	0.49	0.51	0.63	0.52	0.51	0.47	0.44	0.36	0.44	0.35	0.36
Total	99.98	100.08	99.99	99.95	99.95	100.05	99.96	99.97	100.05	99.88	99.93	100.03	100.06
L.O.I.	0.65	-0.39	-0.56	-0.61	-0.62	-0.52	-0.18	-0.62	-0.39	0.12	-0.16	-0.21	-0.16
Mg#	53.1	60.4	60.5	58.3	60.6	59.0	60.4	63.0	63.1	59.0	63.7	59.2	58.7
Trace elements (ppm)													
Sc	15.6	19.7			24.5		20.0	25.6	25.5		25.2	18.0	
V	147	200			238		188	218	208		207	156	
Cr	304	277			222		258	248	259		283	228	
Co	43.4	46.2			50.3		44.8	51.2	50.9		50.4	44.3	
Ni	177	151			172		150	205	205		208	164	
Cu	64.3	47.0			59.1		55.0	60.5	59.9		56.6	49.1	
Zn	141	122			132		115	117	119		112	108	
Rb	40.6	34.2			31.9		33.7	28.5	27.6		25.8	19.5	
Sr	720	617			699		624	573	577		585	453	
Y	17.0	22.3			25.3		22.4	22.2	21.2		20.9	18.5	
Zr	293	213			256		212	205	186		179	143	
Nb	58.0	41.9			63.4		43.6	46.5	44.2		42.2	25.8	
Ba	583	492			505		502	426	407		404	217	
La	36.3	30.8			47.2		31.5	33.5	28.9		28.4	16.8	
Ce	71.5	62.3			96.5		64.0	69.2	60.7		58.0	35.9	
Pr	8.62	7.76			11.5		7.82	8.48	7.48		7.08	4.54	
Nd	33.3	30.8			43.3		31.7	32.8	29.4		28.0	19.4	
Sm	7.26	6.76			8.10		6.90	6.72	6.03		5.97	4.61	
Eu	2.42	2.22			2.54		2.19	2.04	1.95		1.93	1.58	
Gd	6.45	6.53			7.35		6.31	5.97	5.69		5.46	4.75	
Tb	0.91	0.96			1.03		0.94	0.85	0.84		0.82	0.74	
Dy	4.28	4.80			5.24		4.81	4.52	4.46		4.22	3.89	
Ho	0.66	0.83			0.94		0.83	0.81	0.78		0.77	0.71	
Er	1.46	2.04			2.23		1.94	1.98	1.91		1.90	1.66	
Tm	0.18	0.26			0.30		0.24	0.27	0.25		0.25	0.22	
Yb	1.01	1.47			1.80		1.44	1.57	1.53		1.52	1.25	
Lu	0.13	0.20			0.25		0.21	0.23	0.22		0.22	0.18	
Hf	6.47	4.81			5.76		4.88	4.67	4.29		4.10	3.27	
Ta	3.74	2.51			3.93		2.65	2.77	2.73		2.44	1.49	
Pb	2.72	2.96			4.15		3.55	2.84	2.54		2.21	1.54	
Th	5.28	4.61			5.81		4.65	4.31	3.96		3.67	2.31	
U	1.27	0.97			1.38		1.04	1.01	0.95		0.92	0.55	
[La/Sm] _N	3.23	2.94			3.77		2.95	3.22	3.10		3.07	2.36	
[Nb/Th] _N	1.29	1.07			1.28		1.10	1.27	1.31		1.35	1.31	
[Ta/U] _N	1.51	1.33			1.46		1.31	1.40	1.47		1.36	1.39	
Sr/Sr*	1.22	1.15			0.90		1.14	0.99	1.12		1.20	1.40	
Nb/U	45.67	43.42			45.94		41.92	46.04	46.33		46.07	46.99	
Zr/Hf	45.29	44.28			44.44		43.44	43.90	43.36		43.66	43.73	
Pb/Ce	0.04	0.05			0.04		0.06	0.04	0.04		0.04	0.04	

Supplementary Table 3 Continued

Locality	Hainan Island (Wang et al., 2011)												
Sample	08HN-25C	08HN-26A	08HN-26B	08HN-26C	08HN-26D	ZK03-18.1	ZK03-20.1	ZK03-24.4	ZK03-25	ZK03-27	ZK03-27.5	ZK03-29.1	ZK03-30
Rock Type	OT	OT	OT	OT	OT	QT	QT	BS	BS	BS	AB	AB	OT
Major elements (wt. %)													
SiO ₂	50.30	51.20	51.20	51.40	51.40	52.40	52.40	46.10	46.10	46.80	46.70	46.20	46.70
TiO ₂	2.06	2.13	2.28	2.15	2.18	1.86	1.95	2.51	2.56	2.72	2.62	2.68	2.75
Al ₂ O ₃	13.90	14.10	14.00	14.20	14.10	14.10	13.90	13.20	13.10	13.90	13.40	13.40	13.70
TFe ₂ O ₃	12.50	11.60	11.80	11.50	11.60	12.40	11.70	13.70	13.60	14.70	13.70	13.60	14.80
MnO	0.14	0.13	0.13	0.13	0.13	0.10	0.15	0.19	0.19	0.18	0.22	0.18	0.18
MgO	8.11	7.08	6.81	6.88	6.85	6.68	7.03	7.57	7.91	6.62	7.32	7.38	5.54
CaO	8.52	8.95	8.80	8.93	8.91	8.88	8.70	9.88	10.10	10.30	10.30	10.40	10.50
Na ₂ O	3.00	3.20	3.25	3.20	3.22	2.81	3.06	3.74	3.27	2.02	2.93	3.02	2.20
K ₂ O	1.20	1.34	1.37	1.35	1.37	0.51	0.88	2.01	1.93	1.46	1.48	1.83	2.14
P ₂ O ₅	0.35	0.35	0.36	0.35	0.36	0.26	0.29	1.21	1.22	1.30	1.23	1.34	1.39
Total	100.07	100.08	100.00	100.09	100.12	100.00	100.05	100.11	99.98	100.00	99.90	100.03	99.90
L.O.I.	-0.26	-0.42	-0.61	-0.40	-0.51	2.17	1.22	1.29	2.34	2.15	2.88	2.64	2.93
Mg#	58.8	57.4	56.1	56.9	56.6	54.3	57.0	55.0	56.2	49.8	54.0	54.5	45.1
Trace elements (ppm)													
Sc	20.1	21.8		21.5				16.2				16.6	
V	154	193		190				150				152	
Cr	250	252		241				131				114	
Co	43.3	43.5		40.6				42.9				44.0	
Ni	168	107		93				129				115	
Cu	59.1	57.9		52.2				51.8				49.7	
Zn	113	126		112				161				160	
Rb	15.7	22.9		21.9				55.4				35.6	
Sr	461	504		479				1327				1341	
Y	19.3	21.1		20.4				33.2				34.7	
Zr	146	170		165				361				360	
Nb	24.5	26.6		26.9				122.0				118.0	
Ba	223	236		245				858				916	
La	17.0	19.5		19.7				97.2				100.0	
Ce	36.3	42.1		41.3				175.0				180.0	
Pr	4.67	5.38		5.34				19.7				20.5	
Nd	19.6	21.9		22.3				72.2				77.1	
Sm	4.82	5.34		5.44				13.00				14.10	
Eu	1.66	1.82		1.91				4.12				4.48	
Gd	4.64	5.26		5.45				11.9				12.3	
Tb	0.71	0.80		0.83				1.54				1.52	
Dy	3.93	4.27		4.32				7.66				7.63	
Ho	0.70	0.76		0.74				1.29				1.28	
Er	1.73	1.94		1.83				3.09				3.03	
Tm	0.22	0.25		0.23				0.39				0.38	
Yb	1.29	1.46		1.37				2.24				2.27	
Lu	0.19	0.20		0.20				0.31				0.31	
Hf	3.38	3.89		3.87				8.55				8.48	
Ta	1.46	1.58		1.67				12.30				12.00	
Pb	1.67	2.14		2.60				5.73				5.58	
Th	2.32	2.82		2.89				13.40				12.90	
U	0.48	0.66		0.69				2.53				3.01	
[La/Sm] _N	2.28	2.36		2.34				4.83				4.58	
[Nb/Th] _N	1.24	1.11		1.09				1.07				1.08	
[Ta/U] _N	1.57	1.23		1.24				2.49				2.04	
Sr/Sr*	1.39	1.34		1.27				1.01				0.97	
Nb/U	51.47	40.30		39.04				48.22				39.20	
Zr/Hf	43.20	43.70		42.64				42.22				42.45	
Pb/Ce	0.05	0.05		0.06				0.03				0.03	

Supplementary Table 3 Continued

Locality	Hainan Island (Wang et al., 2011)											
Sample	ZK03-31	ZK04-10.5	ZK04-26.8	ZK04-30.7	ZK04-9.2	ZK05-20.1	ZK05-22.3	ZK05-25.4	ZK05-28.1	ZK05-32.1	ZK05-33.6	ZK05-36.5
Rock Type	BS	QT	QT	QT	QT	QT	QT	QT	QT	QT	OT	QT
Major elements (wt. %)												
SiO ₂	45.90	52.80	52.90	54.20	52.70	51.80	52.00	51.60	51.60	50.90	49.40	47.50
TiO ₂	2.66	1.93	1.91	2.73	1.88	1.81	1.97	1.92	1.89	1.96	1.99	2.14
Al ₂ O ₃	13.10	13.90	14.30	19.80	13.90	14.10	14.00	13.80	14.10	14.40	14.60	15.40
TFe ₂ O ₃	14.10	12.10	11.40	8.63	11.80	11.80	11.80	12.10	11.60	12.30	13.70	14.10
MnO	0.27	0.16	0.19	0.13	0.14	0.12	0.12	0.13	0.13	0.13	0.13	0.36
MgO	7.00	5.97	4.83	1.86	6.53	7.77	7.13	8.09	8.07	8.07	8.56	7.40
CaO	10.10	9.05	11.50	8.29	8.97	9.06	9.01	8.95	9.18	8.75	8.41	10.34
Na ₂ O	3.46	3.14	2.96	3.50	3.09	2.81	2.98	2.73	2.76	2.74	2.54	2.24
K ₂ O	2.16	0.77	0.83	0.39	0.73	0.43	0.62	0.40	0.31	0.45	0.42	0.30
P ₂ O ₅	1.32	0.25	0.26	0.47	0.24	0.28	0.30	0.31	0.31	0.31	0.29	0.36
Total	100.07	100.06	101.08	100.00	99.97	99.98	99.93	100.02	99.96	100.01	100.04	100.15
L.O.I.	4.68	2.43	4.21	3.66	1.63	1.52	1.57	1.05	1.95	2.59	2.79	8.64
Mg#	52.3	52.1	50.6	32.2	54.8	59.2	57.0	59.6	60.4	59.0	57.8	53.7
Trace elements (ppm)												
Sc		21.1			21.6			20.7			23.5	
V		138			143			144			154	
Cr		214			226			199			282	
Co		37.7			44.0			41.4			47.0	
Ni		90			173			160			174	
Cu		67.7			61.7			65.4			69.0	
Zn		120			108			110			134	
Rb		16.5			3.2			5.3			4.8	
Sr		439			372			397			349	
Y		19.5			18.0			19.1			20.0	
Zr		117			110			121			123	
Nb		20.2			21.5			25.4			25.5	
Ba		224			202			182			194	
La		16.6			16.0			18.5			19.0	
Ce		31.9			31.4			35.8			37.0	
Pr		3.98			3.83			4.39			4.61	
Nd		16.8			16.1			18.1			18.9	
Sm		4.52			4.05			4.48			4.53	
Eu		1.63			1.55			1.62			1.64	
Gd		4.92			4.58			4.81			4.98	
Tb		0.76			0.72			0.75			0.78	
Dy		4.20			3.94			4.34			4.32	
Ho		0.77			0.73			0.75			0.79	
Er		1.89			1.84			1.87			1.93	
Tm		0.24			0.23			0.24			0.26	
Yb		1.54			1.46			1.49			1.57	
Lu		0.22			0.21			0.21			0.23	
Hf		3.39			3.18			3.37			3.52	
Ta		1.21			1.25			1.45			1.54	
Pb		1.89			1.64			2.01			2.60	
Th		2.56			2.46			2.80			2.77	
U		0.54			0.53			0.58			0.46	
[La/Sm] _N		2.37			2.55			2.67			2.71	
[Nb/Th] _N		0.93			1.03			1.07			1.08	
[Ta/U] _N		1.15			1.21			1.28			1.71	
Sr/Sr*		1.55			1.37			1.29			1.08	
Nb/U		37.34			40.64			43.72			55.31	
Zr/Hf		34.51			34.59			35.91			34.94	
Pb/Ce		0.06			0.05			0.06			0.07	

Reference

- Blichert-Toft, J., Chauvel, C., Albarède, F. (1997) Separation of Hf and Lu for high-precision isotope analysis of rock samples by magnetic sector-multiple collector ICP-MS. *Contrib. Mineral. Petrol.* **127**, 248-260.
- Bouvier, A., Vervoort, J.D., Patchett, P.J. (2008) The Lu–Hf and Sm–Nd isotopic composition of CHUR: Constraints from unequilibrated chondrites and implications for the bulk composition of terrestrial planets. *Earth Planet. Sci. Lett.* **273**, 48-57.
- Flower M. F., Zhang M., Chen C., Tu K. and Xie G. (1992) Magmatism in the south China basin: 2. Post-spreading Quaternary basalts from Hainan Island, south China. *Chem. Geol.* **97**(1), 65-87.
- Ho K., Chen J. and Juang W. (2000) Geochronology and geochemistry of late Cenozoic basalts from the Leiqiong area, southern China. *J. Earth Sci.* **18**(3), 307-324.
- Tu K., Flower M. F., Carlson R. W., Zhang M. and Xie G. (1991) Sr, Nd, and Pb isotopic compositions of Hainan basalts (south China): implications for a subcontinental lithosphere Dupal source. *Geology* **19**, 567-569.
- Wang X., Li Z., Li X., Li J., Liu Y., Long W., Zhou J. and Wang F. (2011) Temperature, pressure, and composition of the mantle source region of Late Cenozoic basalts in Hainan Island, SE Asia: a consequence of a young thermal mantle plume close to subduction zones? *J. Petrol.* **53**, 177-233.
- Zou H. and Fan Q. (2010) U–Th isotopes in Hainan basalts: Implications for subasthenospheric origin of EM2 mantle endmember and the dynamics of melting

beneath Hainan Island. *Lithos* **116**(1), 145-152.

For Peer Review Only